UNIVERSITY OF SOUTHAMPTON

THE ELECTRODEPOSITION OF Cu - Zn - Sn ALLOYS FROM ALKALINE CYANIDE SOLUTIONS

by

Lucica Picincu

A thesis submitted for the degree of

DOCTOR IN PHILOSOPHY

Department of Chemistry

January 2000

UNIVERSITY OF SOUTHAMPTON

Abstract

FACULTY OF SCIENCE

CHEMISTRY

Doctor in Philosophy

THE ELECTRODEPOSITION OF Cu - Zn - Sn ALLOYS FROM ALKALINE CYANIDE SOLUTIONS

By Lucica Picincu

The electrodeposition of Cu-Zn-Sn alloys from a commercial alkaline cyanide bath has been investigated. Cyclic voltammetry, potential step and chronopotentiometric experiments were carried out to investigate the mechanism of electrodeposition of the alloy. Also, Hull cell deposition experiments and plating of brass strips at both constant current and constant potential were carried out. Deposits were examined by SEM and EDS to define their morphology and composition. These deposits from freshly prepared solutions were compared with plates using commercial bath solutions as well as the coatings produced on components on the commercial plating line (both those deemed satisfactory and those with defects).

Voltammetry of the solution with optimized composition showed that the deposition of Cu-Zn-Sn alloy is a complex process which is kinetically controlled by chemical reactions in homogenous solution. Also, it was found that a highly reflective alloy deposit with a composition in the range 47 - 51 % copper, 8 - 12 % zinc and 38 - 43 % tin can be obtained under a range of conditions from this bath. These deposits were of uniform appearance and made of overlapping rounded but rather flat features.

Studies were performed where the concentration of one component of the alkaline cyanide solutions was varied systematically (e.g.the concentrations of free CN^-, free OH^-, metal ions, additive) and this enabled correlations to be deduced between the types of defects found on rejected connectors with plating conditions. For example, a "tiger stripe" deposit could be replicated in the laboratory with solutions which were high in hydroxide or copper ions or low in tin or cyanide ions or by using a high current density. These were rough deposits composed of many overlapping centers and were found to have a high copper and a low tin content. A "tarnished" deposit could be replicated from solutions low in hydroxide or copper ions or high in tin or cyanide ions. These were deposits composed of angular crystallites which had a high tin and a low copper concentration. Many of the bath characteristics can be understood in terms of the speciation of the metal ions in the plating bath.

Table of contents

LIST OF SYMBOLS and ABBREVIATIONS

A	*Arhenius constant (dimensionless)*
A	*Electrode area* ***(cm^2)***
a	*Activity coefficient*
c_O	*Concentration of reduced species* ***(mol dm^{-3})***
c_R	*Concentration of oxidized species* ***(mol dm^{-3})***
E_A	*Activation energy* ***(J mol^{-1})***
E	*Potential* ***(V)***
E_P	*Peak potential* ***(V)***
$E_{1/2}$	*Half wave potential* ***(V)***
F	*Faraday constant* ***(98485 C mol^{-1})***
I	*Current* ***(A)***
j	*Current density* ***(A cm^{-2})***
j_0	*Exchange current density* ***(A cm^{-2})***
j_L	*Limiting current density* ***(A cm^{-2})***
k_s	*Standard rate constant*
K	*Formation constant*
L	*Ligand*
M	*Metal*
m	*Number of moles of electroactive species* ***(mol)***
n	*Number of electrons per molecule of reactant (dimensionless)*
R	*Gas constant* ***(8.314 J K^{-1} mol^{-1})***
T	*Temperature* ***(K)***
t	*Time* ***(s)***
α	*Transfer coefficient (dimensionless)*
η	*Overpotential* ***(V)***
ν	*scan rate* ***(V s^{-1})***
w_a	*Wagner number*

Acknowledgements

First I would like to thank my supervisor Derek Pletcher for his assistance and encouragement throughout the duration of my PhD.

I would also like to thank my industrial sponsors Huber & Suhner for providing the financial support for the research and especially my contact there Dr. Alison Smith.

Many thanks to our lab technician Alistair Clark for his help in the countless sessions of SEM.

I would also to thank all my lab mates with whom I practised and improved my English while running long experiments or polishing the electrodes.

Lastly, but not least many thanks to my husband, Genus, and my children Irina and Razvan for their love and support especially after having "bad days" in the lab.

1.1 Why Electroplating

Electroplating is a process in which a thin layer of a material is deposited on to the surface of a substrate by the means of electrolysis in order to improve the properties of the surface. The process of electrodeposition has several different objectives, e.g.:

a) enhanced corrosion protection
b) improved reflectivity of the surface, e.g. to improve its appearance
c) modify the substrate properties, e.g. heat or abrasion resistance, hardness, electrical or thermal conductivity.
d) to alter dimensions (build up of material for restoration).

Very often, the process is used to give the substrate a combination of the above characteristics. Therefore, electroplating is a very common process used by diverse industries, e.g. jewelry, engineering components manufacture, car industry, electronics, etc. In addition, electrodeposition minimizes the use of precious metals, therefore reducing considerably the cost by using only a deposit thick enough to obtain the needed performance[1,2,3].
Electroplating has become an important coating technique, because of the following advantages[4]:

a) the metal coating is well-adherent.
b) the surface properties can be improved dramatically by quite a thin deposit.
c) there is a good control of deposits thickness
d) most conducting substrates are coatable

However, there are a few disadvantages:
a) the rate of deposition is limited to 20-100 $\mu m\ h^{-1}$
b) pre-treatment is required for some substrates

c) the solutions used are often toxic, necessitating careful control as well as effluent treatment.

d) not all metals can be electrodeposited from aqueous solutions.

1.2 Metal plating

At a first glance, metal deposition appears a fairly simple electrochemical process. An ion from the solution accepts electrons to become an atom incorporated into a metal lattice. In reality, the situation is much more complicated. Firstly, it is very important that the process is reproducible and that the deposit always has the same chemical, physical and mechanical properties. Only a bath that is stable over a long period of time could secure a reproducible and predictable deposit. Secondly, it is important that the deposit quality is maintained over a range of operating conditions, since changes in concentrations and current densities occur, especially when different objects are being plated. Also, it should be mentioned that the properties of a deposit depend on the operating conditions: *e.g.* temperature, bath composition, current density. Therefore, it is impossible to define a single set of conditions for electroplating one metal. Moreover, the situation becomes much more complicated when two or more metals are being co-deposited as an alloy.

Schematically, an electroplating bath (fig.1) is composed of the following[4]:

1) The cathode which is the electronically conducting workpiece to be plated.
2) The anode which can be soluble or insoluble.
3) The electroplating bath that is composed of a soluble form of the metal to be plated, a conducting salt, buffer and additives.
4) An inert vessel (tank) containing the electrodes and the plating bath. Usually, the electroplating tank is made of steel, rubber-lined steel, polypropylene or polyvinyl chloride.
5) An electrical power source.

During electroplating, a layer of metal is deposited onto the cathode surface.

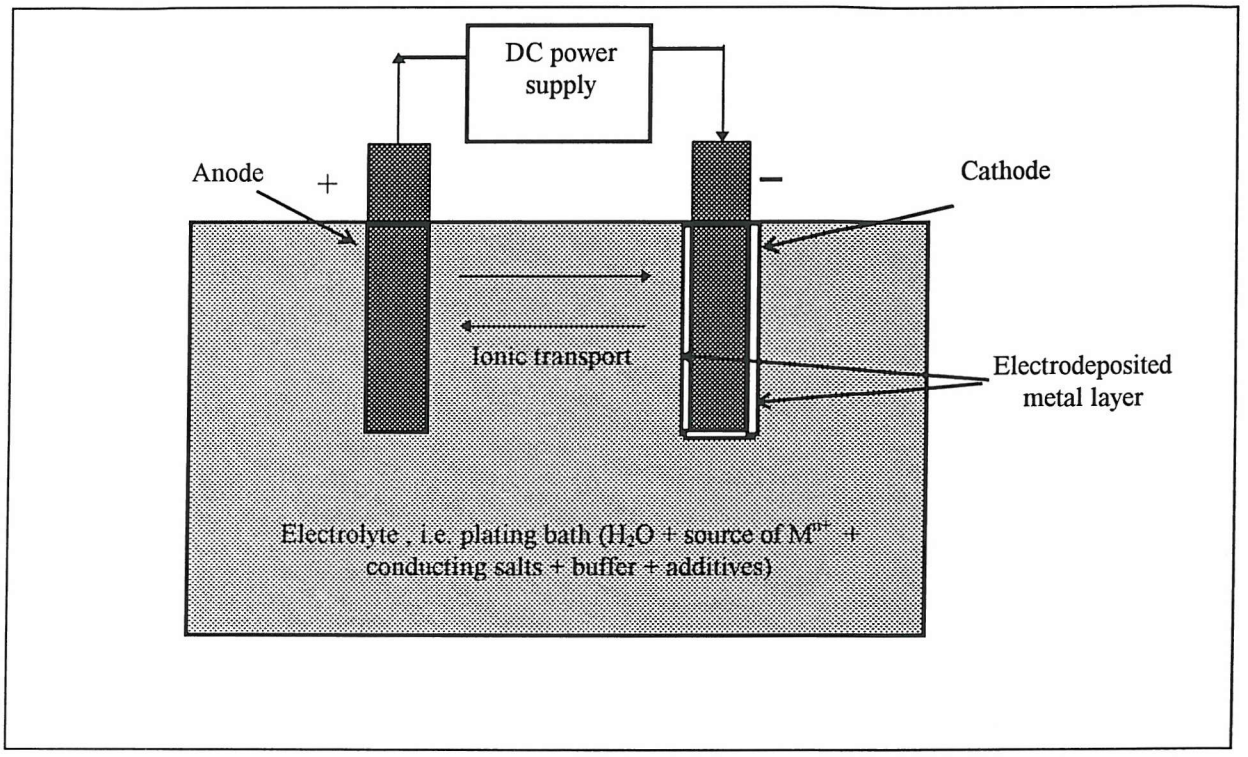

Figure 1.1 *- A typical electroplating bath*

The cathode often also called the working electrode or the substrate, may have different shapes and sizes and could be a single metal, an alloy or any other conducting material, e.g. conducting ceramic. The desired reaction occurring at the cathode is the reduction of the metal ions with the formation of a metal film[4].

$$M^{n+} + ne^- \rightarrow M \qquad (1.1)$$

Often in the case of alloy deposition the metal species in solution are complex ions.

$$ML_x^{n+} + ne^- \rightarrow M + xL \qquad (1.2)$$

Moreover, in aqueous solution, hydrogen evolution is always a possible competing reaction. Hydrogen evolution depends strongly upon the pH of the bath as well as of the nature of the cathode surface (both substrate and deposit).

$$2H_2O + 2e^- \rightarrow H_2 + 2OH^- \qquad (1.3)$$

1.2.1 Deposition of metal

The equation that governs electrodeposition is the reduction of a metal species at the electrode surface, equation 1.1. The thermodynamics of the above reaction is represented by the Nernst equation:

$$E_e = E^\theta + \frac{RT}{nF} \ln \frac{a_{M^{n+}}}{a_M} \qquad (1.4)$$

in which E_e is the equilibrium potential, a_M^{n+} is the activity of the metal ion in the solution, a_M is the activity of the metal, T is the temperature, n is the number of the electrons involved in the metal deposition reaction, F is the Faraday constant and R is the gas constant. Assuming the activity of a metal is one (pure metal, M, is being deposited), the above equation can be approximated[5-7]:

$$E_e = E^\theta + \frac{RT}{nF} \ln a_{M^{n+}} \qquad (1.5)$$

For ideal solutions the activity can be approximated by the concentration and in electrochemistry it is common to make the assumption that $a_M^{n+} = c_M^{n+}$ so that the Nernst equation is used in the form:

$$E_e = E^{\theta} + \frac{RT}{nF} \ln c_{M^{n+}} \qquad (1.6)$$

For a complete view of the deposition process, the kinetics of the electron transfer have to be considered in the discussion. This is governed by the Burtler - Volmer equation:

$$j = j_0[\exp\frac{(1-\alpha)nF}{RT}\eta - \exp\frac{-\alpha nF}{RT}\eta] \qquad (1.7)$$

where j is the current density and j_o represents the exchange current density and the overpotential: $\eta = E - E_e$

The exchange current density is a function of the concentration of oxidized and reduced species in solution as well as a standard rate constant k_s:

$$j_0 = nFk_s(c_0)^{1-\alpha}(c_R)^{\alpha} \qquad (1.8)$$

Also, the exchange current density is dependent on temperature and this effect is normally described by an Arrhenius type equation:

$$\log j_0 = A \exp\frac{-E_A}{RT} \qquad (1.9)$$

In an electroplating process the back reaction is normally insignificant and therefore the rate of electrodeposition can be estimated by an equation of the type:

$$j = -j_0 \exp\frac{-\alpha nF}{RT}\eta \qquad (1.10)$$

Equation 1.10 shows that the current density observed at each potential depends strongly on: the overpotential, the exchange current density, as well as the transfer coefficient and temperature.

In addition, the electrode reaction may not be as simple, as many electroplating processes involve the reduction of a complexed metal species. Hence, prior to electrode reaction there may be a chemical predissociation step, e.g.:

$$Cu(CN)_2^- \leftrightarrow Cu^+ + 2CN^- \qquad (1.11)$$

$$Cu^+ + e \rightarrow Cu \qquad (1.12)$$

The formation of a compex ion may be represented as :

$$M^{n+} + mL \rightarrow ML_m^{n+} \qquad (1.13)$$

in which the formation constant of the complex is:

$$K = \frac{[ML_m^{n+}]}{[M^{n+}][L]^m} \qquad (1.14)$$

Therefore equation 1.6 becomes:

$$E_e = E^\theta - \frac{RT}{nF}\ln K - \frac{mRT}{nF}\ln[L] + \frac{RT}{nF}\ln[ML_m^{n+}] \qquad (1.15)$$

Since for cyano complexes K is large, the ln K term becomes dominant and causes a large negative shift in the equilibrium potential. Also, a large concentration of the ligand increases the negative shift effect in the equilibrium potential. Therefore, the stronger the complexing agent present in the system, the more negative the equilibrium potential becomes. This can

have some interesting effects. For example, in a mixed copper-zinc bath containing cyanide, since K(Cu) > K(Zn), it is possible for the two metals to be deposited at the same potential and, therefore, the alloy brass may be plated from such solutions. In most media, Cu would be deposited at much more positive potentials than Zn.

1.2.2 The mechanism of metal deposition

The mechanism for the formation of a new phase can be best explained by discussing the deposition of a metal onto an inert cathode (e.g. graphite). Metal deposition reactions involve mass transport of the metal species in solution and electron transfer at the cathode surface. In addition, there are steps which are unique to processes involving metal growth. In the formation of a metal deposit there could be four such stages[6] (figure 1.2):

1) nuclei formation (gathering of a small number of metal atoms into a nucleus which is sufficiently large to be stable).
2) growth of each individual center.
3) the overlap of the enlarged centers with the formation of continuous layers.
4) thickening

It may also be possible that well organized metal lattices are formed. Hence, either electron transfer occurs preferentially at certain lattice sites or the metal deposition process requires surface diffusion of adatoms from the site of formation to the point where it is incorporated into the lattice.

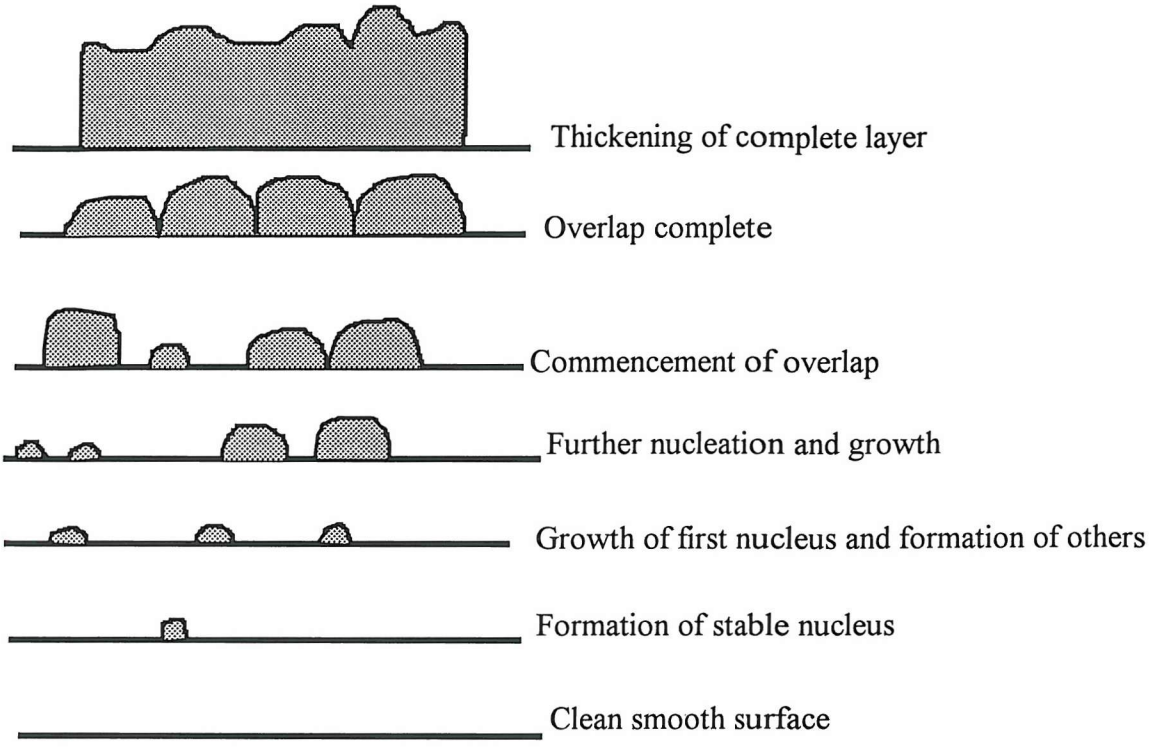

Figure 1.2 *- Various stages of metal deposition on a cathode*

Hence, the metal deposition is a multistep process in which each of the stated processes could be the rate determining step.

1.2.3 Throwing power

The ability of a bath to produce deposits of an even thickness over the whole of the electroplated surface has been termed the throwing power[1-4,8]. An uniform deposit can be obtained when the potential is the same at all points over the electrode surface. However, difficulties are encountered in the case of an object with a complex shape. Figure 1.3 shows schematically a cell in which the working electrode has a non-uniform geometry. The

voltage applied across the two electrodes (figure 1.3) is the sum of the cathode overpotential, anode overpotential and the IR drop in solution.

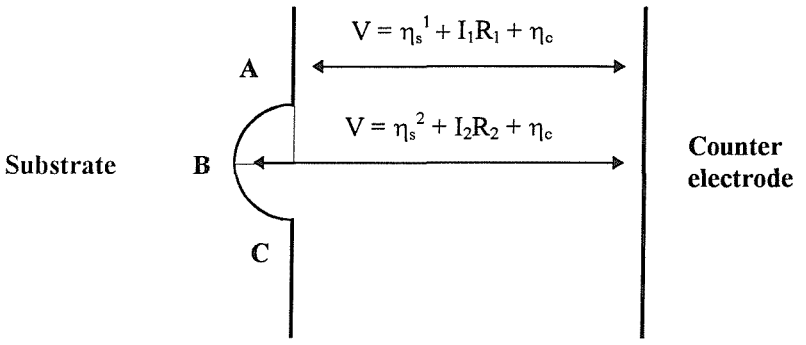

Figure 1.3 - A typical cell with a non-uniform cathode

Assuming that the anode has a uniform, flat surface, it is clear that the cathode overpotential and the resistance of the electrolyte between points on the working electrode and the counter electrode are different at nonequivalent positions ($I_1 > I_2$ because $R_1 < R_2$, and hence $j_1 > j_2$ - figure 1.4).

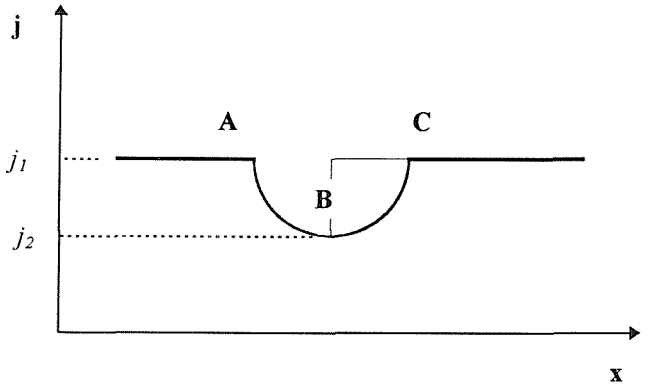

Figure 1.4 - *The current density distribution in a cell with a non-uniform cathode.*

Also, an important role in the uniformity of the deposit is played by a dimensionless number called the Wagner number[4,9].

$$W_a = \frac{\kappa d\eta}{di} L \qquad (1.16)$$

where κ is the electrolyte conductivity, dη/di is the reciprocal slope of an i-η curve, and L is a characterisitc length. The Wagner number can be written

$$W_a = \frac{d\eta / di}{L / \kappa} \qquad (1.17)$$

and regarded as the ratio of "polarization resistance per unit area" to the electrolyte resistance per unit area. In practice, under conditions of a more uniform secondary current distribution, W_a has to be high. This is possible when dη/di is high (by adding additives to the system), large κ (caused by a high concentration of an inert electrolyte), or a small L.

Factors which improve the throwing power are:

1) the electrolyte conductivity - an increase in the conductivity of electrolyte leads to a decrease in IR drop in the bath which causes differences in potential over a complex cathode surface.
2) the presence of complexing agents produce a change in the Tafel slope. Therefore, in the case of a high Tafel slope, any variation in the potential, produces a small difference in the deposition rate:

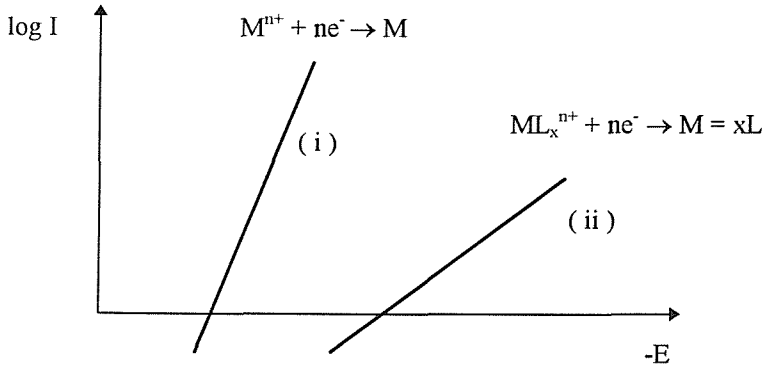

Hence, an increase of the Tafel slope leads to an improvement in the throwing power.

3) competing electrode reactions - e.g. hydrogen evolution reaction. Hydrogen evolution occurs at points on the surface where the potential is more negative. A more even deposit is obtained as a result of the increase in IR drop, hence the decrease in the faradaic efficiency will lead to an enhanced throwing power.

1.2.4 The rate of deposition

The mass of electroplated metal *w* can be estimated from the Faraday's law[4,10]:

$$w = \phi \frac{Mq}{nF} \qquad (1.18)$$

where ϕ is the current efficiency for metal deposition, M is the molar mass of metal, q is electrical charge passed, n is the number of electrons involved in the metal deposition reaction and F is Faraday constant. As the electroplating processes are carried out mostly in batches at a constant current density *j* for a period of time *t*, the averaged rate of mass deposition per unit area is :

$$\frac{w}{At} = \phi \frac{jM}{nF} \qquad (1.19)$$

This expression can also be written in terms of useful current density, $j_M = \phi j$

$$\frac{w}{At} = \frac{j_M M}{nF} \qquad (1.20)$$

So, the rate of deposition, expressed as weight deposited in unit time (g s^{-1}) depends on the molar mass of metal, the number of electrons transferred per ion and the current efficiency.

Therefore in cases where there is a choice of n, e.g. Cu, a low oxidation state of metal produce a higher deposition rate for a given current density.

The averaged rate of deposition on a thickness x basis can be estimated from the equation:

$$\frac{x}{t} = \phi\frac{iM}{\rho AnF} = \phi\frac{IM}{\rho nF} \qquad (1.20)$$

where ρ is the density of the metal.

1.2.5 The quality of the deposit

A satisfactory deposit must be adherent and have the desired properties. Such properties depend on a number of process variables - e.g. electrolyte composition, pH, temperature, addition agents, current density, cell geometry, agitation. One of the most important parameters is the optimum current density range in which the deposit exhibits the desired qualities: brightness, uniformity, etc. In order to assess the behavior of a plating bath, a number of laboratory tests have been developed. The Hull cell test [4,11-15,20] it is the most common.

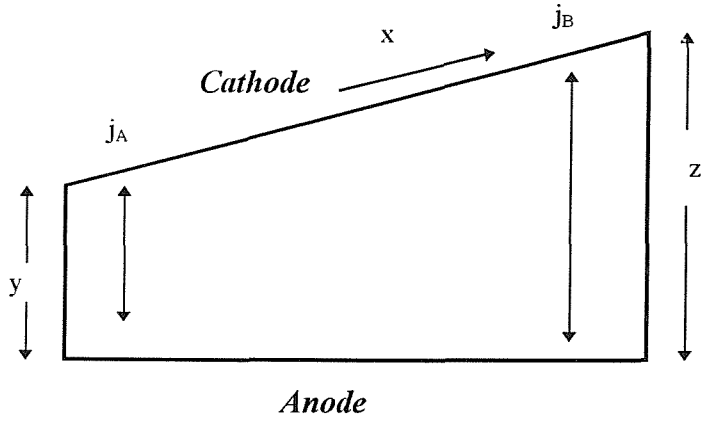

Figure 1.4- Hull Cell

The results of a Hull cell test indicates the useful current density range in which the process can be operated. It also can be used to gain information about the influence of electrolyte composition (additives, impurities, etc.).

Because of the inclination of the cathode, the Hull cell test allows a controlled variation of the current density over the cathode surface to be achieved in a single test. For example, the shortest distance between the electrodes becomes a high current density area, where a thicker deposit will result -*eg:* in figure 1.4 $j_A > j_B$. Typically, the current density ranges from 0.25 mA cm^{-2} to 250 mA cm^{-2}.

Actual local current densities are a function of cell dimensions and electrolyte conductivity. The actual current densities have been correlated with an expression of the type:

$$j_x = I(a\text{-}b \log_{10} x) \qquad (1.21)$$

where *a* and *b* are constants depending on the cell size.

It should be emphasized that in practice, for particular plating baths the current density distribution is often supplied by the plating house distributing the bath.

However, it should be stressed that the Hull cell is employed as a simple empirical tool which enables comparative checks to be made on plating bath in order to help process control and trouble shooting operations.

1.2.6 Anode

The anode used in electrodeposition process [3,4,8,10] can be made from a soluble or insoluble material. An *insoluble anode* does not dissolve in the electrolyte, and is usually made of graphite, PbO_2, $DSAO_2$. The desired process occurring at the anode is usually the discharge of the hydroxyl ions or water to give oxygen evolution.

At the anode:

$$4OH^- - 4e^- \rightarrow 2H_2O + O_2 \qquad (1.22)$$

or

$$2H_2O - 4e^- \rightarrow O_2 + 4H^+ \qquad (1.23)$$

If the solution is insufficiently buffered, the anode reaction will lower the pH.

In addition, because metal ions are reduced at the cathode, and are not being replaced at the anode, the concentration of the metal ions in the solution decreases.

Also, another disadvantage of using insoluble anodes is the possible oxidation at the anode of bath constituents - e.g. addition agents.

Soluble anodes are made of the metal being deposited at the cathode and serve as the replenishing source of the metal ions. They maintain a constant metal concentration in the bath by the means of dissolving at the same rate as the metal deposition at the cathode. To ensure a smooth dissolution, the anode should have a high surface area. Ideally they should not passivate (they should undergo uniform dissolution only under the influence of current) and produce metal ions in their lowest oxidation state. The anode may produce sludge (insoluble material that falls from the anode during electrodeposition) and this has to be removed from the bath at intervals.

The desired anode reaction is the dissolution of the same metal that will be plated:

$$M \rightarrow M^{n+} + ne^- \qquad (1.24)$$

or in a complexing medium:

$$M + mL \rightarrow ML_m^{n+} + ne^- \qquad (1.25)$$

1.2.7 Plating bath

It is important that the solution employed in an electroplating process is stable for a long period of time so reproducible deposits can be obtained. A classical plating bath [3,4,8] is composed from a mixture of salts of the electroactive species, electrolytes, additives and sometimes complexing agents so an electroplate with desired properties and quality can be obtained.

Electrolyte

The electrolyte is added in high concentration to give the bath a high electrical conductivity. This causes a decrease in the iR drop in solution, with the result of a more uniform potential over the cathode surface, and therefore an improved throwing power. Electrolytes used in electroplating process are mainly aqueous solutions of high concentration of acid or base - since protons and hydroxyl ions have a good conductance. In addition to providing increased conductivity, added acid or base can prevent hydrolysis of the metal ion in solution; they effectively buffer the solution. If a bath is operated at a pH between 2 and 12, an effective buffer must be added. Without effective buffering, the electrode reactions can lead to large pH swings close to the electrode. For example, hydrogen evolution as a competing reaction at the cathode could lead to an increase in pH at the cathode surface and precipitation of metal ions as the hydroxide (leading to poor quality deposits).

The electroactive species

The metal to be plated is present in high concentration (usually 1-3 mol dm^{-3}) to prevent significant depletion from the solution at the cathode surface. Typically, the metal ion is present in the form of a hydrated ion - in the case of rapid plating of simple objects - or as a complex with ligands like CN^-, Cl^-,or NH_3 - when a high throwing power is of importance.

The metal ion should be reducible within the potential range of the solvent and it should be stable in solution over a wide range of pH and temperature.

Complexing agents

Complexing agents are used to change the potential where metal deposition occurs. The addition of a ligand causes the deposition potential to move negative through thermodynamic and/or kinetic factors. This can be used in alloy deposition and, for example, if a chemical reaction can occur between the substrate and the metal ion in solution:

$$M_s + M^{n+} \rightarrow M_s^{n+} + M \qquad (1.27)$$

Such processes are called cementation and lead to poorly adherent deposits. The presence of complexing agents can also lead to a change in Tafel slope which improves the throwing power.

Compexing agents can also prevent passivation of the anodes and hence aid dissolution. The most common complexing agents used in electroplating include cyanide, hydroxide and sulphamate ion.

Additives

A large selection of the organic additives are used in the electroplating bath. Although present in low concentration they have a dramatic impact on the morphology, structure and properties of the cathode deposit. Additives are usually considered to act by a mechanism of adsorption on the cathode surface. They, or reduction products are sometimes occluded into the deposit. Adsorption may increase the deposition overpotential - since the electron transfer has to occur through the adsorbed layer.

Since the additives can alter one or more properties of the deposit, they can be classified, *e.g.* as brighteners, levellers, structure modifiers and wetting agents.

(i) ***Brighteners.***

A deposit is bright when the wavelength of the incident light is greater than the microscopic roughness of the deposit so the light is reflected rather than scattered. The brighteners or their decomposition products are most likely to be adsorbed at "active sites" where metal deposition in otherwise most rapid. This diminishes the tendency for the deposit to roughen. Brighteners may also modify the nucleation process causing the formation of fine-grained deposit. Brighteners are normally present in relatively high concentration.

(ii) ***Levellers***

Levellers are added in small concentrations and are often incorporated in the deposit. The adsorbed levelers reduce the rate of electron transfer at peaks in the deposit where there is a high rate of diffusion, shifting the areas of higher current density towards the depressions. Deposition rate there becomes faster, and the surface profile smoothens.

(iii) ***Structure modifiers***

These have the role of changing the structure of the deposit. Sometimes they are used as stress relievers as they adjust the stress in the deposit.

(iv)*Wetting* agents

Wetting agents are added to accelerate the release of the hydrogen gas bubbles from the electrode surface and prevent hydrogen embrittlement of the metal.

1.3 Alloy electroplating

A large proportion of electroplated metals are used in the form of alloys rather than as pure, single metals[1-3, 20, 31,32],. This is because the properties of the alloys can be tailored to satisfy the mechanical or chemical requirements of an application more successfully than pure metals. The enhancement in properties must compensate the increased difficulty involved in the operation of the alloy plating process. The composition and properties of the alloy can be altered by changes of one or more of the deposition parameters - such as electrolyte composition, temperature, current density.

For instance, the many colors and shades of gold alloys (*e.g.* rose, green, or white) can be achieved by codepositing gold with copper, nickel, tin or silver under specific deposition conditions. The chemical and corrosion resistance of electrodeposited alloys could be superior to that of either of the parent metals in certain environments: *e.g.* lead-tin alloy containing 6% tin has a higher corrosion resistance than the parent metals and a high - phosphorous nickel alloy has a much better resistance to concentrated hydrochloric acid than pure nickel. The hardness of electrodeposited alloys can also be greater than that of the electrodeposited parent metals. Moreover, they exhibit a better hardness compared to the corresponding thermal alloys which are hardened by conventional metallurgical processes such as heat treatment or coldworking - e.g. the cobalt-phosphorus alloys have a hardness equal to that of electrodeposited chromium.

Very often the grains of many electrodeposited alloys are too small to be seen with the microscope but their size can be estimated by the means of X-ray diffraction.

1.3.1 General conditions for alloy plating

Generally, the procedure for alloy plating is very much the same as the one for single metal deposition: a current is passed between electrodes through a solution with the result that metal deposits at the cathode.

During a simple electroplating process the rate of deposition could be estimated by an equation of the type:

$$j = -j_0 \exp\frac{-\alpha nF}{RT}\eta \qquad (1.26)$$

where j_0 is termed as the exchange current density, η is the overpotential, T is temperature, α is the transfer coefficient.

However, when two or more metal ions are being reduced at the cathodic surface, the process is much more complicated as the metal ratio in the alloy is not the same as that in the solution.

For instance, in the case of brass deposition, for a given applied current density:

$$j = j_{Cu} + j_{Zn} + j_{Sn} + j_{H2} + j_{O2} \qquad (1.27)$$

where j_M is the current density for the deposition of each metal, j_{O2} is the current density for oxygen evolution and j_{H2} is the current density for the hydrogen evolution.

The ratio of $j_{Cu}/ j_{Zn}/ j_{Sn}$ determines the alloy composition.

It needs to be recognized that the discussion of an alloy plating system is much more complicated than a single metal.

Firstly, the equilibrium potential is now governed by an expression of the type:

$$E_e = E^{\theta} + \frac{RT}{nF} \ln \frac{a_{M^{n+}}}{a_M} \qquad (1.28)$$

While the assumption $a_M{}^{n+} = c_M{}^{n+}$ is equally valid, it is no longer true that $a_M = 1$. A first estimate would be that a_M is related to the fraction of the metal in the alloy. As a result, the reference point for overpotential is not the same.

Secondly, the kinetics of each metal deposition reaction is probably not the same as for a single metal.

In order to deposit an alloy, the essential ratio of $j_{Cu}/ j_{Zn}/ j_{Sn}$ (for the desired composition) must be created. This can be achieved by adjustment of both thermodynamic and kinetic parameters.

As summarized above, the thermodynamics is largely determined by the concentration of the metals in solution and the presence of the complexing agents. For example alloys containing copper normally require the presence of a strong complexing agent. Practical alloy plating baths often combine more than one complexing agent each of which interacts primarily with

one metal ion; this facilitates the adjustment of the thermodynamics factor determining the deposition potential.

1.4 Cu - Zn - Sn

The ternary alloy copper-tin-zinc can be electrodeposited from alkali cyanide baths with the result of a pleasing deposit which can range in color from yellow to dark gold, or white color[8,16,20,32]. Such solutions can be considered as a combination of brass-plating and bronze-plating baths.

The deposition of brass, bronze as well as of Cu/Zn/Sn alloy goes back to the early 1840's[3]. Industrially, the Cu/Zn/Sn ternary alloy can be deposited by either rack or barrel options and it has become increasingly important because of its application in the electronics industry for connectors.

Very little data dealing with the deposition of copper-zinc-tin alloys have been published in scientific journals or books. Mainly, the information is proprietary, or disclosed only in the patent literature. Diggin and Jernsedt[17] do not give information about the bath composition although it treats the precautions to be taken when operating the bath. Mohler,[18] reviews in his paper several plating processes including the one in discussion. Jacky[19] and Jordan[20] give some data regarding the bath and alloy composition. However, the alloy metal ratio of 55 to 60% Cu, 20 to 30% Sn and 10 to 20% Zn is different than the one studied in this project as a result of the small concentration of the metals ions in solution employed in their systems.

Also, it should me mentioned that as a result of little technical information on the relation between the alloy composition and the bath variables, the control of the plating operation is usually empirical. However to ensure the deposit remains within a certain color and composition, the bath parameters must be controlled closely and even small changes will result in a deposit with a completely different appearance. In order to operate the bath continuously it will be necessary to control the following variables:

1. metal ion concentration
2. free cyanide concentration
3. free hydroxide concentration
4. sodium carbonate concentration
5. additive concentration
6. temperature
7. pH

1.4.1 The metals

Complexation of Cu(I), Sn(II) and Zn(II) in aqueous cyanide and hydroxide solutions has been widely studied[10-43]. The generally agreed major solution species and formation constants for their formation are reported in table 1.1

	cyanide			**hydroxide**		
	major species	***K***	***ref.***	***major species***	***K***	***ref.***
Cu(I)	$Cu(CN)_3^{2-}$	$3.8x10^{28}$	31			
Zn(II)	$Zn(CN)_4^{2-}$	10^{17}	31	$Zn(OH)_4^{2-}$	10^{40}	43
Sn(II)		-		$Sn(OH)_2^{2-}$	10^{26}	42

Table 1.1 shows that as the weakest complex is $Zn(CN)_4^{2-}$ and the $Zn(OH)_4^{2-}$ is the strongest complex.

1.4.2 Free Cyanide

Next to the metal ratio, the free cyanide is one of the most important variables in the bath. Sufficient cyanide ion is needed in the system in order to complex all copper and zinc ions. Free cyanide also influences thermodynamics and kinetics of metal deposition reaction - as discussed above. It represents the quantity of cyanide which is not needed in the formation of the complex solutions. However it is important to maintain its concentration within strict

limits as there is loss of cyanide occurring during anodic oxidation and hydrolysis. Also, a high concentration in cyanide slows down the plating of copper and also will result in a more rapid decomposition to form carbonate. In contrast, low concentrations of free cyanide will speed the plating rate with the result of a deposit very high in copper.

1.4.3. Free hydroxide

The free hydroxide is the principal conducting ion in the bath and also complexes Sn(IV). It is also essential for safety reasons to ensure the electrolyte is maintained at a sufficient high pH, to avoid formation of gaseous HCN.

The free hydroxide controls also the amount of tin in solution as the complex ion. Without sufficient hydroxide, the carbon dioxide in the air would decompose the stannate ion and cause basic tin compounds to precipitate and thus the ratio of the three metals in solution will be disturbed.

1.4.4 Carbonates

These are used to provide solution buffering in the solution layer close to the cathode and improved conductivity. They are necessary in a cyanide plating bath up to a certain concentration. Beyond that, they start adversely influencing plating, quality, cost and output. Therefore, it is important to take into account that in cyanide plating baths carbonates occur naturally with time, as a result of one or a few of the following mechanisms[44]:

1. reaction of sodium hydroxide with atmospheric CO_2 according to the following equation:

$$2NaOH + CO_2 \rightarrow Na_2CO_3 + H_2O \qquad (1.29)$$

2. decomposition of cyanide at the anode due to the oxidation to cyanate and subsequent hydrolysis of CNO^- to CO_3^{2-} and NH_3 :

$$HCN + 2H_2O \rightarrow NH_4HCO \qquad (1.30)$$

$$NH_4HCO + 2H_2O \rightarrow 2NH_3 + H_2CO_3 \qquad (1.31)$$

1.4.5 Additive

No bright ternary alloy is obtained unless addition agents are added in the bath. Several compounds are reported to be used as additives. Brenner [3] reports the use of quaternary ammonium compounds with long chains. Jordan [20] reports the use of either fatty alcohol phosphate ester ethoxylate or of Pb acetate or K-Na tartrate as additive.

The additive used in this project is known commercially as Copper Glo and it is believed to be an aliphatic tertiary aminoxide with a long chain amido subsituent. the following major structure:

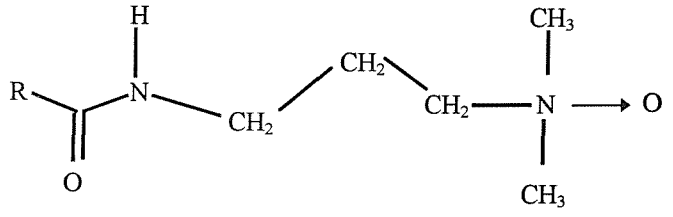

1.4.6 Bath temperature

This it is an important parameter as it has a marked effect upon the alloy composition. The bath temperature influences the:

1. surface diffusion of adatoms. High temperatures accelerate the adatoms diffusion with an effect on the deposit quality.

2. exchange current densities which vary strongly with temperature, usually obeying an Aarhenius relationship.
3. diffusion coefficient of the species in solution:

$$D = D^0 \exp(-E_A / RT) \qquad (1.32)$$

4. rate of homogenous reactions in the system.

Hence, in order to obtain a deposit with a certain composition, the temperature should be kept within strict limits. Bath temperatures are, depending on the process, from 45 - 66 C but in all cases the set temperature must be controlled to ± 2 C.

1.4.7 The pH

The pH of the bath has to be kept between 12.6 and 13.0 and sodium hydroxide is used to increase the pH value. When the pH drops below 12, hydrolysis of the tin salt may occur and therefore the metal ratio in solution is disturbed. Also, the pH has to be maintained high for safety reasons in order to avoid the formation of HCN .

1.4.8 Agitation

Stratification of the plating bath can occur in alloy plating just as it does in the deposition of a single metal. Agitation of the alloy plating bath can directly affect the composition of the alloy by reducing the thickness of the cathode diffusion layer. This is a simple mechanical action which does not produce any change in the electrochemical properties of the solution or the mechanism of the plating process. The effect of agitation on the composition of the deposit is due to the concentration changes produced at the cathode-solution interface. During alloy deposition the cathode diffusion layer is depleted in metal ions, and the concentration ratio of the metals in the layer differs from that in the bath. By agitating the

bath, the thickness of the diffusion layer decreases, hence the metal ratio of the diffusion layer gets more closer to the one in solution

1.5 The purpose of this study

The aim of this study is to understand the chemistry and electrochemistry of the Cu-Zn-Sn electroplating bath. Studies to find the relation between the quality, morphology and composition of deposits with the electrodeposition conditions and for optimum electrodeposition conditions which produce reflective, uniform deposit were carried out.
In the first stage of this investigation, the standard plating bath (ie. that used in commercial plating) was studied. Voltammetric experiments as well as Hull Cell test have been employed to study the electrodeposition of Cu-Zn-Sn alloy which is being plated at Huber & Suhner Bicester.

In a second stage of this work, parameters and concentration of the plating solution have been altered one at the time and the effect on the electroplating process was defined.
The electrochemistry of single metal ions only (i.e. Cu(I), Zn(II) and Sn(IV)) in cyanide media were also investigated.

Finally, connectors or plating baths which have been provided by Bicester plating line were analyzed for a deeper understanding of the bath age has on the alloy.

2.1 Chemicals and Reagents

The chemicals employed in this project are listed in Table 2.1. Aqueous solutions were made with deionized water from a "Analyst" Whatman water purifier. The brass Hull cell panels, 100 mm x 75 mm, (Ossian), which had a protective film and the silver plated ones were supplied by Huber & Suhner. Also, some of the chemicals were supplied from Huber & Suhner at Bicester so that the chemicals used for the project were identical to those on the plating line.

Reagents	*Physical condition*	*Supplier*	*Purity / %*
NaCN	Solid	Huber & Suhner	highly purity
CuCN	Solid	Huber & Suhner	highly purity
$Zn(CN)_2$	Solid	Huber & Suhner	highly purity
$Na_2[Sn(OH)_6]$	Solid	Huber & Suhner	highly purity
$Na_2(CO)_3$	Solid	Merck	99.9
Copper Glo	solution	Huber & Suhner	
NaOH	Solid	Merck	99.9 AnalaR
HCl	1 M solution	Fisher Scientific	99.9 AnalaR
$AgNO_3$	0.1 M solution	Merck	99.9 AnalaR
Trimethyl amine oxide	solid	Lancaster Synthesis	98
Dimethyl octamyl N oxide	solid	Aldrich	99
Sodium hypochlorite	solution	Merck	
$BaCl_2$	Solid	Pronalys Ar	99

Table 2.1 - List of chemicals

After use all cyanide containing solutions were poured into excess concentrated hypochlorite and the resulting solutions were returned to Huber & Suhner for processing in their effluent treatment plant.

2.2 Electrochemical instrumentation

The *experiments at strip electrodes* were initially performed with the help of a potentiostat and waveform generator. Both were Hi-Tek Model DT 2101 and Model PPR1 respectively. Current voltage curves were recorded on a XY recorded (Gould 6000 series).
Later on, these experiments were carried out with a EG&G PAR Model 263A. The data aquisition was performed using an Opus 386/16 MHz computer via a GPIB-PC 2A (National Instruments) interface using the EG&G software, version 4.23. The voltammograms were imported into a Dell Pentium 75 computer for analysis using the same software.

The solutions studied in the electrochemical cell were thermostated with the aid of a Camlab thermostat. Usually the temperature was 333 K as for the commercial bath.

The *experiments for Hull cell depositions* were carried out in a Hull cell (supplied by Huber & Suhner) with the help of a Powerline power supply. Prior to plating, the solution was thermostated in situ with the aid of a built in thermostat.

The *electrocleaning* was performed with the aid of a Powerline power supply.

The *free cyanide and free hydroxide* was analyzed with the help of an automatic 686 Titroprocessor in which the titrant was fed automatically with a 665 Dosimat. The Titroprocessor was equipped with four non-volatile memories available for standard

methods. From these memories only the first three were employed in this project. Prior to each determination the processor had to be loaded with the appropriate parameters.

2.3 SEM

Scanning Electron Microscopy were performed with the aid of a JEOL 6400 analytical SEM which was also equipped with a Tractor Series II X-ray. The samples were mounted with conducting cement (Leit-C from Agar Aids) on to metallic studs. EDS analysis was carried out at an accelerating voltage of 20 kV and it was performed by moving the electron beam around the sample. It was found that different analysis performed on the same sample lead to very close results. Also, for reproducibility purposes, most of the experiments have been repeated several times on samples which were plated at different times. The results obtained are reported in this thesis at the nearest $\pm$ 0.5 value.

The EDS was calibrated from time to time by using standard metals. A much more accurate method of finding the alloy composition would be by dissolving it in acid and then analyzing the resulting solution with the aid of AA. However, this method is impracticable in this case as the substrate is unstable in acid. The thickness of the deposit was not known as H_2 evolution accompanies the electroplating process. However, the current efficiency could be found by weighing the sample before and after the plating.

2.4 Electrochemical cells

2.4.1 Voltammetric cell

Early experiments employed Ag microelectrodes and also a home built brass RDE. With these electrodes, the data was not entirely reproducible as a result of difficulties encountered during the cleaning procedure. Hence, it was considered that the best electrodes would be disposable strips which were cut from Hull cell panels of A = 1 cm^2. These electrodes had

identical surfaces and preparation to the Hull cell electrodes and were used once before being discarded.

Voltammetry and other experiments which employed the strip electrode were carried out in a glass cell with a volume of ~40 cm^3 although only 15 cm^3 of solutions were used. The cell was equipped with a water jacket so that the experiments could be carried out at 333 K (the commercial plating temperature).

Prior to voltammetry or electrodeposition experiments Hull cell panels (100 mm x 75 mm) were cathodicaly electrocleaned (1A for 60 s) in an alkaline bath at 313 K, cut into strips 5 mm wide, and then etched in a commercial acid for a few minutes. After thorough washing with water, the electrodes were then dipped into the plating solution so that an exposed area of 1 cm^2 was in use. The working electrode was in the same compartment as the Pt gauze counter electrode while the reference electrode (SCE) was separated from the working electrode by a Luggin capillary. The quality of electroplates were judged by visual observation and also by SEM.

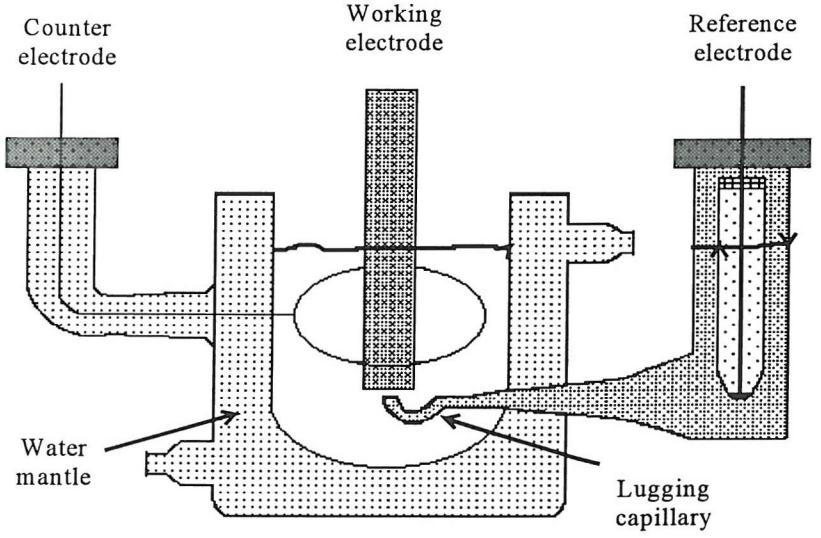

Figure 2.1 *Glass cell used for experiments with the strip electrode*

2.4.2 Hull cell

The Hull cell experiments give valuable information about the useful current density range in which the system can be operated. A plating experiment is also used to determine the state of health of the plating bath in order to ensure continuous productions of satisfactory deposits.

The Hull cell is composed of an undivided cell made of Perspex with a capacity of ~300 cm^3. The working electrode was a brass panel which in some cases had a silver undercoat and the secondary electrode was made of steel. The brass panels (100 mm x 75 mm) (Ossian) were supplied by Huber & Suhner and were already prepolished. Also the side of the panel which was to be plated was protected with a polythene film which was removed just before the electrocleaning procedure.

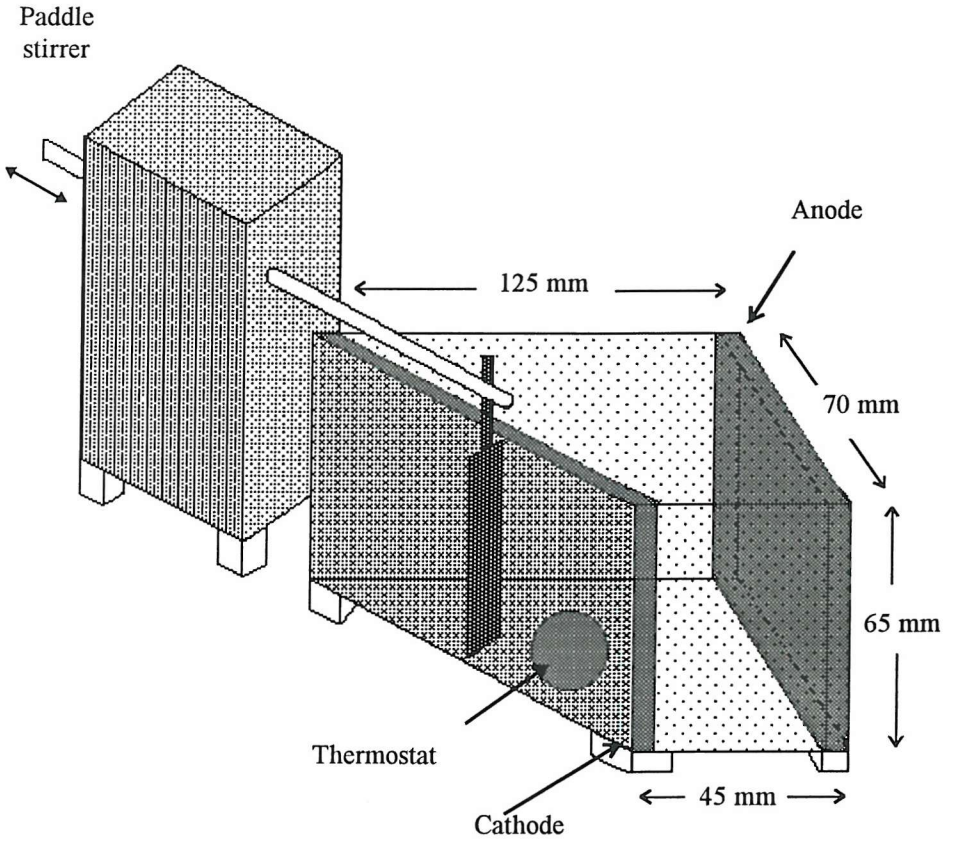

***Figure 4.2** - The Hull Cell*

The electrocleaning was performed at 313 K in a Entrep solution 35 g l^{-1}. The Hull cell panel was cathodically electrocleand at 1A for 60 s with the aid of a Powerline power supply type. A steel anode was used in this procedure.

In order to achieve a large operating current density range, the separation of the brass plate and steel counter electrode ranged from 45 mm to 125 mm. The current density range achieved is 0 mA cm^{-2} to 45 mA cm^{-2}. Since during the plating process hydrogen evolution occurs, the solution is agitated with a paddle that moves slowly across the surface of the brass plate. Prior to each experiment the solution was thermostated to 333 ± 2 K with the help of the built in thermostat.

A standard Hull cell test for state of health monitoring is performed at 1 A for 120 s, during which, in normal conditions, a reflective, complete deposit is obtained. However, for an accurate determination of elemental composition, the plating time has to be increased, so that the electron beam does not penetrate into the brass substrate. Also, for the same reason, as shown later in the thesis, a number of Hull cell tests have been performed on panels that had a silver undercoat. This was applied by Huber & Suhner at Bicester using their standard procedure. Ag undercoated electrodes were pretreated before use.

2.4 Experimental procedures

Prior to all experiments the brass electrodes were electrocleaned in a Entrep solution 35 g l^{-1} and then etched in a solution of Picacid 35 g l^{-1}. Both these solutions were supplied by Huber & Suhner.

The plating solutions were freshly prepared and the ratio free CN^-/ free OH^- optimized to the desired value using the procedure programmed into the Titroprocessor 686.. Prior to plating the solution was thermostated at 333 K, in situ as the cell was equipped with a mantle. For experiments performed in the Hull Cell, the solution was thermostated by using the built in

thermostat with which the cell was fitted. After depositon, the samples were analyzed with the help of SEM and EDS procedures.

2.4.1 Solution preparation

All solutions were prepared using chemicals procured by Huber & Suhner in deionized water produced by a Whatman water purifier. After preparation, the ratio CN^-/OH^- was checked with the aid of a Titroprocesor 686. The ratio was then optimized to the desired one. It should be mentioned that no check of the metal ion concentration or additive was performed as no adequate instrumentation was available. Then, the solution was stored in enclosed vials under the fume cupboard.

2.4.2 Determination of free hydroxide

The free hydroxide was determined with the help of a Titroprocessor 686. The free hydroxide was determined by titration with 1 M HCl with the help of the GET method-General Equivalence-point Titration. This method, uses titration with continuous reagent feeding and automatic evaluation, and measures the pH with the aid of a Long Life combined glass electrode (type 6.0239.100 produced by Metrohm). For an accurate determination of the free hydroxide, the pH electrode had to be calibrated with buffer solution with the aid of the MEAS mode of the Titroprocessor.

Prior to this, 20 ml of the plating solution was placed into a beaker to which 10 ml $BaCl_2$ solution 0.8 M was added. A further 30 ml of deionized water was added and then the solution was automatically titrated with 1 M HCl which was supplied by a 665Dosimat. The titration was performed with the help of a pre-calibrated combined pH glass electrode. At the end of titration, the concentration of hydroxide was printed out by the titroprocessor. If the concentration was low, more NaOH was added to the plating solution and the above procedure was repeated.

2.4.3 Determination of the free cyanide

The determination of the free cyanide is performed by titration with 0.1 M $AgNO_3$. It employs the MET method- Monotonic Equivalence-point Titration, titration with incremental reagent feeding and automatic evaluation. The free CN^- concentration is measured with the help of a Ag titrode (type 6.04430.100 produced by Metrohm) which is connected to the Titroprocessor.

To 1 ml of the plating solution was added 5 ml 1.2 M NaOH solution and 60 ml of deionized water. The beaker was then attached to the titroprocessor and titrated with a 0.1 M $AgNO_3$ solution with the help of the Dozimat. A silver titrode was used as the sensing electrode. At the end of titration, the concentration of free cyanide was printed automatically by the built in printer. Then, if necessary, the appropriate correction was made, and the above procedure was repeated.

2.4.4 Electrocleaning procedure

Prior to each experiment, the brass or silver undercoat electrodes had to undergo an electrocleaning procedure. This procedure is used to ensure that components to be electroplated are free of any grease and impurities. Hull cell panels were electrocleaned immediately before plating. In the case of experiments using brass strip electrodes, the panel was cut in to strips after electrocleaning.

For this, the panel was dipped in an Entrep solution 35 g/l which was heated to 313-318 K with the aid of a hot plate. A current of 1 A was then applied cathodically to the panel for 60 s. This time is considered sufficient for the electrode to be cleaned. A stainless steel electrode was employed as anode. This experiment was performed with the aid of a Powerline power supply. Then the panel was washed with copious amounts of water.

2.4.5 Etching

After electrocleaning, the panel was etched in a solution of Dipacid 35 g l^{-1} for 2 min. When the experiments employed strip electrodes, each individual strip was etched immediately before use. They were washed thoroughly with water before use.

Studies of the Alloy Electroplating Bath

The electroplating of alloys is an established part of the metal finishing industry. Typical baths as well as the general concepts to understand alloy deposition are described in a number of textbooks [3,8,20]. Huber & Suhner Ltd have developed an alkaline cyanide plating bath (tradename - SUCOPLATE®) operated at 333 K for the electrodeposition of a bright, abrasion resistant Cu-Zn-Sn alloy for finishing electronic components [20].

The objective of this thesis is to understand the electrochemistry of the SUCOPLATE electroplating solution. For this, a large number of voltammetric techniques have been employed. Also, SEM and EDS techniques have been used to detect the alloy morphology as well as its composition. The approach has been to carry out experiments in a plating solution with the same composition as the commercial electroplating line (the "standard" plating bath). Then the investigation has been broadened to solutions where the concentration of one component in the bath was systematically varied. In this way, it was hoped to understand the role of each species in the bath.

3.1 The standard plating bath

All experiments in these section were carried out with freshly prepared solutions with the following composition:

	$g\ l^{-1}$	mM
CuCN	9.1	102
$Zn(CN)_2$	5.4	46
$Na_2[Sn(OH)_6]$	5.7	24
Na_2CO_3	6.5	61
free NaCN	25.0	551
free NaOH	2.1	50
Copper Glo solution	5.0	

Copper Glo solution is an electroplating additive supplied by Lea Ronal Ltd where the active ingredient is believed to be an aliphatic tertiary amine oxide with a long chain amido substituent. The solution was thermostatted at a temperature of 333 K and, consistent with commercial practice, was not deoxygenated. The substrate for electroplating was brass strip 5 mm wide cut from a plate supplied for Hull Cell depositions and mounted so that it dipped into the solution to a depth of 10 mm; these make convenient disposable electrodes.

3.1.1 Cyclic Voltammetry

Figure 3.1 shows cyclic voltammograms recorded with a potential scan rate of 20 mV s^{-1} at a brass strip electrode in the plating bath at 333 K. The positive limits are - 1260 mV vs SCE, a potential where the current is zero and no alloy was deposited; corrosion of the brass commences at potentials positive to this value. The negative potential limit is - 2000 mV where H_2 evolution is clearly observed.

Figure 3.1 A shows the first scan on the brass electrode. The main feature is a cathodic peak, E_p = - 1680 mV vs SCE and I_p = 5.2 mA cm^{-2}. This peak current density is a large fraction of the commercial plating current density (6 mA cm^{-2} is a typical value) but significantly less than would be estimated for a diffusion controlled reduction of all the Cu(I), Zn(II) and Sn(IV) in solution. When compared with the response for a diffusion controlled process, however, this cathodic peak is too symmetrical, the current dropping too rapidly beyond the peak. This can arise when there is inhibition of the metal deposition reaction which could occur, for example due to adsorption of hydrogen atoms or an organic on the freshly deposited alloy surface in this potential range. In fact, a sudden spurt of H_2 evolution, correlated with the peak on the voltammogram. In later sections, further data will be reported which associated a significant fraction of current in this region with transient H_2 evolution. Close to -1.6 V, H_2 was observed early in depositions but not when the steady state was reached. The reverse scan shows no anodic current negative to - 1300 mV; the reduction is irreversible and the Cu-Zn-Sn alloy appears to be stable over the potential range

studied. The reverse scan also shows a narrow potential range around -1520 mV where the current is higher than on the forward scan and this is consistent with the process leading to the cathodic peak on the forward scan involving a nucleation step for the formation of a new phase on the electrode surface. After this single cycle, the brass is obviously covered with a uniform and shiny alloy layer and, indeed, the total cathodic charge passed (~ 130 mC cm^{-2}) is sufficient to deposit a layer ~ 0.2 μm thick if metal deposition was the only electrode reaction taking place.

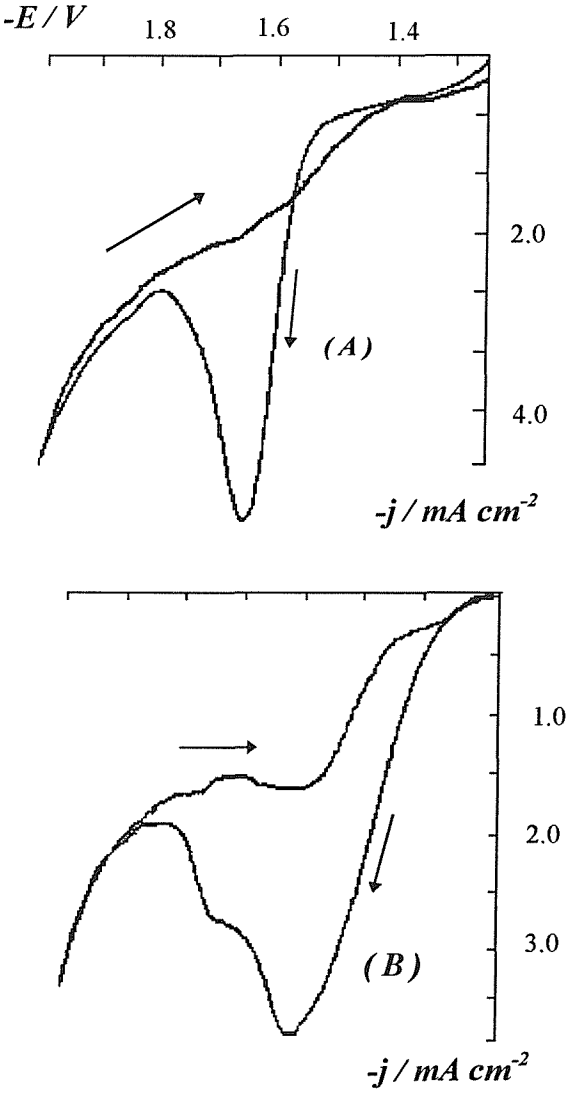

Figure 3.1 *Cyclic voltammograms for the plating bath at a fresh brass strip electrode* ***(A)*** *first scan,* ***(B)*** *fourth scan after continuous potential cycling. Potential scan rate: 20 mV* s^{-1}*.Temperature 333K*

Figure 3.1 B reports the current/potential response during the fourth continuous potential cycle and there are significant differences. While the cathodic peak remains at a similar potential, it is smaller with a peak current density of 4 mA cm^{-2}. It is also much broader because reduction starts much earlier at -1380 mV (cf. - 1520 mV on the first cycle). The fourth scan also shows a new shoulder at - 1760 mV. If there is a pause of 100 s with agitation between the 3rd and 4th scan, the positive shift in the foot of the first cathodic peak and the shoulder at - 1760 mV are again seen although the currents are larger than without the pause. The changes between the 1st and 4th cycles therefore result from the different surface properties of brass and the Cu-Zn-Sn alloy (not changes to the solution adjacent to the electrode). It is tempting to interpret the positive shift in the reduction potential only in terms of a nucleation phenomenon during the first cycle. In fact, however, H_2 evolution is also observed around -1500 mV on the 4th scan but not the 1^{st} cycle.

In cyclic voltammetry, the extent of diffusion control is usually probed by variation of the potential scan rate. Such experiments, however, gave complex results and experiments at faster scan rates led to peaks whose shape imply a role for adsorption processes. Therefore, the importance of mass transport in determining the magnitude of the current densities was examined using a rotating disc electrode. Figure 3.2 shows voltammograms recorded at a rotating brass disc electrode, rotation rates 400 rpm and 3600 rpm. A reduction wave, $E_{1/2}$ $\approx$ - 1660 mV vs SCE can be discerned but well formed plateaux are not observed. Rather, negative to the wave, the current shows some decrease consistent with passivation. It should, however, be noted that the currents are significantly higher at the faster rotation rate but not the factor of three predicted by the Levich equation for a mass transfer controlled current. Moreover, the limiting current density at 400 rpm is 28 mA cm^{-2} compared to a value of 130 mA cm^{-2} estimated from the Levich equation for mass transport control with respect to all the Cu(I), Zn(II) and Sn(IV) in the bath (assuming a diffusion coefficient of 6 x 10^{-6} cm^2 s^{-1} for each metal species in solution). Therefore, the alloy deposition appears to be partially mass transport controlled in the plateau region. In consequence, it must be

concluded that there is also partial control by some chemical processes in solution, perhaps the interconversion of metal complexes before electron transfer.

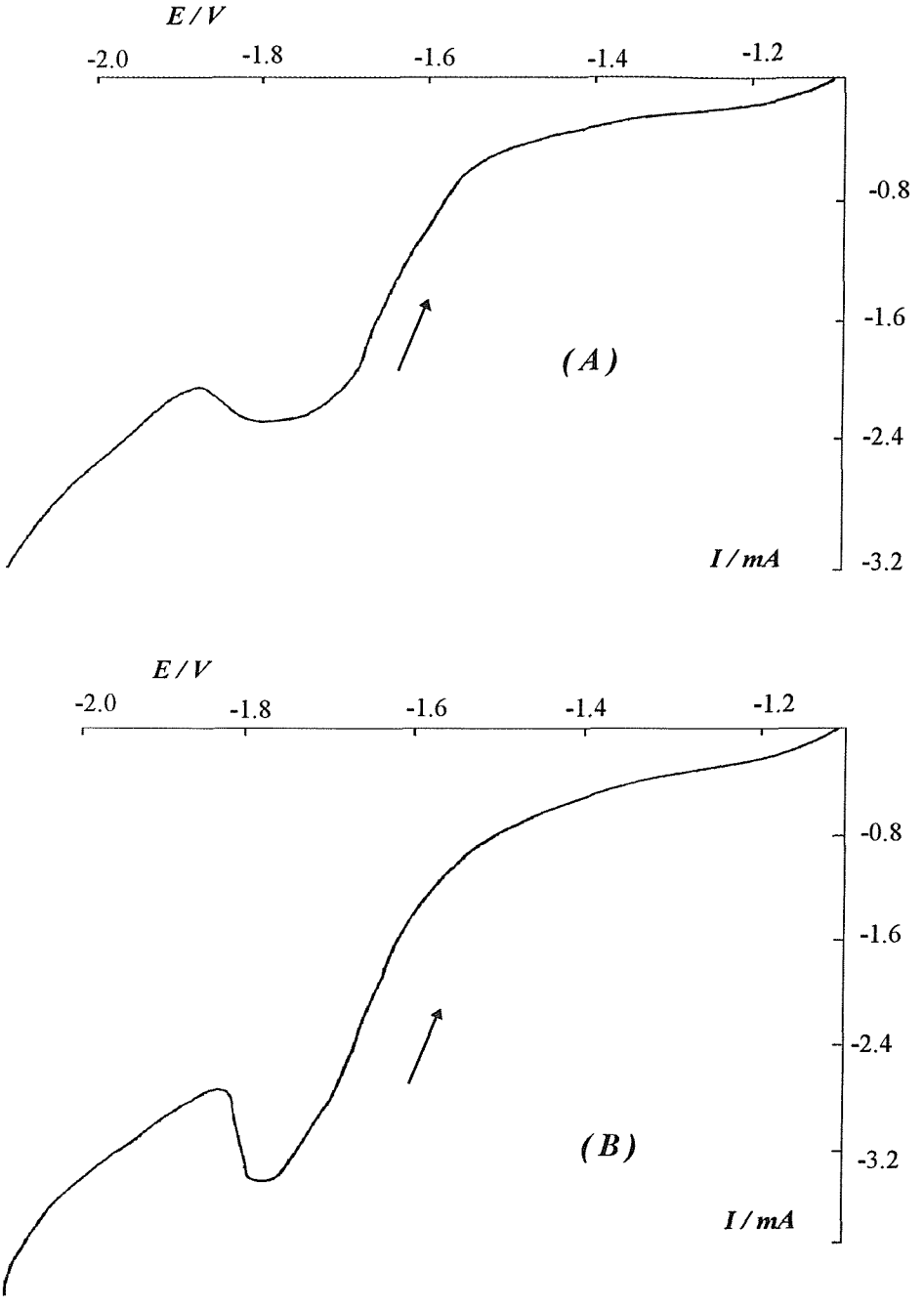

Figure 3.2 *- Voltammograms for electroplating bath at a polished brass RDE (d = 3 mm). Rotation rate (A) 400 rpm and (B) 3600 rpm. Potential scan rate: 20 mV s^{-1}. Temperature:333 K*

Further evidence in support of this conclusion results from voltammetry at temperatures below 333 K. The currents observed are strongly dependent on temperature and, indeed, no significant waves or peaks were observed at 298 K- see Section 3.5.

3.1.2 Steady State / Sweep Experiments

A series of experiments were carried out, each using a fresh brass strip electrode. The potential of the brass strip electrode was held constant at a value in the range - 1500 mV to - 2200 mV vs SCE until the current reached a constant value (typically 50 - 500 s) and then the potential was scanned in a positive direction. Figure 3.3 shows a typical voltammogram, in fact that recorded after the potential had been held at - 2200 mV for 60 s.

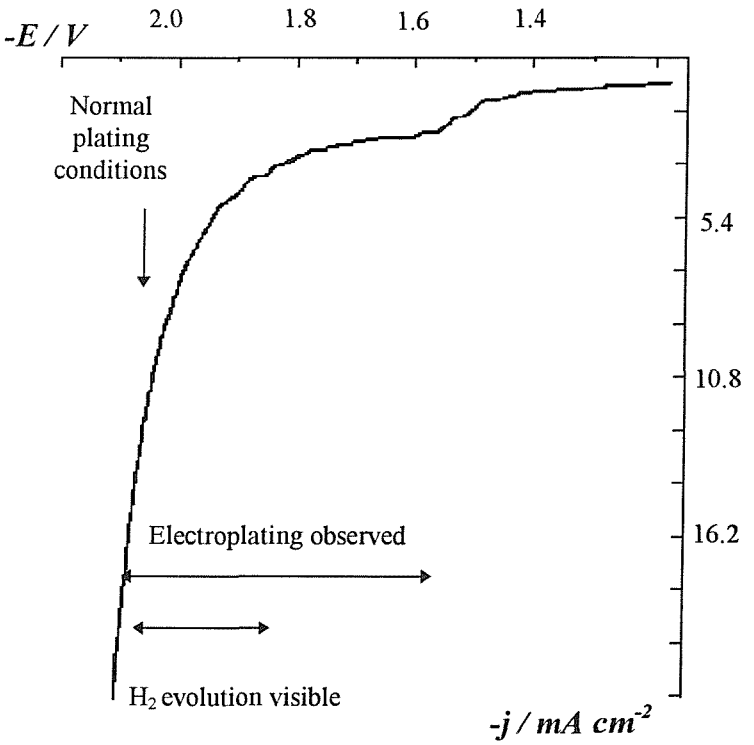

Figure 3.3- Steady state voltammogram recorded for the plating bath at a fresh brass strip electrode after it had been held at -2.2 V vs. SCE for 60s. Potential scan rate: 20 mV s^{-1}. Temperature: 333 K

The voltammogram again shows a reduction wave at - 1650 mV with a limiting current density of ~ 2 mA cm^{-2}. Negative to - 1800 mV the cathodic current rises steeply. Observation of gas evolution and alloy deposition allows the source of these currents to be identified, see table 3.1:

Potential/ mV vs SCE	**Current density/ mA cm^{-2}**	**Alloy Deposition**	**H_2 Evolution**
- 1400	- 0.4	none observed after 600 s	none visible
- 1500	- 0.8	none observed after 600 s	none visible
- 1600	- 1.4	tarnished with bronze tinge	transient
- 1700	- 2.3	highly reflecting	slight
- 1800	- 2.6	highly reflecting	slight
- 1900	- 3.5	highly reflecting	slight
- 2000	-5.5	highly reflecting	vigorous
- 2100	-7.0	highly reflecting	vigorous
-2200	- 20	highly reflecting	vigorous

Table 3.1 *Steady state currents and visual observation during potentiostatic experiments.*

(i) Alloy was deposited at all potentials negative to - 1500 mV vs SCE. The deposits showed strong adhesion and appeared both reflecting and uniform. Hence, the reduction wave is associated with metal deposition although the limiting current is low compared to the commercial plating current density of 6 mA cm^{-2}.

(ii) At the bath pH of 13.2, the equilibrium potential for H_2 evolution is ~ 1032 mV vs SCE and hence H_2 evolution is thermodynamically favourable over all the potential range studied. In practice, hydrogen evolution was always visible at potential negative to - 1800 mV and appears to be the major reaction leading to the increase in current in this

potential range. It will be emphasised later that transient H_2 evolution was observed early in depositions, especially around - 1600 mV.

3.1.3 Chronopotentiometry

The current density often used in commercial plating, 6 mA cm^{-2}, corresponds to a potential of - 2050 mV vs SCE. This was also confirmed by chronopotentiometry, see figure 3.4 When a current density of 6 mA cm^{-2} is applied, the potential changes rapidly from the open circuit value to - 1760 mV but within 2 s, reaches a steady state value of -2050 mV vs SCE. The figure also shows the responses at other current densities; the results are entirely consistent with the voltammetry. With current densities in the range 4 - 10 mA cm^{-2}, the E/t curves all show evidence for an electrode reaction around - 1700 mV before the potential moves to a steady state value in the H_2 evolution region.

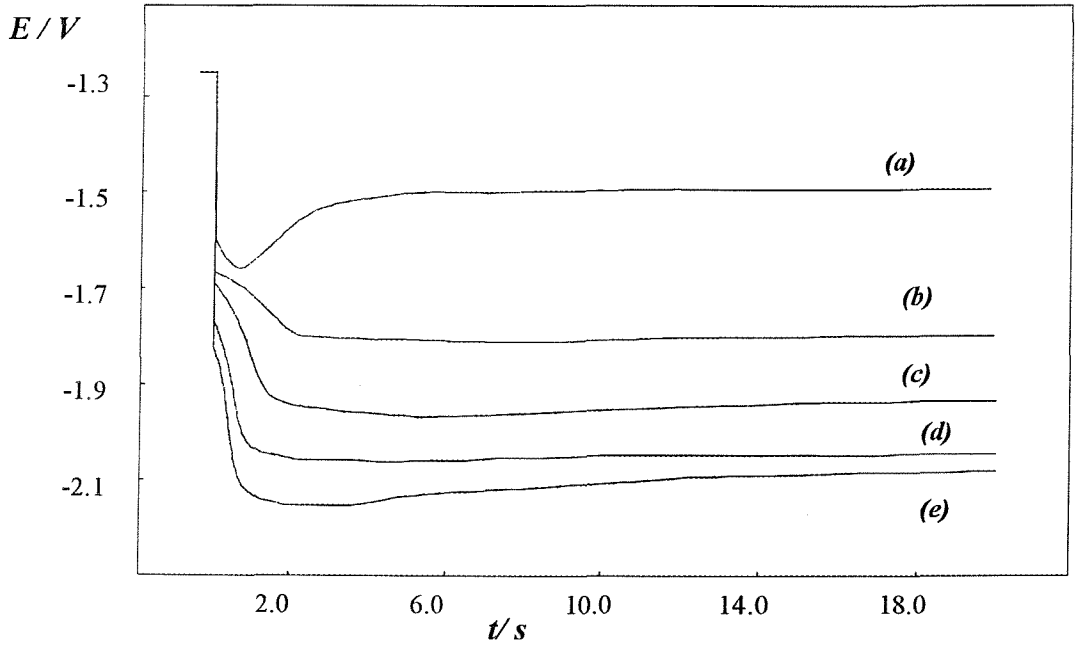

Figure 3.4: *Chronopotentiometry for a fresh brass strip electrode in the electroplating bath. Current densities:(a) 2mA cm^{-2}, (b) 3mA cm^{-2}, (c) 4mA cm^{-2}, (d) 6mA cm^{-2}, (e) 10mA cm^{-2}. Temperature: 333 K*

The response at 2 mA cm^{-2} is different. The steady state potential is - 1550 mV and the steady state is reached via an excursion to more negative potentials. This is typical of an electrode reaction where phase formation is occurring and the rate of nucleation of the new phase on the electrode surface influences the response. At higher current densities nucleation becomes too fast to see this excursion.

3.1.4 Chronamperometry

The nucleation and early growth of a metal layer is better studied by potential step experiments and figure 3.5 reports I/t transients for a series of potential steps from - 1250 mV to values in the range - 1320 mV to - 1400 mV. It can be seen that at these potentials well positive to the wave in the steady state voltammogram, alloy deposition is occurring, all be it at a very low rate.

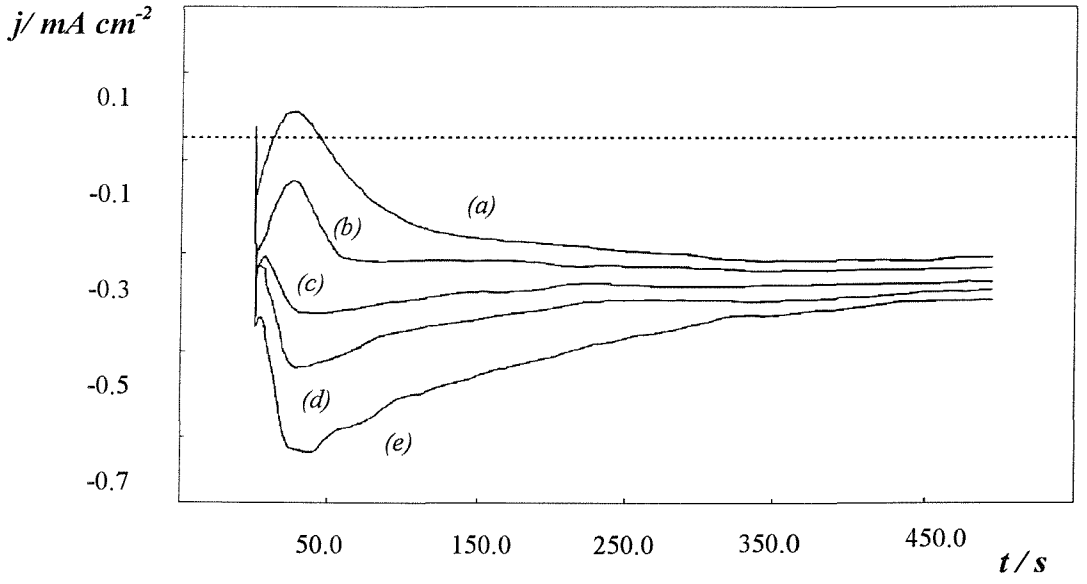

Figure 3.5 *Current time transients in response to potential step experiments from -1250 mV to: (a) -1.32 V, (b)-1.34 V, (c) -1.36 V, (d) -1.38 V, (e)- -1.4 V. Fresh brass strip electrodes in the electroplating bath at 333 K*

At each potential, an early fall in current is followed by a rising cathodic current over a time scale of 50 - 150 s and eventually a steady state current is reached.

As the potential is made more negative, the time scale for the rise in current becomes shorter and there is a trend for the transient to pass through a maximum before decaying towards an increasing steady state current. If the potential is stepped to - 1700 mV, only a falling I/t transient is observed and the steady state current is ~ 2.2 mA cm^{-2}, close to that observed by steady state voltammetry. The early parts of the rising portions of the transients could be fitted to linear $I^{1/3}$ vs t plots as expected for continuous nucleation and three dimensional growth of centres under electron transfer control. At long times the currents become kinetically controlled.

Certainly, the overall picture is consistent with a mechanism for alloy deposition where nucleation of the Cu-Zn-Sn alloy phase on the brass surface is followed by three dimensional growth of the nuclei and overlap of the centres into a continuous layer. This layer then thickens under partial mass transfer and partial kinetic control. The influence of nucleation is, however, only evident at low overpotentials and it is clear that in the conditions of commercial plating, nucleation is very rapid.

3.1.5 Scanning Electron Microscopy

A large number of scanning electron micrographs were obtained during this programme. Many samples were prepared in the laboratory and others were taken from the commercial plating lines (both jig and barrel plating). Energy dispersive spectroscopy (EDS) - figure 3.6 -was used for routine elemental analysis of the plated layers. In order to ensure that the determination of the elemental composition was not influenced by penetration of the electron beam into the brass substrate, it was found essential either to use deposits which were relatively thick or to undercoat the samples with a silver strike (as is also common in commercial practice). Also, the EDS system is calibrated routinely using standard samples.

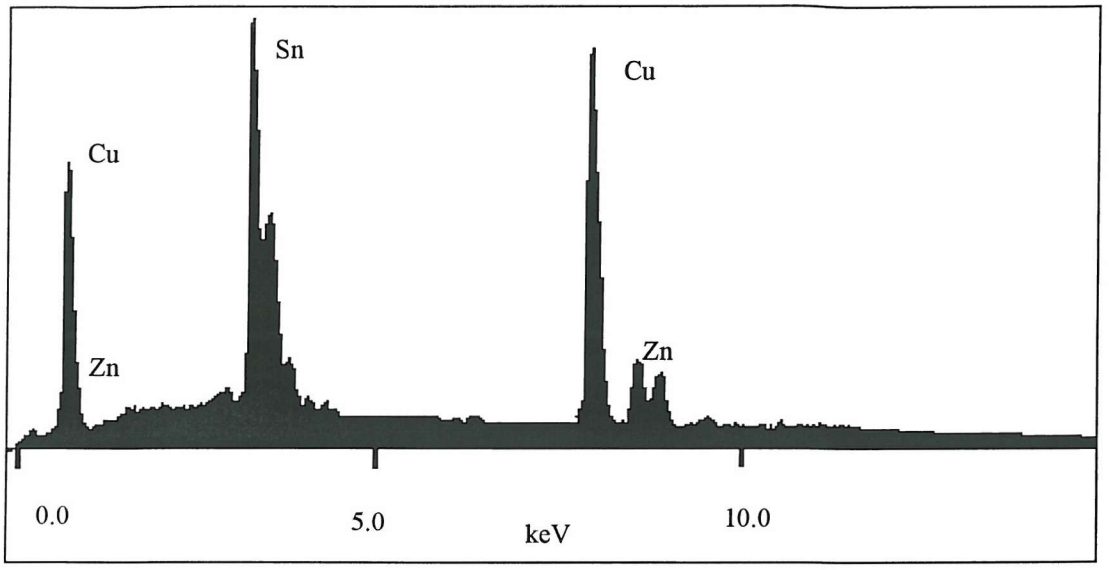

Figure 3.6 *- the EDS of a Hull Cell sample at the position of 6 mA cm^{-2} plated from a standard solution for 5 min.*

For example, in a common Hull cell test where plating was carried out at 1 A for 120 s, the deposit at the position for 6 mA cm^{-2} appeared good but was not thick enough to obtain reliable compositional data by EDS; the % Cu and % Zn were always high due to the electron beam entering the brass substrate.

Figure 3.7 is an SEM of a sample cut from a Hull cell brass plate. It can be seen that the surface is covered by an array of scratches resulting from the polishing procedure.

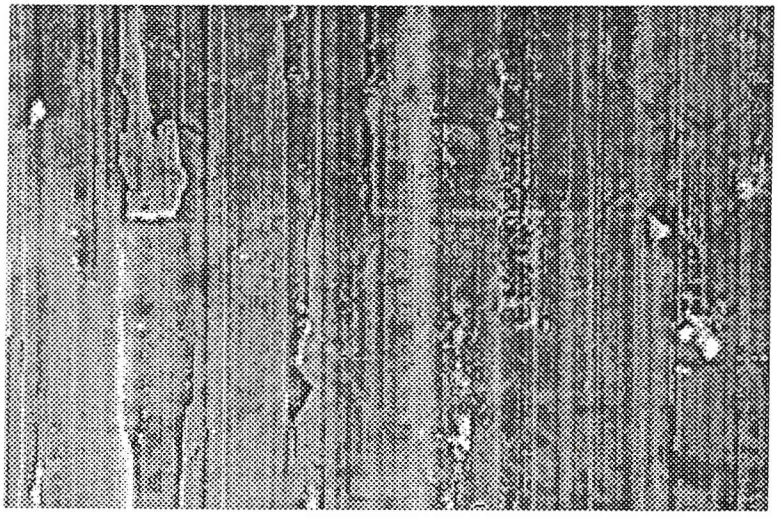

Figure 3.7 *- SEM of a brass substrate*

Figure 3.8 shows an SEM of a brass strip electrode which has been plated at a constant potential of - 2050 mV and it can be seen that the surface of the plate is almost featureless although there are a few lines which may result from the scratches on the brass.

A very similar, featureless surface was obtained by plating at 6 mA cm^{-2} whether on a strip electrode, a Hull cell plate or, indeed, on commercial samples. Also undercoating with a silver strike, did not change the surface after alloy plating.

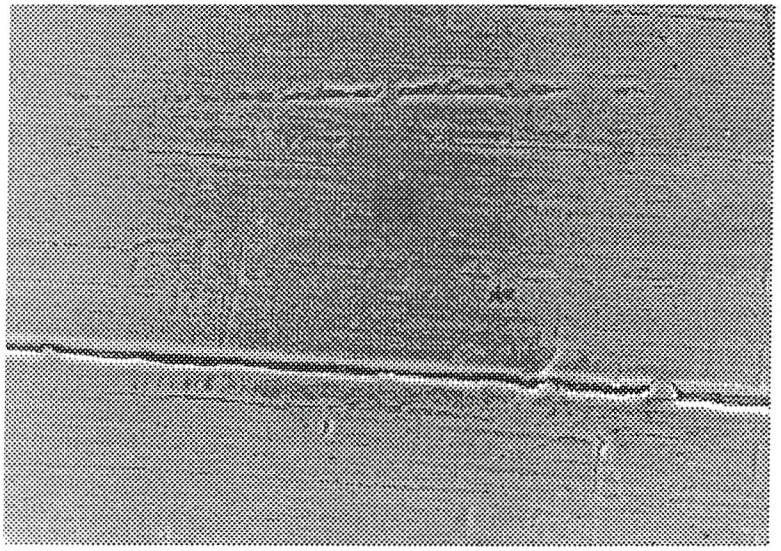

scale ⟷ 1 μm

Figure 3.8- *SEM of the surface after the deposition of Cu-Zn-Sn alloy at -2050 mV for 120 s. T = 333 K*

The elemental composition for a number of samples plated in different conditions in the laboratory as well as a sample from the commercial line are reported in table 3.2.

Electroplating conditions	**Elemental composition %**		
	Cu	**Zn**	**Sn**
Brass substrate	68	32	
Ag plated brass strip, I = 6 mA cm^{-2}	50	9	41
Ag plated brass strip, E = - 2050 mV	50	9	41
Hull cell, Ag plated plate at position for j = 6 mA cm^{-2}	51	8	41
Hull cell brass plate, thick alloy deposit♣ at position for I = 6 mA cm^{-2}	54	8	36
Typical plating line electroplate	48	8	43

Table 3.2 *Composition of substrate and alloy deposits determined by EDS analysis. Laboratory depositions using a total charge of ~ 1 C cm^{-2} except ♣ = ~ 10 C cm^{-2}.*

With the exception of the thick deposit, the elemental compositions are very similar and this was confirmed with many other samples. It was concluded that the composition of highly reflecting and fault free deposits lay in the ranges:

Cu	47 - 51 %
Zn	8 - 12 %
Sn	38 - 43 %

This alloy composition is quite different from the molar ratio of the metal ions in solution (Cu:Zn:Sn = 60:28:12). This is not possible if the deposition is mass transport controlled and clearly the kinetics of tin deposition must be favourable compared particularly to zinc. The Hull cell is generally used for quality control of this alloy plating bath. It has been found that a particular appearance of the whole plate after deposition of alloy at 1 A for 120 s correlates well with a healthy bath with an acceptable composition. The test leads to a plate where most of the surface appears uniformly coated with highly reflecting alloy but at the high current density side there is an area which is darker and striped in appearance (known as "tiger stripe") figure 3.9 a.

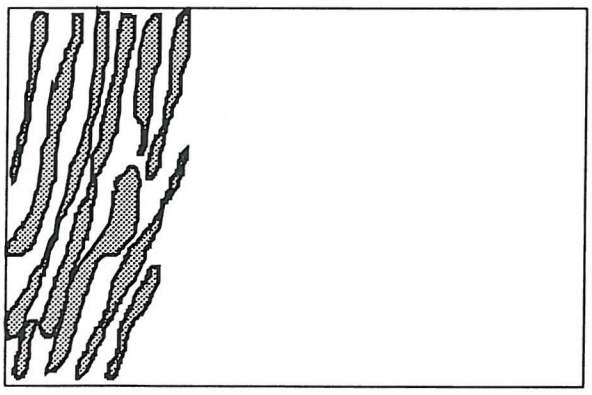

***Figure 3.9 a** - A plated Hull Cell panel showing "tiger striped" deposit at the high current density side*

Figure 3.9 b illustrates an SEM of a tiger stripe on a Hull cell plate and it can be seen that the deposit is now made up of many overlapping small hemispherical centers.

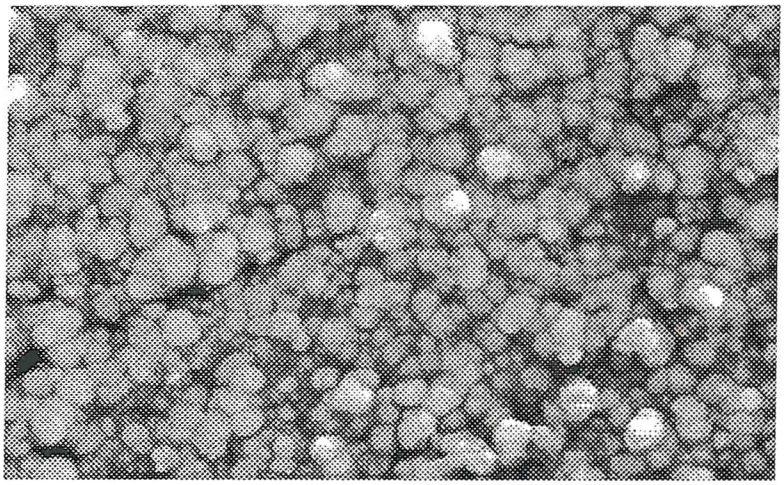

Figure 3.9 *b of the Cu-Zn-Sn alloy deposit from a Hull cell at the position for a current density of 40 mA* cm^{-2} *. Deposition time 120s. T = 333 K*

scale ⟷ 1 μm

Table 3.3 reports the compositions for deposits on different areas of a silver undercoated Hull cell plate.

Hull cell plate

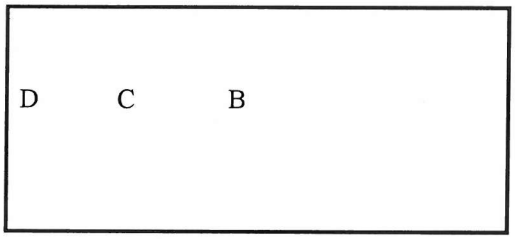

Sample	*j* / mA cm^{-2}	Cu/ %	Zn/ %	Sn/%
B	6	50	10	40
C	13	53	10	37
D	45	57	12	31

Table 3.3 *EDS analysis of a sample from Hull cell deposit on a Ag coated brass plate.*

It can be seen that with increasing current density, the % Cu increases at the expense of tin in the electroplate and the deposit darkening can be associated with high copper.

In a further series of experiments, deposition was carried out onto silver undercoated strip electrodes at a series of potentials. The compositions are shown in table 3.4.

Potential/ mV	Current density/ mA cm^{-2}	Deposit appearance	Elemental Composition/% Cu	Zn	Sn
- 1500	1.0	reflective, red			
-1550		reflective, red	66	2	31
- 1600	2.3	white, reflective	58	6	36
- 1700	2.3	white, reflective	53	9	41
- 1900	3.6	white, reflective	47	8	45
- 2050	6	white, reflective	51	8	41

Table 3.4 - the change in alloy metal ratio with deposition potential. Total charge passed: 800 mC

Data in table 3.4 shows that at all potentials studied a shiny, reflective alloy was deposited. At more positive potentials, the alloy has an increased content in copper and it is low in tin, thus explaining its red color. Also, there is an agreement between these experiments and the ones performed in the steady state -section 3.1.2. A plot of E vs. I resembles the steady state voltammogram - figure 3.3 .

3.1.6 Conclusion

- It is shown that a Cu-Zn-Sn alloy layer may be plated onto brass or brass with a Ag strike under a range of controlled current or controlled potential conditions; it has a composition within a defined range as well as maintaining a uniform and highly reflecting appearance. In the conditions typical of commercial electrodeposition, hydrogen evolution accompanies the metal ion reduction reactions and this will enhance local mass transport and may also improve the throwing power of the bath. Certainly, the electron micrographs are essentially featureless. At very high current density, the deposit is rich in copper and low in tin and this leads to a darker striped deposit; electron microscopy shows that such deposits are made up of overlapping hemispheres with sub-micron radii.

- In steady state voltammetry, a single reduction wave at - 1650 mV may be identified with the electrode reactions leading to alloy deposition. It was never possible to identify separate waves/peaks for the reduction of Cu(I), Zn(II) and Sn(IV) species. The height of this wave and its dependence on rotation rate would indicate that the limiting current is partially controlled by mass transfer. On the other hand, the strong variation of the current density with the temperature and the composition of the alloy (ie. quite different from the solution composition) clearly indicate rate control by homogeneous chemical reactions prior to electron transfer. It is likely that the speciation of the metal ions must change before reduction is possible. The mixed control for metal ion reduction will also determine the alloy deposition rate at the more negative potential consistent with commercial conditions.
- Non-steady state experiments allow the investigation of the nucleation and early growth of the alloy phase on the cathode surface but nucleation is clearly a very rapid process in commercial conditions. They also disclose that the ratio of hydrogen evolution/metal deposition can change with time and the voltammograms contain peaks which would be consistent with a processes involving the Copper Glo additive and hydrogen atoms.

3.2 The effect of free cyanide on alloy deposition

The concentration of cyanide ion is one of the most important parameters in the alkaline cyanide electroplating bath. Substantial published data [21-31,34-36,39-43] indicates that cyanide ion acts as a complexant for both copper and zinc metal ions. As a result, it has a great influence on the thermodynamics and the kinetics of the Cu-Zn-Sn deposition reaction. Therefore, a closer investigation of the effect the free cyanide concentration on the deposition of a Cu-Zn-Sn alloy has been carried out by the means of a number of voltammetric techniques and electron microscopy. The experiments carried out in this section employed freshly prepared solutions of the plating bath in which the concentration of the free cyanide was deliberately increased/decreased and the effect on alloy deposition was studied. The composition of the solutions were:

		$g\ l^{-1}$			mM	
CuCN		9.1			102	
$Zn(CN)_2$		5.4			46	
$Na_2[Sn(OH)_6]$		5.7			24	
Na_2CO_3		6.5			61	
free NaOH		2.1			50	
free NaCN	48	25.0	or 19	1057	551	or 418
Copper Glo solution		5.0				

The solution was thermostated at a 333K and, as on the plating line, was not deoxygenated. The electrodes for electrodeposition were usually fresh brass strips although in a few experiments a silver undercoat had been applied.

3.2.1 Cyclic voltammetry

The electrochemistry of alkaline cyanide plating baths with different concentrations in free cyanide have been studied. Cyclic voltammograms were recorded at disposable brass strip electrodes (A = 1 cm^2) at 333 K. The potential was scanned from -1260mV to -2000 mV vs. SCE at a scan rate of 20 mV s^{-1}.

Figures 3.10 a,b,c show the first scan recorded at brass strip electrodes from solutions with different concentrations in free cyanide: 48 g l^{-1}, 25 g l^{-1} and 19 g l^{-1}. The forward scan has one main feature consisting of a reduction feature at approximately -1650 mV vs. SCE. As seen in figure 3.10 b, a solution containing standard cyanide concentration (25g l^{-1}) gives a sharp reduction peak of j_P = 5.2 mA cm^{-2} which represents a large fraction of the commercial plating current density. When the cyanide concentration is high (48 g l^{-1}) a larger reduction peak of j_P = 10 mA cm^{-2} was recorded (figure 3.10 a). In both situations the peaks have symmetrical shapes with a sharp fall in the current beyond E_P = -1650 mV. Also, H_2 evolution is observed around this potential and it seems to decrease negative to the peak before recommencing towards the negative limit.

In contrast, for a solution low in cyanide (19.5 g l^{-1}), figure 3.10 c, a drawn out reduction wave with j_L = -4.5 mA cm^{-2} was recorded at $E_{1/2}$ = -1650 mV vs SCE. The reduction process in all three solutions continues on the back scan but it is irreversible as there is no anodic current negative to -1250 mV. However, the reduction peak recorded on the reverse scan for a solution with a high concentration of cyanide shows the complex behaviour of the system. With all three solutions a metal deposit on the brass substrate was clearly visible after a single scan. With 25 and 48 g l^{-1} cyanide this deposit was bright, silvery and highly reflecting. With the low cyanide it was markedly yellow in appearance.

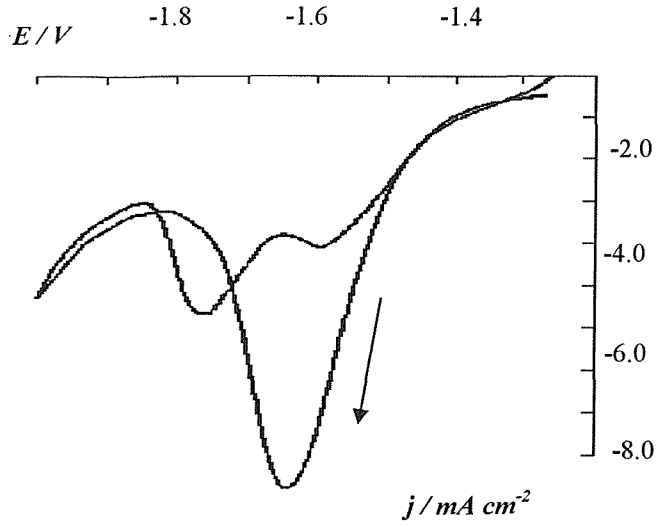

Figure 3.10 a *- Cyclic voltammogram of a electrolplating bath high in cyanide performed at a brass electrode.*
T = 333K, scan rate: 20 mV s^{-1}

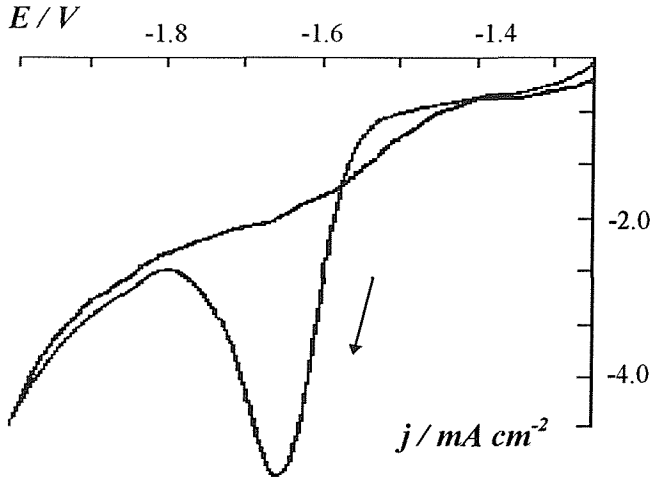

Figure 3.10 b *- Cyclic voltammogram of a standard electrolplating bath high in cyanide performed at a brass electrode.*
T = 333K, scan rate: 20 mV s^{-1}

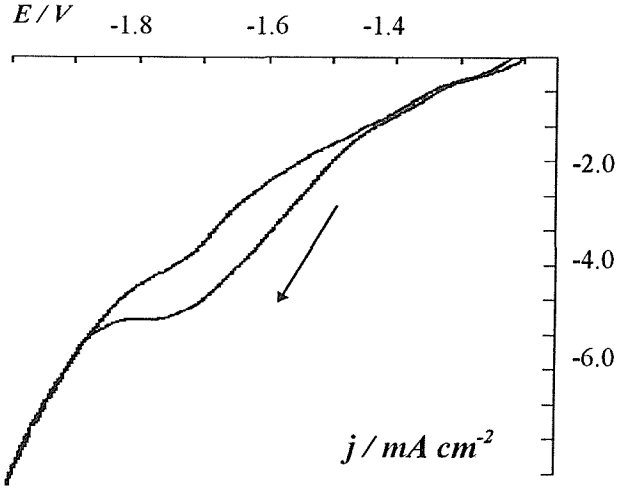

Figure 3.10.c *- Cyclic voltammogram of a electrolplating bath low in cyanide performed at a brass electrode.*
T = 333K, scan rate: 20 mV s^{-1}

Figures 3.11 a,b,c, show the current/potential response after four continuous potential cycles. Again, reduction features are seen, although with some differences compared to those on the first scan. For instance, voltammograms recorded from standard solutions or solutions high in cyanide show a much larger cathodic charge passed during the 4th cycle. Also, the peaks are much broader than those recorded on the first scans as a result of additional features. For example, a solution high in cyanide shows a reduction wave of about 4 mA cm^{-2} at $E_{1/2}$ = -1500 mV, then a small additional peak at -1750 mV. A standard solution, shows a shift in the reduction potential to more positive values as discussed in the previous section. In contrast, no change in voltammetry is seen for solutions low in cyanide. Therefore, with this solution the changes in the surface of the metal do not seem to produce any difference in the potential/current response- figure 3.11.c

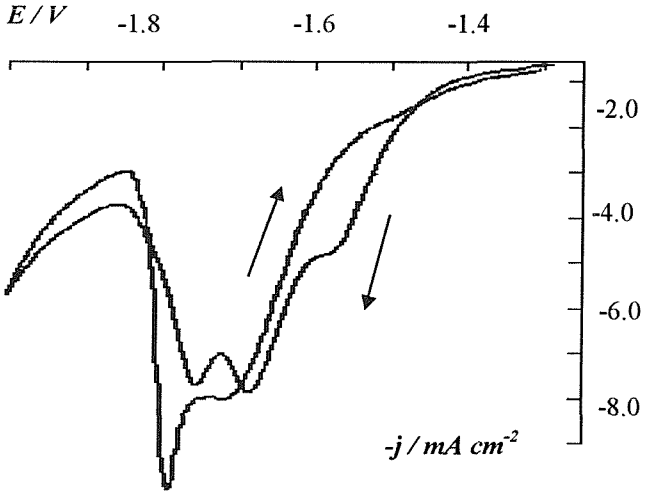

Fig 3.11 a *Voltammogram after four continuous cycles performed in a plating bath high in cyanide. Working electrode: brass, reference electrode SCE, scan rate = 20mV s^{-1} T = 333 K*

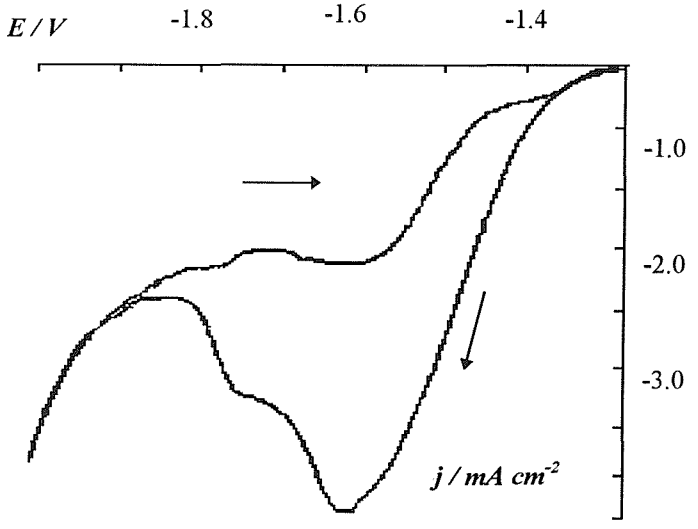

Fig 3.11 b *Voltammogram after four continuous cycles performed in a standard plating bath. Working electrode: brass, reference electrode SCE, scan rate = 20mV s^{-1} T = 333 K*

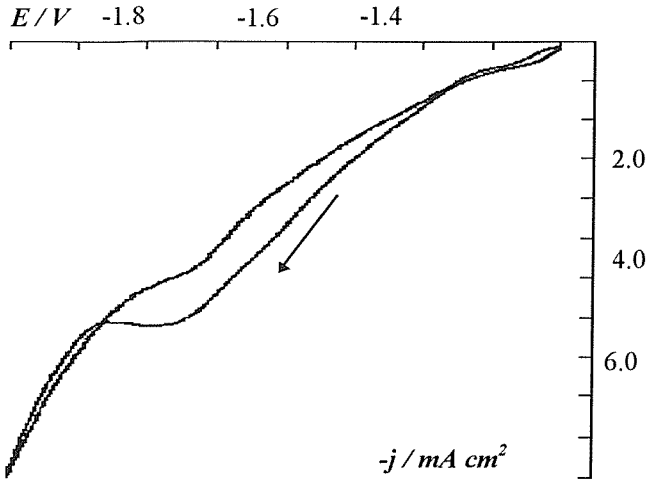

Fig 3.11 c *Voltammogram after four continuous cycles performed in a plating bath low in cyanide. Working electrode: brass, reference electrode SCE, scan rate = 20mV s^{-1} T = 333 KK*

If after the fourth scan, the solutions are agitated, no change in voltammetry is observed. Hence, the changes between the first and fourth scan cannot be attributed to changes in the solution composition in the diffusion layer and therefore must result from the difference in the surface properties of brass and the Cu-Zn-Sn alloy.

The cyanide ion appears to be implicated in the origin of the cathodic peaks and the decreases in current in the potential range - 1750 mV to -1950 mV.

3.2.2 Steady state / sweep experiments

A series of experiments have been carried out, at fresh brass strip electrodes. The potential of the brass electrode was first held constant at a value in the range -1600 mV to -2000 mV vs. SCE until a steady state current was reached then the potential was scanned in a positive direction.

Figures 3 12 a,b,c show 3 typical voltammograms for solutions standard, high and low in cyanide recorded after the potential had been held at -2000 mV for 60 s. All voltammograms have one main feature consisting of a reduction wave/peak in the region of $E_{1/2}$ = -1550 mV vs. SCE. Also, negative to -1800 mV there is a strong variation in the reduction current.

Hydrogen evolution was observed negative to -1800 mV, and certainly it contributes to the current toward the more negative limit.

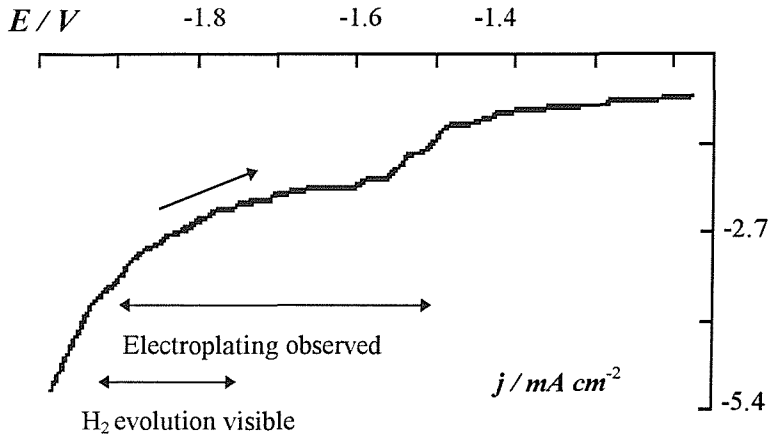

Figure 3.12 a *-The current / potential response from a linear potential scan after the potential had been held at -2.0 V vs. SCE in a standard solution for 60 s*

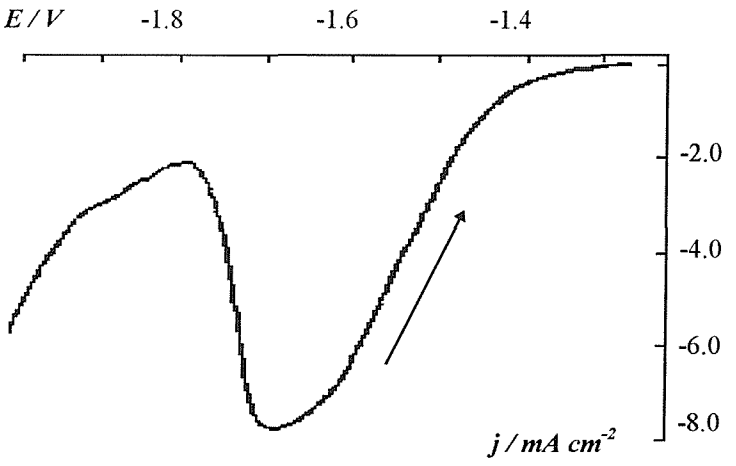

Figure 3.12 b *-The current / potential response from a linear potential scan after the potential had been held at -2.0 V vs. SCE in a solution high in cyanide for 60 s*

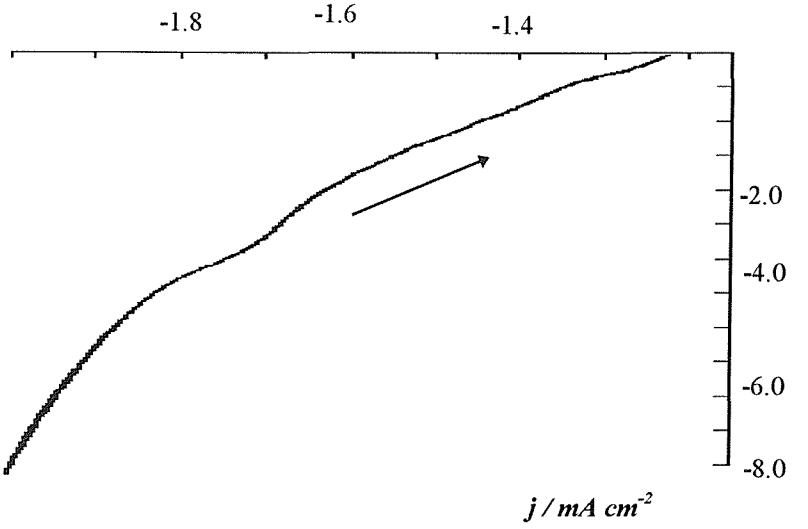

Figure 3.12 c *-The current / potential response from a linear potential scan after the potential had been held at -2.0 V vs. SCE in a solution low in cyanide for 60 s*

However, significant differences between the voltammograms can be noted. For instance, a large reduction peak of 8 mA cm^{-2} is recorded at Ep = -1600 mV for a solution high in cyanide - figure 3.12 b. This peak appears to be associated with hydrogen evolution as gas bubbles can clearly be observed around this potential. On the contrary, a drawn out reduction wave of 3.5 mA cm^{-2} is recorded for a solution low in cyanide (19g l^{-1}), figure 3.2.2.1 c, and a well formed reduction wave is recorded for a standard solution. It should be noted also, that there is a resemblance between these voltammograms and the back scans on the cyclic voltammetry (figure 3.11 a,b,c).

Table 3.5 shows the steady state j/E data and for all three systems.

$E_{dep.}$ / mV	$j_{s.s.}$ / mA cm^{-2} 19 g l^{-1} CN	$j_{s.s.}$ / mA cm^{-2} 25 g l^{-1} CN	$j_{s.s.}$ / mA cm^{-2} 48 g l^{-1} CN
-2000	8.0	5.5	6.0
-1800	4.0	2.6	2.0
-1700	-	2.3	7.0
-1600	2.5	1.4	2.7
-1500	1.0	0.8	2.0

Table 3.5 *The variation of steady state current with cyanide concentration during potentiostatic experiments*

Data in table 3.5 shows that at more negative potentials, the currents are higher in the low cyanide solutions and the deposits from this solution are tarnished and copper colored. Even the steady state I-E response for the high cyanide solutions is peaked around - 1700 mV and copious hydrogen evolution was apparent in these conditions. The deposits from high cyanide solutions were milky, and non reflecting.

3.2.3 Chronoamperometry

Experiments in which the nucleation and growth of metal layer were studied have been carried out from solutions containing high, low or standard cyanide concentration. In these experiments I/t transients were recorded at brass electrodes in a series of potential steps from - 1250 mV to values in the range of -1320 mV to -1400 mV. There are some similarities between the transients obtained from solution standard (figure 3.5) and high in cyanide (figure 3.13). An initial decrease in the current is firstly recorded followed by an increase until a steady state current is reached. Also, for both systems, there is a decreasing timescale for the rise in the current as the potential is made more negative. This is attributed to a faster nucleation.

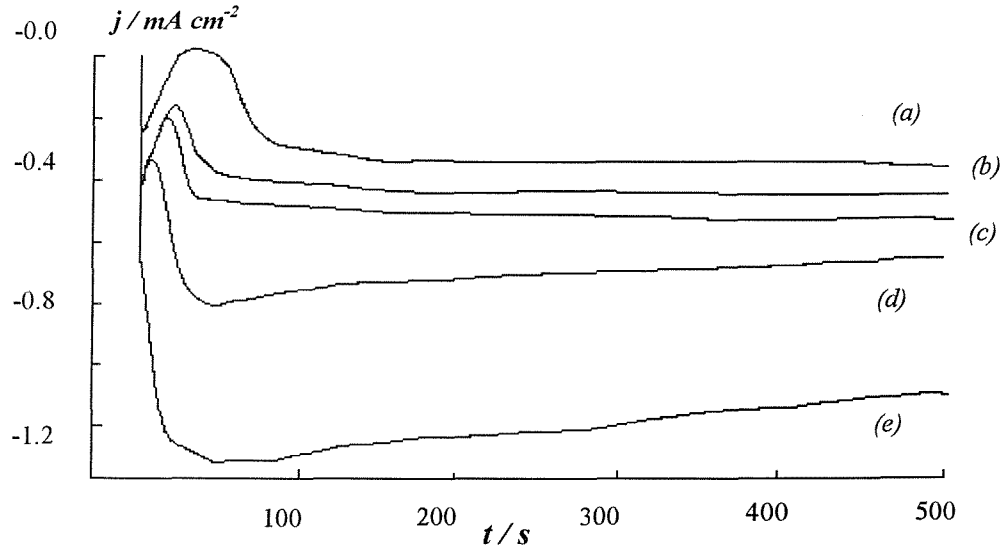

Figure 3.13 *- Chronoamperometric experiments of a solution high in free cyanide at brass electrodes. (a): -1320 mV, (b): -1340 mV, (c): -1360mV, (d): -1380mV, (e): -1400mV. T = 333 K*

Probably, the overall picture is consistent with a mechanism in which the nucleation of Cu-Zn-Sn alloy phase on the brass surface is followed by three dimensional growth of the nuclei

and overlap of the centers into a layer which thickens under partial mass transfer and partial kinetic control by the rate of a homogenous reaction. This is however evident only at low potentials, as in the plating line conditions (much more negative potentials) nucleation occurs at a very rapid pace. No deposits were observed by eye on the timescale used for these transient experiments. In contrast, different behaviour is seen for systems low in cyanide (figure 3.14).

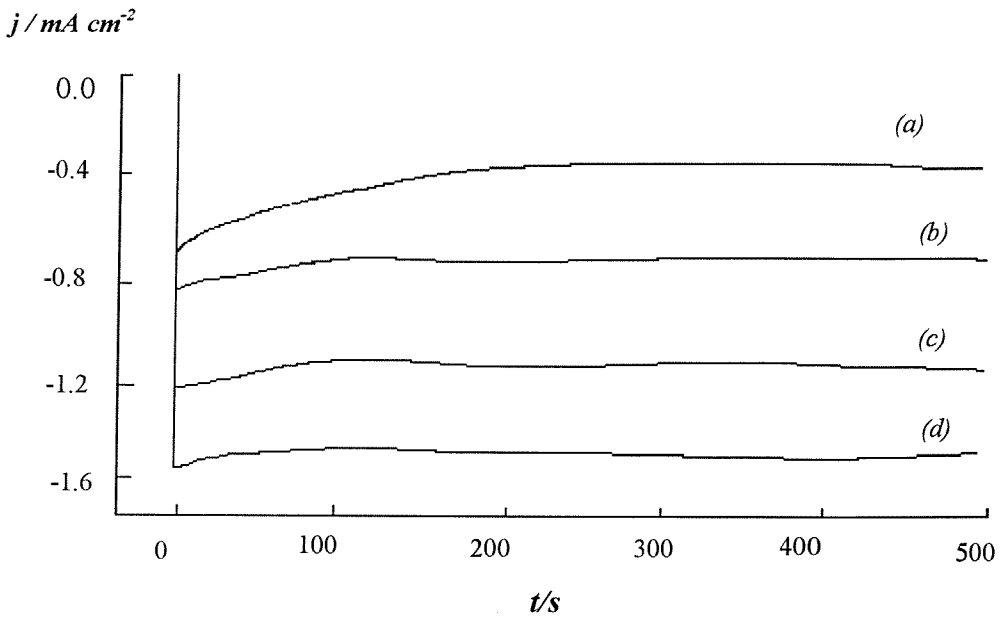

Figure 3.14 *- Chronoamperometric experiments of a solution low in free cyanide at brass electrodes. (a): -1320 mV, (b): -1350 mV, (c): -1380mV, (d): -1400mV. T = 333 K*

Firstly, there is an instant increase in current is recorded followed by a slow, slight decrease until a steady state current is reached. The short time scale of the increase in the current could be explained by immediate nucleation mechanism followed right away by rapid growth of a continuous alloy layer. The current densities reached in this system are almost double in size compared to the ones achieved in solutions rich in free cyanide. This explains why reflective, uniform deposits were obtained even at very low applied potentials: *e.g.* -1350 mV. It should be mentioned, however, that with such solution, the alloys had a copper appearance.

In all solutions, when the potential is stepped to a more negative value - *e.g.* -2000 mV, only falling I/t transients are observed.

3.2.4 SEM

Brass Hull cell panels have been plated from solutions containing different concentrations of cyanide. In order to ensure a fairly accurate determination of the elemental composition which is not influenced by the penetration of the electron beam into the brass substrate, a thick layer of alloy was plated. Different alloys were obtained in the three different solutions studied. A deposit with a milky appearance was obtained in a system high in cyanide. This appearance suggests high tin in the deposit. Figure 3.15 shows an SEM Hull cell panel plated from such solution at the position of 6 mA cm^{-2} .

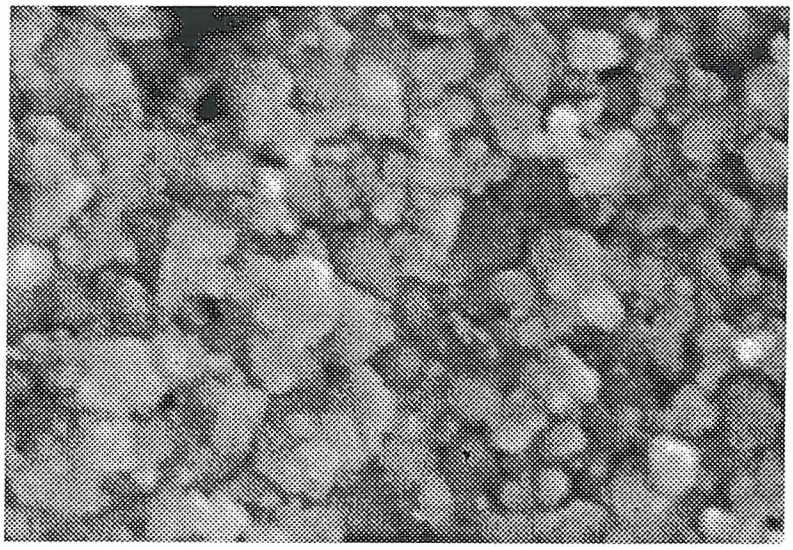

Figure 3.15 *- SEM of a Hull Cell sample high in cyanide at the position of 6 mA* cm^{-2}

scale:⟵⟶ 1 μm

It can be seen that the surface is covered by a well structured deposit composed of clusters of angular spheres of about 0.5μm diameter.

When analysed, the sample was found to have the metal ratio Cu-Zn-Sn of 27-5-68. This is not surprising, since copper and zinc ions are complexed by cyanide ions. As a result, a high concentration in cyanide ions makes it more difficult for the copper and zinc to deposit and the alloy has a high tin content.

It should be mentioned that other Hull cell samples plated from solutions high in cyanide - *e.g.* 31.1 g l^{-1} - showed the same rough structure and the same trend in the metal ratio.

In contrast, samples plated from low cyanide systems had a copper appearance. Figure 3.16 shows an SEM of a sample cut form a Hull cell panel at the position of 6 mA cm^{-2} . When analyzed the SEM shows a featureless deposit that follows the substrates polishing lines. However, the micrograph shows a number of pinholes scattered over the whole area. When analyzed, the sample was found to have a high concentration in copper with a composition Cu-Zn-Sn of 67-9-24.

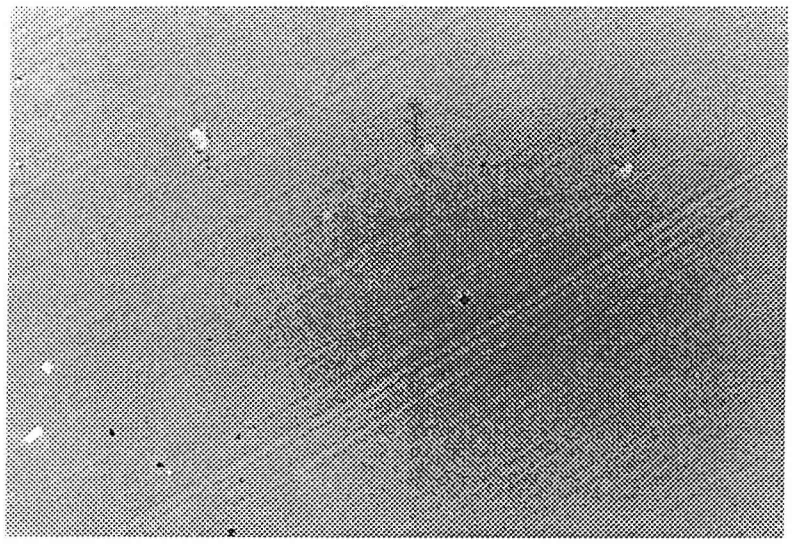

scale: ⟷ 10 μm

Figure 3.16 *- SEM of Hull Cell sample low in cyanide at the position of 6 mA* cm^{-2}

Hence, a low concentration in cyanide ions favors copper deposition at the expense of tin.

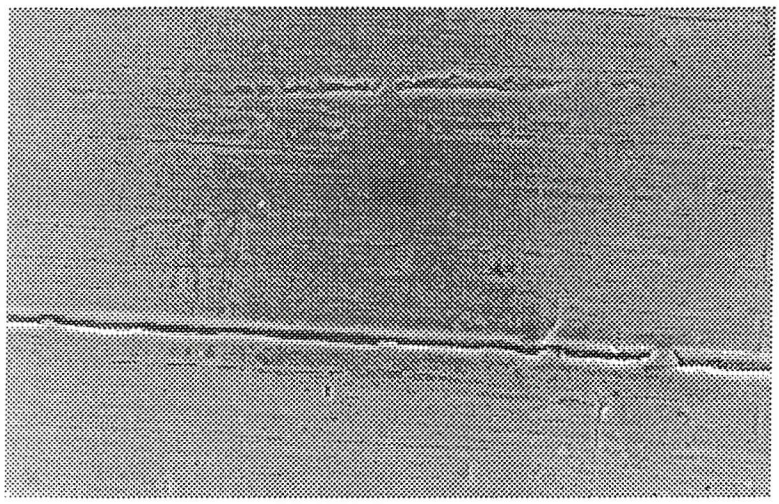

Figure 3.17 *SEM of the alloy deposited at a constant potential of -2050 mV on a brass strip electrode from a standard bath*

scale:⟷ 1 μm

The deposit plated from a standard solution is shown in figure 3.17 and it has been described in Section 3.1.5.

3.2.5 Conclusion

- It was found that the cyanide concentration influences both the alloy composition and the appearance strongly:

[CN] g l^{-1}	Cu %	Zn %	Sn %
19	67	9	24
25	51	8	41
48	27	5	68

Hence,

⇒ a high concentration in cyanide gives a deposit high in Sn - the deposit has a milky, white appearance with low reflectivity

⇒ a low cyanide gives high Cu concentration - this leads to yellow but shiny deposit

- Also, the peak on the cyclic voltammograms are associated with H_2 evolution and more evident when an alloy with a higher Sn content is being deposited.

- There was a strong correlation between the height of the reduction current on the cyclic voltammograms and the cyanide concentration, see table 3.6.

$[CN^-]$ gl^{-1}	I_p / mA cm^{-2}
19.5	4.8
25	5.5
31	7.7
40	8.5
48	10.0

Table 3.6 *- the variation of the reduction current with cyanide concentration*

- The nucleation of the copper rich phase occurs more readily than the standard or tin rich phases - figure 3.18. The transients shown below were obtained by measuring in figures 3.5, 3.13 and 3.14 τ, the growth transient, which is the time from the minimum in current to its peak value.

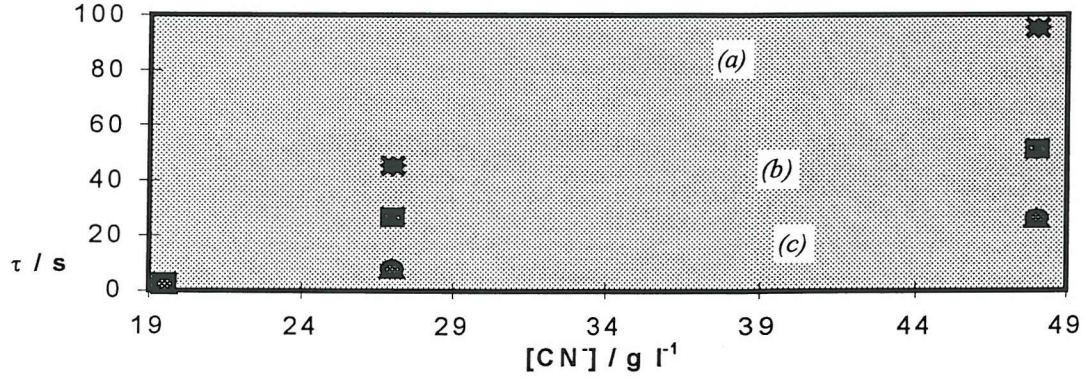

Figure 3.18 *- the effect of [CN⁻] on the growth transient, τ, with the deposition potential. (a): -1320 mV, (b): -1400 mV, (c): -1500 mV*

3.3 The effect of free hydroxide on alloy composition

The free hydroxide concentration(ie. the hydroxide ion not complexed to metal ions) clearly has several roles in the plating bath. It makes a major contribution to the conductivity of the bath. In addition, the hydroxide is essential for safety reasons; the electrolyte has to be maintained at a sufficiently high pH, to avoid the formation of HCN even close to the anode. Probably, its most important role is to control the chemistry of the tin ions in solution, by acting as a complexing agent [20,31-33]. It should be noted that hydroxide can be lost from the bath in several ways: (i) by the absorption of CO_2 from the atmosphere into the open plating bath, especially if the bath is allowed to cool to room temperature at weekends (ii) by hydrolysis of species such as CN^- (iii) by involvement in anode reactions.

Hence, it is important to determine the effect that the free hydroxide concentration has on the alloy composition and its quality as well as to adjust it on a regular basis.

The experiments carried out in this section consisted of a number of voltammetric techniques, scanning electron microscopy and electron dispersive spectroscopy. Also, freshly made solutions of the plating bath were used in which the concentration of the free hydroxide was deliberately increased/decreased and the effect on the alloy deposition was studied. The composition of the solutions were:

		$g\ l^{-1}$			mM	
CuCN		9.1			102	
$Zn(CN)_2$		5.4			46	
$Na_2[Sn(OH)_6]$		5.7			24	
Na_2CO_3		6.5			61	
free NaOH	0.66	2.1	5.4	15.7	50	128.6
free NaCN		25			551	
Copper Glo solution		5.0				

The electrodes employed in this section were mostly disposable brass strips. However, there is some data reported from connectors from the plating line and also from plated Hull cell

brass panels. All the experiments have been performed at 333 K and as on the plating line the solutions were not deoxygenated.

3.3.1 Cyclic voltammetry

The voltammetry of alkaline cyanide plating baths with different concentrations of free hydroxide have been studied. The pH of all three solutions was in the region of 13.2 - 13.6 and the temperature was 333 K. Cyclic voltammograms have been recorded at disposable brass strip electrodes (A = 1 cm^2). The potential was scanned between -1250 mV to -2000 mV vs. SCE at a scan rate of 20 mV s^{-1}. The positive limit of -1250 mV vs. SCE corresponds to a potential where the current is zero, hence no alloy is deposited at this value and no brass corrosion is occurring. Also, the negative limit of -2000 mV was chosen as H_2 evolution was becoming rapid.

Figures 3.19 a,b,c show the first scan recorded at fresh strips of brass electrodes from solutions with different concentrations in free hydroxide: 0.66 g l^{-1}, 2.1 g l^{-1} and 5.4 g l^{-1}. All three voltammograms have a large reduction peak at $E_P \approx$ -1650 mV. Figure 3.19 b shows the behavior of the standard solution. The same response is obtained from a solution high in hydroxide (5.4 g l^{-1}). A current density of 6 mA cm^{-2} is reached before a sharp fall beyond E_P = -1650 mV (figure 3.19 a). This peak in current appears to result from hydrogen which was observed evolving quite vigorously in this region before a decrease negative to the peak, and a slow recommencement towards the negative limit. A much larger cathodic charge is passed in a solution low in hydroxide. This is partially due to an additional feature before the reduction peak (figure 3.19 c) consisting of a well defined reduction wave of I_L = 8 mA cm^{-2} at $E_{1/2}$ = -1450 mV vs. SCE. This current is certainly attributed to metal deposition as a layer of metal covered the electrode when the potential was scanned between -1250 mV to -1500 mV. Again, the change in response is consistent with easier deposition of tin and certainly tin(IV) will be more weakly complexed in the low hydroxide bath.

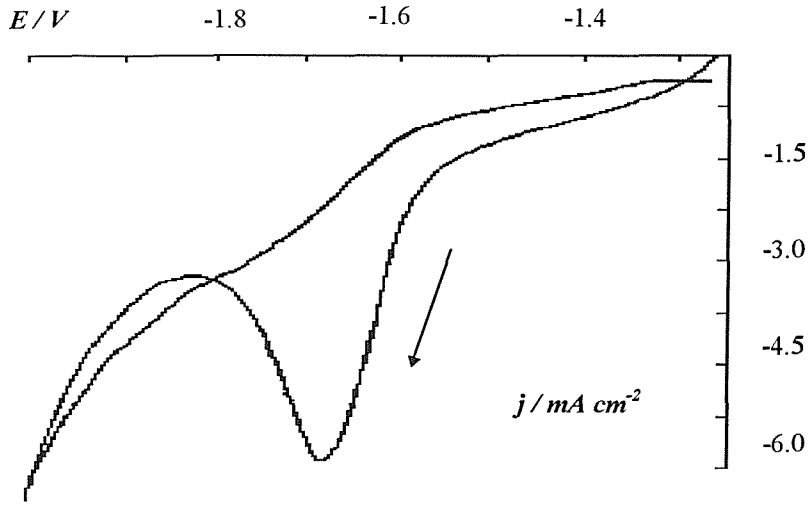

Fig 3.19 a *Cyclic voltammogram of a solution high in hydroxide performed at a brass electrode. T = 333K*

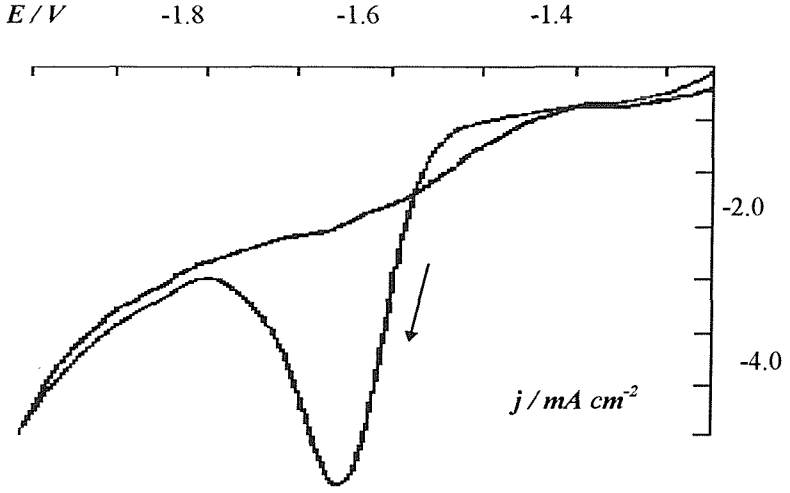

Fig 3.19 b *Cyclic voltammogram of a standard solution performed at a brass electrode. T = 333K*

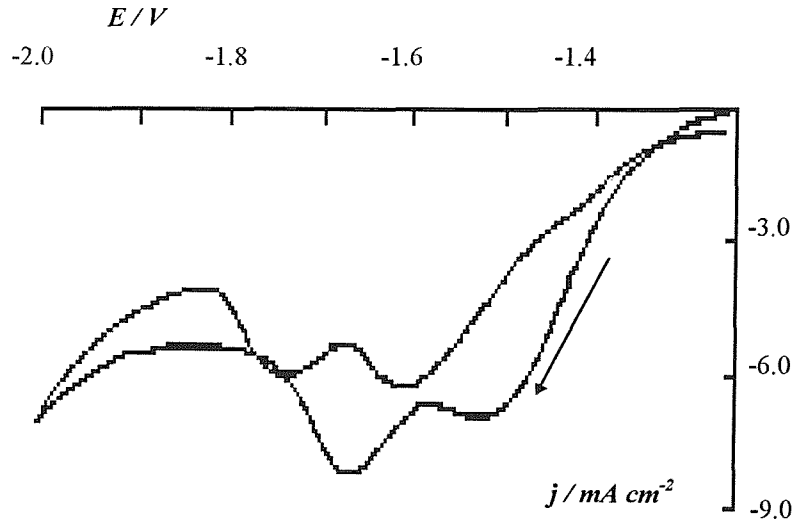

Fig 3.19 c *Cyclic voltammogram of a solution low in hydroxide performed at a brass electrode. T = 333K*

It should be also noted the

complexity of the deposition process in a solution low in hydroxide because of the peaks recorded on the reverse scan. With all these solutions, the brass electrode was covered completely with a layer of alloy after the first scan.

There are some differences recorded on the fourth scans. Figures 3.20 a,b show the current/potential response after four continuous cycles. Reduction features are recorded from all solutions. When high hydroxide is present in solution, figure 3.20 a, two reduction waves are recorded at $E_{1/2}$ = -1500 mV and $E_{1/2}$ = -1700 mV. Hydrogen evolution commences toward the negative limit and is not as vigorous as on the first scan.

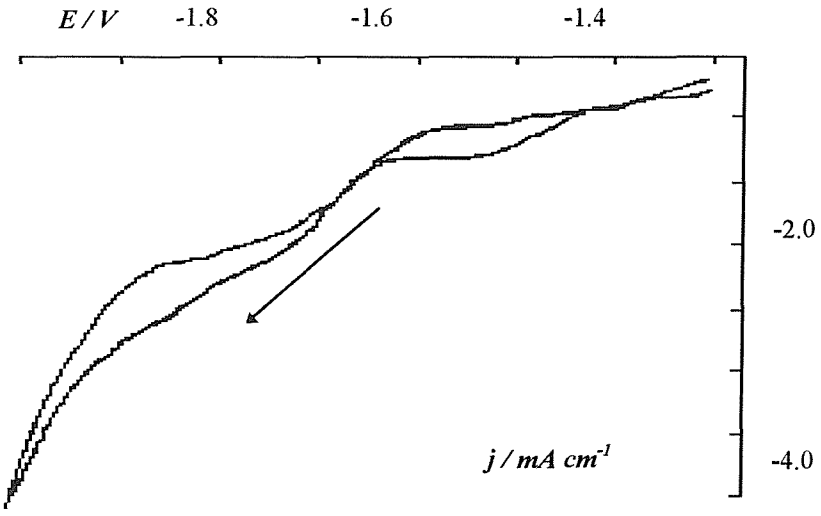

Figure 3.20 a *- Cyclic voltammogram after four continuous cycles in a bath high in hydroxide performed at a brass electrode. T = 333K*

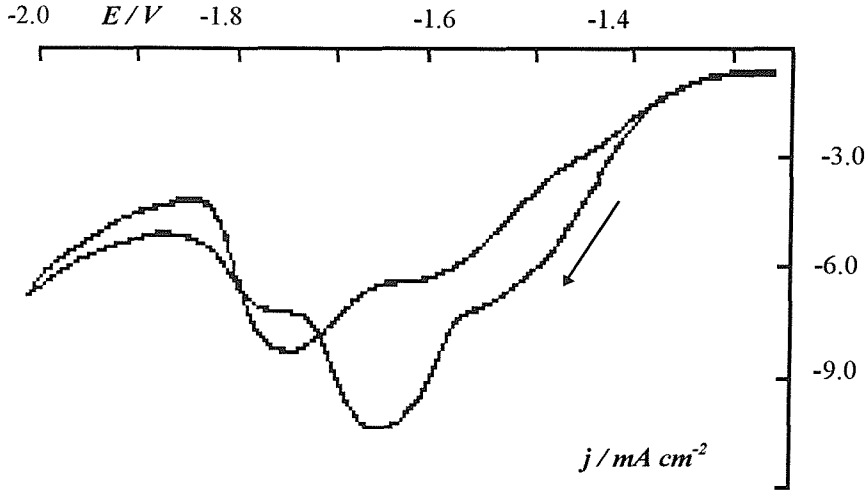

Figure 3.20 b- *Cyclic voltammogram after four continuous cycles in a bath low in hydroxide performed at a brass electrode. T = 333K*

Further experiments in which the solution was stirred, showed the same reduction peak as on the first scan (figure 3.19 a), hence, the difference between the scans is caused by changes in the diffusion layer and not in the electrode surface. Not major changes were recorded on a solution low in hydroxide. However, the larger charge recorded is due probably to changes in the electrode surface (a higher tin content, see later).

3.3.2 Steady state / sweep experiments

The experiments carried out in this section consisted in holding the potential of the electrode at a value in the range of -1400 mV to -2000 mV until a steady state current was reached (see table 3.6) and then the potential was scanned in a positive direction. The electrodes employed in these experiments were made of freshly cut brass strips of A = 1 cm^2.

Figures 3.21 a,b,c show three typical voltammograms recorded after the potential had been held at -2000 mV for 60 s. It should be stressed that the steady state data (table 3.6) is very similar to the voltammograms recorded in this way.

All voltammograms have one main feature consisting of a reduction wave/peak in the region of -1600 mV vs SCE. Also, they show a steep variation in the current negative to -1800 mV. Not much hydrogen evolution was observed in this region but it certainly contributes slightly to the current.

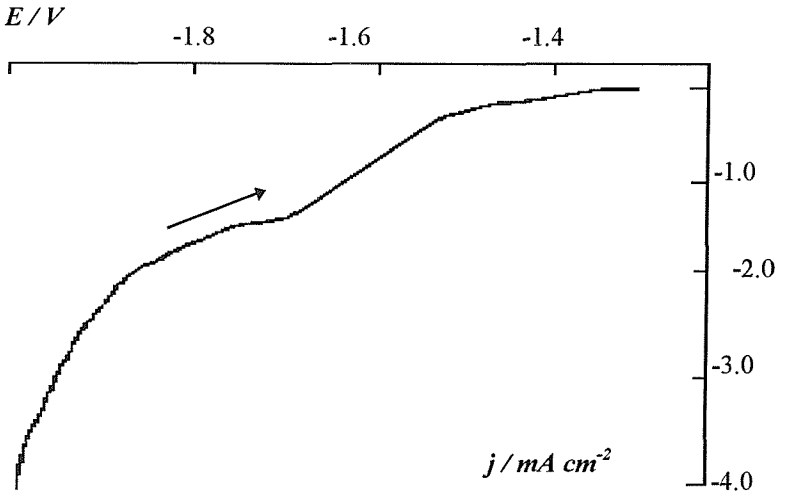

Fig 3.21 a - Back scan for a solution high in hydroxide after the potential had been held at E = -2.0V for 2 min

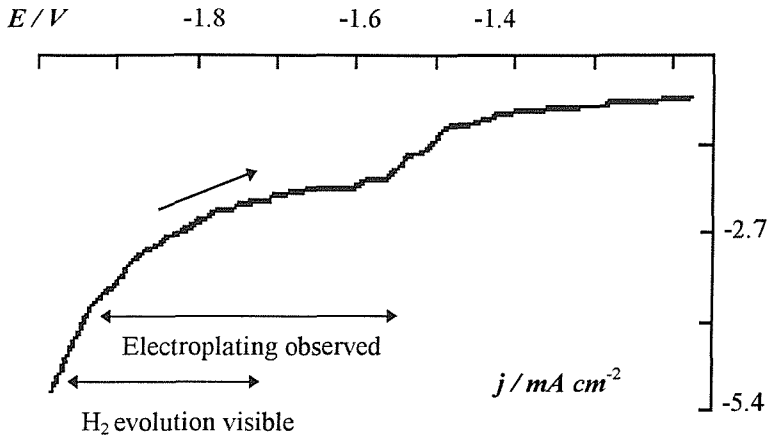

Fig 3.21b *- Back scan for a standard solution after the potential had been held at E = -2.0 V for 2 min*

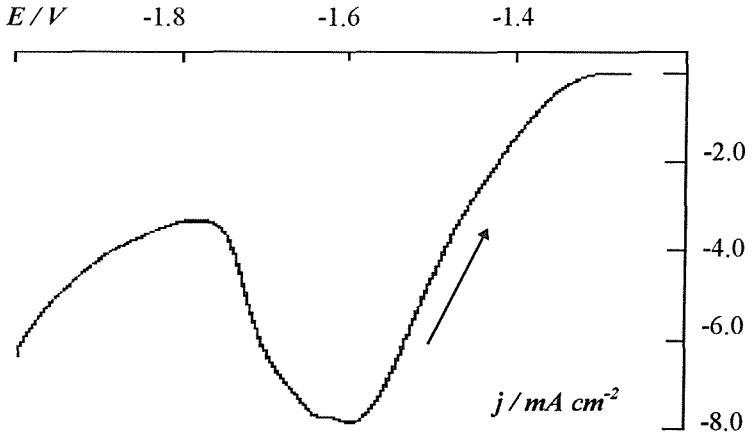

Fig 3.21 c *- Back scan for a solution low in hydroxide after the potential had been held at E = -2.0 V for 2 min*

The most significant difference between these voltammograms is for that recorded for a solution low in hydroxide. The large reduction peak of 8 mA cm^{-2} (figure 3.21 c) seems to be associated with hydrogen evolution which is seen to evolve vigorously in this region. Also, it seems that it could be associated with a high tin content as a poorly reflecting, milky deposit was obtained from this solution. The other two solutions give simple reduction waves of about the same current value which resemble the back scans on the cyclic voltammetry (figure 3.21 a,b).

Table 3.6 shows the steady state j/E data for all three solutions:

$E_{dep.}$ / mV	$j_{s.s.}$ / mA cm^{-2} 0.66 g l^{-1} OH	$j_{s.s.}$ / mA cm^{-2} 2.1 g l^{-1} OH	$j_{s.s.}$ / mA cm^{2} 5.4 g l^{-1} OH
-2000	6.0	5.5	3.8
-1900	3.75	-	2.5
-1800	3.0	2.6	1.9
-1700	2.2	2.3	1.2
-1600	4.4	1.4	-
-1500	4.3	0.8	-
-1400	1.0	-	-

Table 3.6 *- the variation of the steady state current with hydroxide concentration during potentiostatic experiments*

A much smaller current was obtained in solutions high in hydroxide. Also, the deposits obtained from such solutions were tarnished and copper colored, especially at -1600 mV. where EDS analysis showed the alloy composition to be Cu-Zn-Sn of 58-19-23. The voltammetric response for this solution never shows the reduction peak at ~ -1600 mV and this is further evidence that the peak results from H_2 evolution when the alloy depositing has a tin content above a critical value.

In contrast, deposits obtained from solutions low in hydroxide were milky, non reflective and tin colored. EDS analysis showed a high tin deposit with the composition Cu-Zn-Sn of 30-6-64. Also, the hydrogen evolution was observed evolving vigorously at potentials around -1650 mV as recorded on steady state voltammetry (Figure 3.21 a).

3.3.3 Chronoamperometry

Potential step experiments in which the nucleation and early growth of the metal layer were studied have been carried out. These experiments have been performed in solutions which were high, low or had a standard hydroxide concentration. Figures 3.22 a,b,c,d, show the I/t transients recorded in experiments in which the potential was stepped from -1250 mV to values in the range -1320mV to -1400 mV. A few similarities are found between the transients obtained from solutions standard and high in hydroxide. When the potential was stepped to -1320 mV or -1350 mV, an initial decrease in the current is recorded followed by an increase until a steady state in reached. No such transients were recorded from this solution at more negative potentials - *e.g.* -1380 mV and -1400 mV. There was an instant increase, followed by a decay in the current, over a period of 150 sec. The steady state current reached in both solutions is within the same range. However, the steady state is reached more rapidly with solutions high in hydroxide (figure 3.22 a). When the potential was stepped to -1500 mV or -1600 mV a deposit with a copper appearance was obtained from such solution (figure 3.22 b). The I/t transients obtained in this experiments have a completely different shape to the ones studied above. For instance, at -1600 mV, an increase in current is observed on a 15 s time scale, followed by a sharp decrease. Then, the transient increases over a 150 s period until eventually a steady state value is reached. This last rise in the current could be attributed to hydrogen evolution which is observed evolving vigorously at this potential.

In contrast, nice transients were obtained from solutions low in hydroxide. The steady state currents reached from this solution (figure 3.22 d) are about double in size compared to those obtained from solutions high or standard in hydroxides. However, a portion of this current could be attributed to hydrogen evolution which was observed at potentials as low as -1320 mV. Also, it should be mentioned that no deposit was observed by eye during these step experiments in any of the three solutions studied.

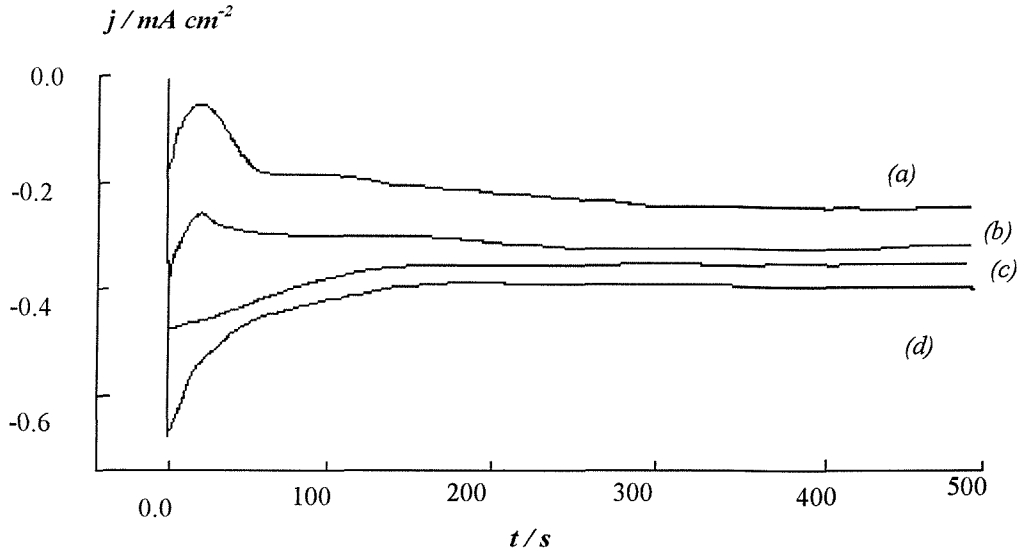

Fig 3.22 a Potential step experiments for a solution high in hydroxide: (a): -1320mV, (b): -1350 mV, (c): -138mV, (d): -1400mV

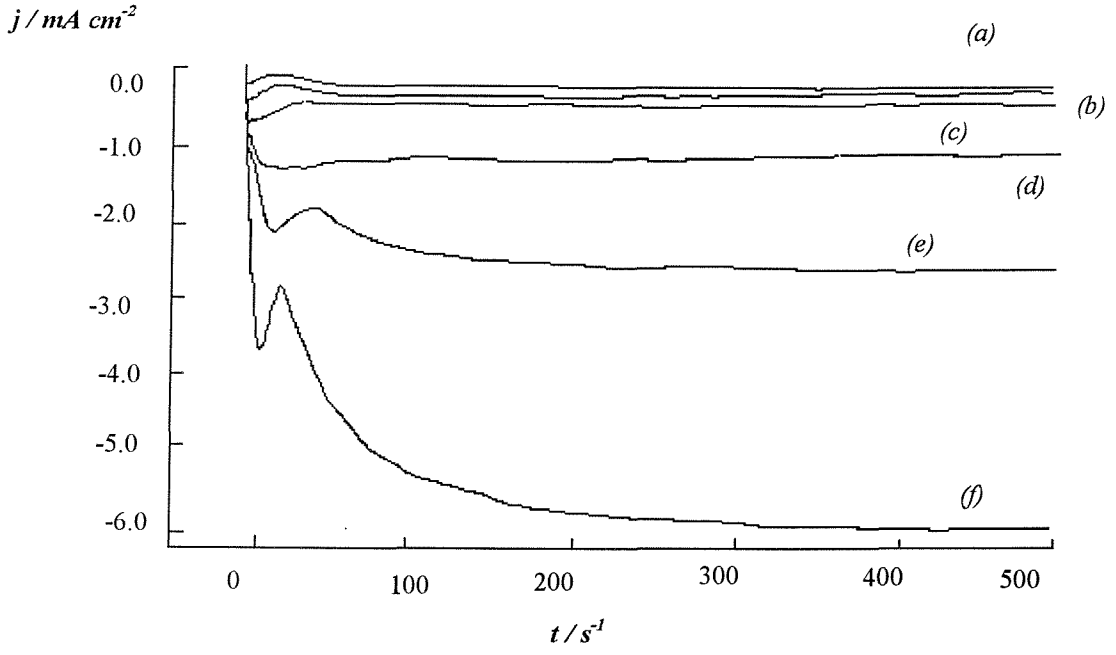

***Figure 3.22 b** Potential step experiments for a solution high in hydroxide: (a): -1320mV, (b): -1350 mV, (c): -1400mV, (d): -1500mV, (e): -1550mV, (f): -1600mV*

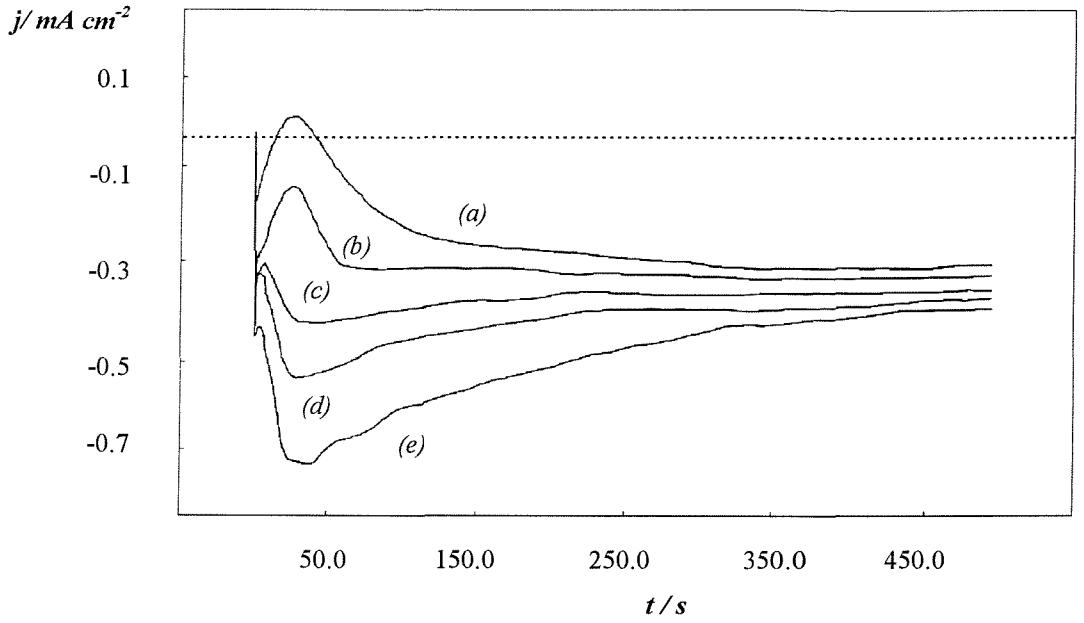

Figure 3.22 c *The current / time response for a standard solution in a series of potential step experiments Potential steppe at (a) -1.32 V, (b) -1.34 V, (c) -1.36 V, (d) -1.38 V, (e) -1.4 V*

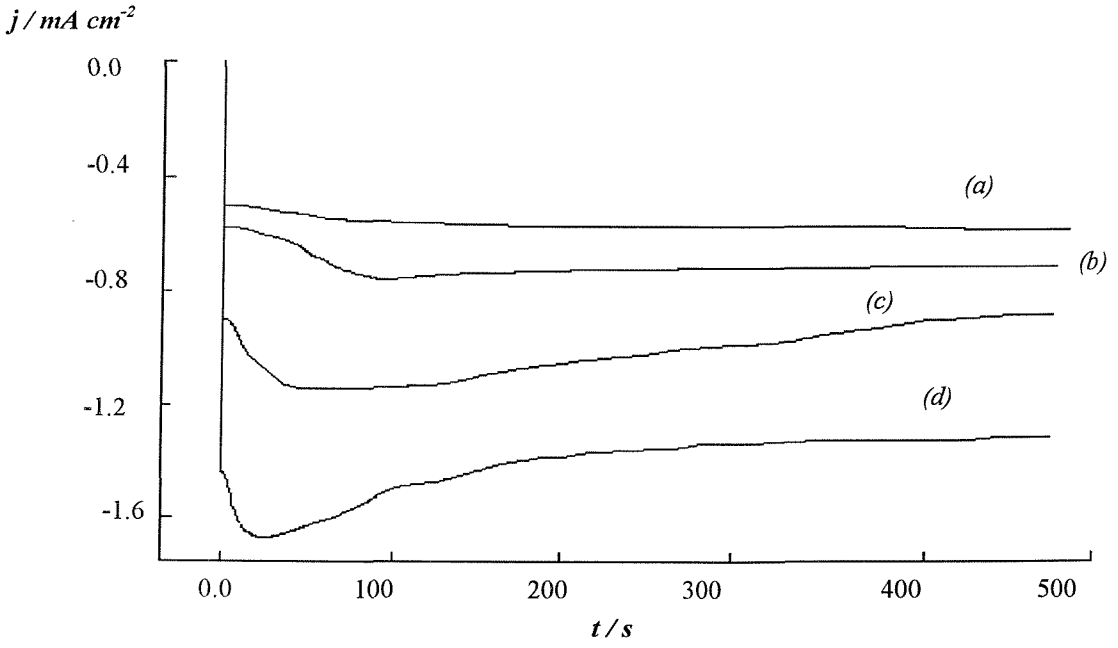

Figure 3.22 d *Chronoamperometric experiments from a solution containing 0.66 g l^{-1} free hydroxide. (a): -1320 mV, (b): -1350 mV, (c): -1380 mV, (d): -1400 mV*

3.3.4 SEM

Hull cell panels made of brass have been plated from solutions containing 5.4 g l^{-1},2.1 gl^{-1} or 0.66 g l^{-1} free hydroxide. As previously reported, for an accurate determination of elemental composition which is not influenced by the penetration of the electron beam into the brass substrate, a thick layer of alloy was plated. Three different alloys were plated from these three solutions (table 3.7).

A tarnished deposit was obtained from a solution high in hydroxide. Figure 3.23 shows an SEM of a Hull panel at the position for 6 mA cm^{-2}, which was plated for 7 minutes. A surface composed of a rough, non uniform deposit formed of compacted small grains is observed. The EDS analysis showed a high concentration in zinc and low in tin with a Cu-Sn-Zn composition of 53-19-28.

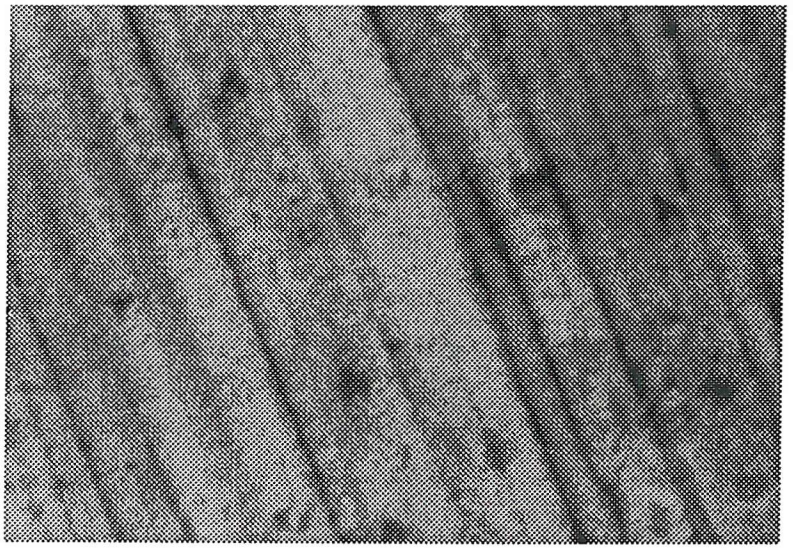

scale: ⟷ 1 μm

Figure 3.23 *- SEM of a Hull cell brass sample at the position of 6 mA cm^{-2} plated for 7 min from a solution containing 5.4g l^{-1} free hydroxide.*

Table 3.7 - data showing different alloy compositions plated from solutions with different OH concentrations.

[OH⁻] / g l⁻¹	*Cu - Zn - Sn / %*	*deposit appearance*	*substrate*
0.66	30 - 6 - 64	non reflective, patterned, milky	brass - Hull Cell at the position of 6 mA cm^{-2}
0.66	43 - 5 - 52	non reflective, milky	silver brass strip, E = -1600 mV
2.1		reflective	brass - Hull Cell at the position of 6 mA cm^{-2}
4	64 - 20 - 14	tarnished	silver connector from the plating line
5.4	53 - 19 - 28	tarnished	brass - Hull Cell at the position of 6 mA cm^{-2}
5.4	58 - 19 - 23	tarnished, copper color	silver brass strip, E = -1600 mV

A connector plated form a solution containing 4 g l^{-1} showed the same trend in the metal ratio which was: 64-20-14. It is clear therefore that more hydroxide in the plating bath complexes the tin in solution making it harder for it to plate. However, it should be stressed that the differences in the composition of the above two samples may arise from the difference in the free hydroxide concentration from the two solutions.

Also, a silver plated brass strip which was plated at -1600 mV in a solution high in hydroxide, showed an alloy poor in tin and rich in copper with the composition Cu-Zn-Sn of: 58-19-23; This explains the tarnished, red colored deposits obtained from such solution.

In contrast, samples plated from solutions low in hydroxide had a completely different appearance. The Hull cell samples showed in the plating region a patterned deposit with a non reflective, tin appearance. Figure 3.24 shows a sample cut from a Hull cell brass panel plated for 7 min at the position for 6 mA cm^{-2} .

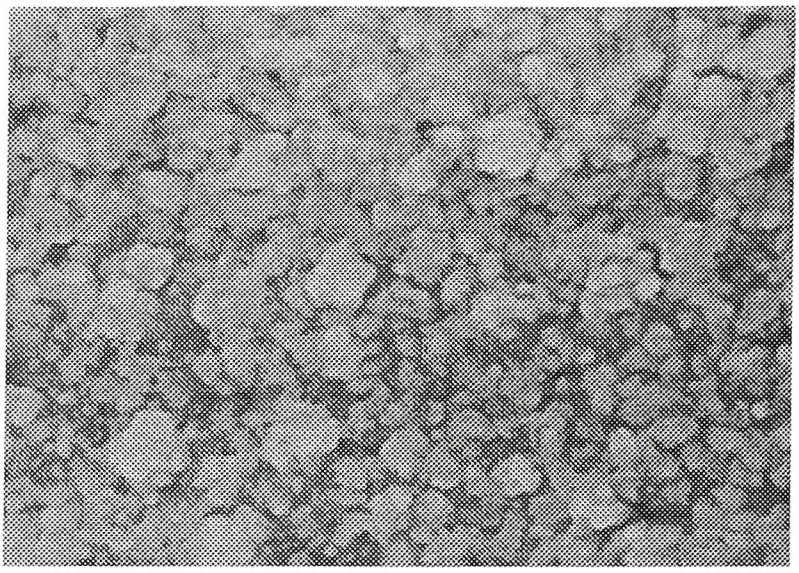

Figure 3.24- *SEM from a Hull Cell sample at the position of 6 mA cm^{-2} plated for 7 min from a solution containing 0.66 g l^{-1} free hydroxide*

scale: ⟷ 1 μm

The SEM shows a rough surface covered with angular grains of 0.5 μm diameter. Also, the alloy composition found was Cu-Zn-Sn of 30-6-64. This is not surprising since the whole panel was covered with a milky, non reflective, patterned deposit in the 6 mA cm^{-2} region. The deposit plated from a standard solution is shown in figure 3.25 and it has been described in Section 3.1.

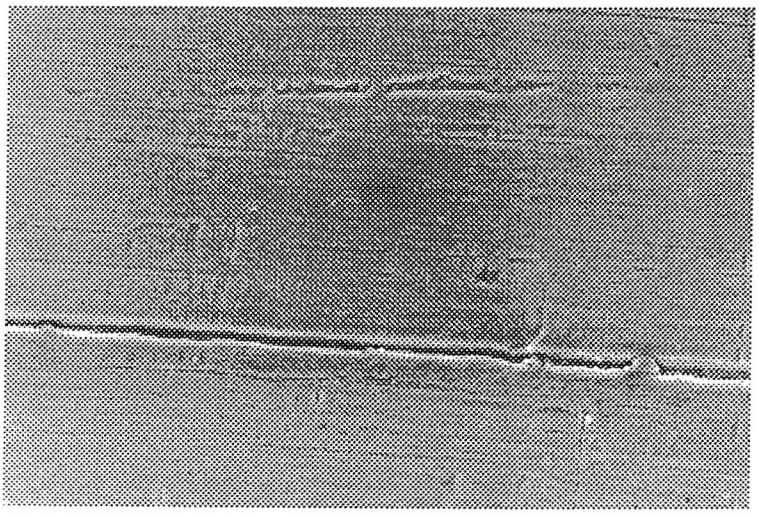

Figure 3.25- *SEM of the alloy deposited at a constant potential of -2050 mV from a standard bath*

scale ⟷ 1 μm

3.3.5 Conclusion

- It was found that the alloy composition is strongly influenced by the amount of free hydroxide in the electroplating bath (table 3.7).
-

OH / g l^{-1}	*Cu-Zn-Sn*
0.66	30-6-64
2.1	51-8-41
5.4	53-19-28

Table3.7 showing the different alloy ratios obtained from solutions high / low in free hydroxide

  * an alloy high in tin and low in copper is plated from a bath with a low concentration in free hydroxide. This leads to rough deposit composed of angular grains of 0.5 μm diameter. Such alloy is non reflective and it has the milky, tin appearance.
  * in contrast, when the plating bath is high in free hydroxide, the alloy becomes rich in zinc and poor in tin. The deposit was tarnished and formed of compacted small granules.

- The peaks on the cyclic voltammograms are associated with H_2 evolution and are observed when the alloy has a tin content above a critical value, e.g. in a solution low in hydroxide.

3.4 The effect of additive concentration on alloy deposition

An alloy has a pleasing appearance when a high reflectivity in the visible part of the spectrum is achieved. Because alloys have an inherent tendency to form grained deposits, addition agents are used to confer the electroplates with additional brightness. For instance, organic addition agents are used in white brass plating and in the deposition of copper-zinc-tin alloys. The mechanism by which these organic additives influence electrodeposition is poorly understood and not widely studied. It is possible that these organic additives undergo electrochemical reductions at the cathode, depleting the added organic species and / or introducing new species, the products of such reductions. Hence, a study of the role the organic additive has on the Cu - Zn - Sn alloy electrodeposition process was performed in this section. The experiments were carried out in solutions in which the concentration of additive was varied and the behaviour was closely monitored mainly by the means of cyclic voltammetric and SEM techniques.

The solutions employed in the study had the composition :

	g l^{-1}	**mM**
CuCN	9.1	102
$Zn(CN)_2$	5.4	46
$Na_2[Sn(OH)_6]$	5.7	24
Na_2CO_3	6.5	61
free NaOH	2.1	50
free NaCN	25	551

Copper Glo solution 0, 0.5, 1.25, 2.5, 5.0, 10.0 g of commercial solution added to 1 litre of electrolyte

Unfortunately, the composition of the commercial plating additive solution, Copper Glo, is not known. It has been suggested that the active ingredient has the structure:

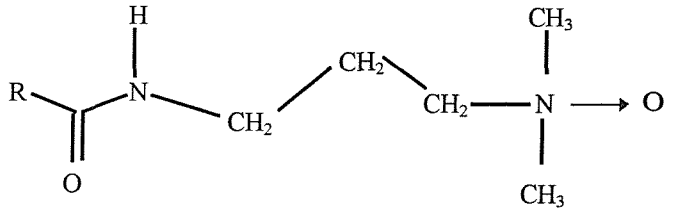

but the length of the alkaline chain, R, is not stated and Copper Glo may be a mixture of amino oxides with variable chain lengths. It is also not clear whether the "active" group is the N → O group or the role of this functional group is merely to make the additive water soluble. Moreover, the concentration of the additive in the commercial solution is not disclosed. Hence, in the thesis the amount of additive is stated as grams of commercial additive solution / litre of plating bath.

As on the plating line, the experiments have been performed at 333 K, and the solutions were not deoxygenated. Also, the electrodes were disposable brass strips and some experiments used Hull Cell panels.

3.4.1 Cyclic voltammetry

Cyclic voltammetric studies of standard solutions containing different amounts of organic additive have been carried out at disposable brass electrodes of A = 1 cm^2 at 333 K. All the cyclic voltammograms have been recorded at a scan rate of 20 mV s^{-1} and the potential was scanned from -1260 mV to -2000 mV vs. SCE.

Figures 3.26 a, b, c, d and e show the cyclic voltammograms recorded from electrolytes with 0 g l^{-1}, 0.5 g l^{-1} , 2.5 g l^{-1} , 5 g l^{-1} and 10 g l^{-1} of additive solution. It can be seen that different responses were recorded from these solutions.

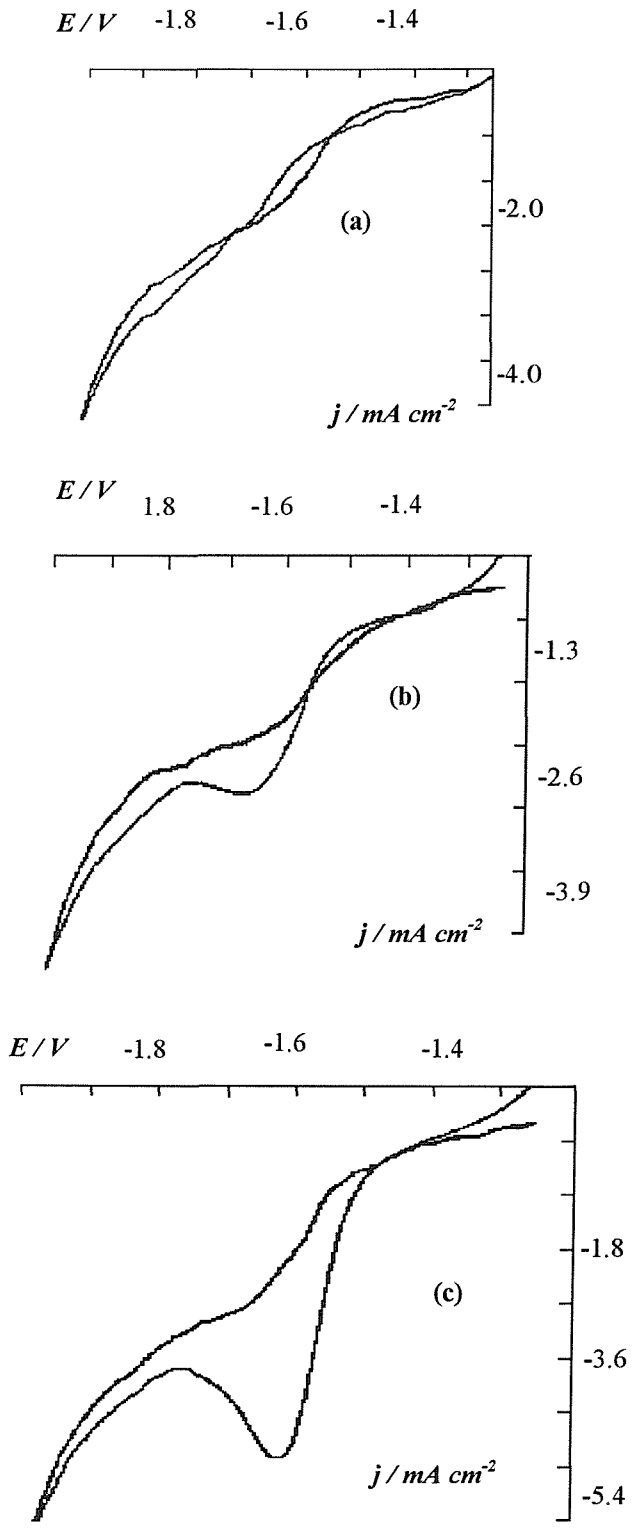

Fig 3.26 - the current potential response of standard solutions containing different additive concentrations. (a) 0 g, (b) 0.5 g, (c) 2.5 g, of additive solution in 1 litre of electrolyte.

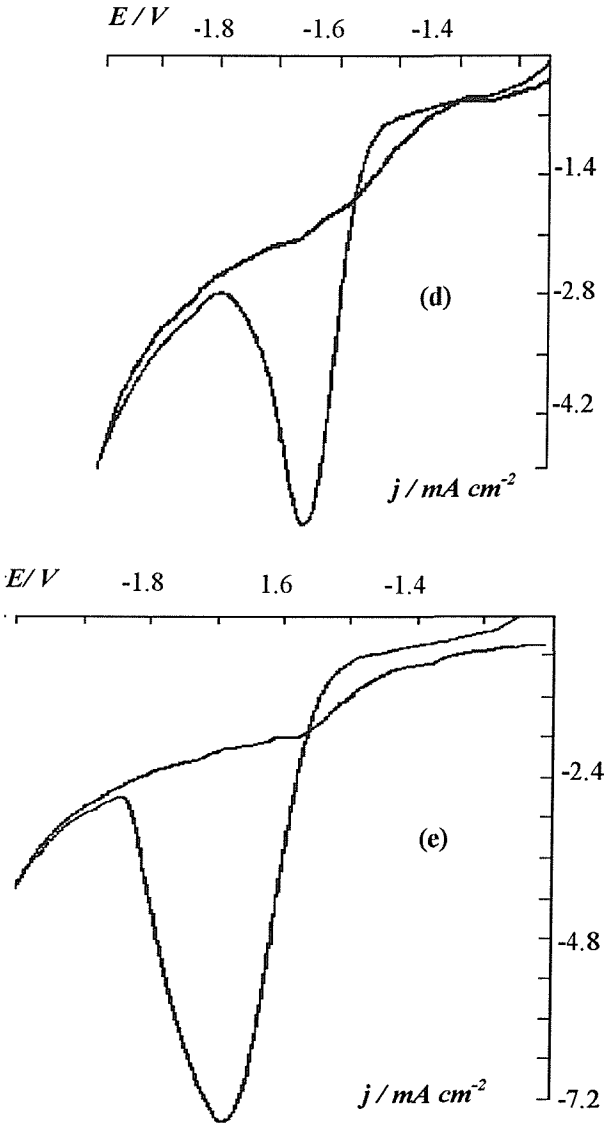

Fig 3.26 - the current potential response of standard solutions containing different additive concentrations (d) 5 g and (e) 10 g of additive solution in 1 litre of electrolyte.

When no additive was present in the bath, figure 3.26, a reduction wave with a limiting current density of 2 mA cm^{-2} was recorded at $E_{1/2}$ = -1600 mV. This wave is associated with alloy deposition as a good quality metal layer was deposited onto the electrode surface even when the potential was scanned between -1250 mV and -1600 mV.

When 0.5 g l^{-1} additive was added to this solution, figure 3.26 b, this reduction

current takes the shape of a small peak of j_P = - 2.2 mA cm^{-2} at E_P = -1650 mV. The increase in the current is caused by the hydrogen evolution which could be seen evolving in the peak region (E ≈ - 1600 mV). Figures 3.26 c, d and e, report data collected from alkaline cyanide solutions containing 2.5, 5, 10 g l^{-1} additive. It could be seen that a gradual increase in the height of the peak is recorded as the amount of the additive increases. For example, the reduction current increases from 4.0 mA cm^{-2} at 2.5 g l^{-1} additive, to 8 mA cm^{-2} for a 10 g l^{-1} additive.

Also, the hydrogen evolution which was observed evolving in the region of E = -1600 mV was becoming more vigorous with the increase in additive concentration. In all these solutions, after a complete scan, a continuous layer of alloy covered the electrode surface.

It can be concluded therefore that the voltammetric response changes strongly with the additive concentration. This change could, however, only be associated with the hydrogen evolution which was observed evolving in the peak region. Indeed, the additive could be present only to cause transient H_2 evolution during the early stages of metal deposition - before the potential shifts to a steady state value of -2000 mV, see figure 3.3. Such H_2 evolution would influence the current distribution during the early phase formation and could lead to a more, even, brighter deposit.

Figure 3.27 shows the current - potential response recorded from a solution which contains 10 g of additive solution to 1 litre of electrolyte after four continuous cycles. There are several changes from the first scan. Firstly, as in the standard bath, a positive shift in the reduction process of about 100 mV is registered. This shift leads to a much broader peak due to reduction which starts at about -1380 mV. It should be noted also, that there is an additional shoulder recorded at E = -1780 mV. Also, during the fourth scan the height of the reduction peak is much smaller than the one recorded on the first scan, with a peak current density of 4.5 mA cm^{-2}. The same height in the reduction peak was recorded from all solutions containing additive. However, it was found that on the fourth scan the cathodic charge passed was increasing gradually with the amount of the additive.

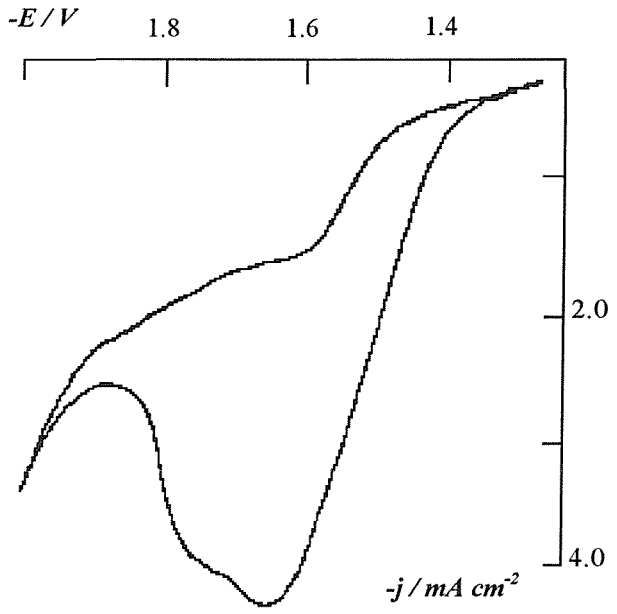

Figure 3.27 *- Cyclic voltammogram recorded after four continuous cycles from an alkaline cyanide solution containing 10 g l^{-1} of additive solution added to 1 litre of electrolyte*

Figure 3.28 a, b, and c, show scans from -2.0 V to -1.2 V (i.e. starting with electrodes coated with alloy) recorded from solutions containing 0, 2.5 and 10 g l^{-1} of additive solution added to 1 litre of electrolyte after four continuous cycles. It can be seen that with all these solutions, a reducing wave with well defined plateaux were recorded and the responses are very similar. These waves occur at the same potential: $E_{1/2}$ = - 1550 mV having the same value limiting current of j_L = - 2 mA cm^{-2} (figure 3.28). During these scans, hydrogen evolution was not seen occurring.

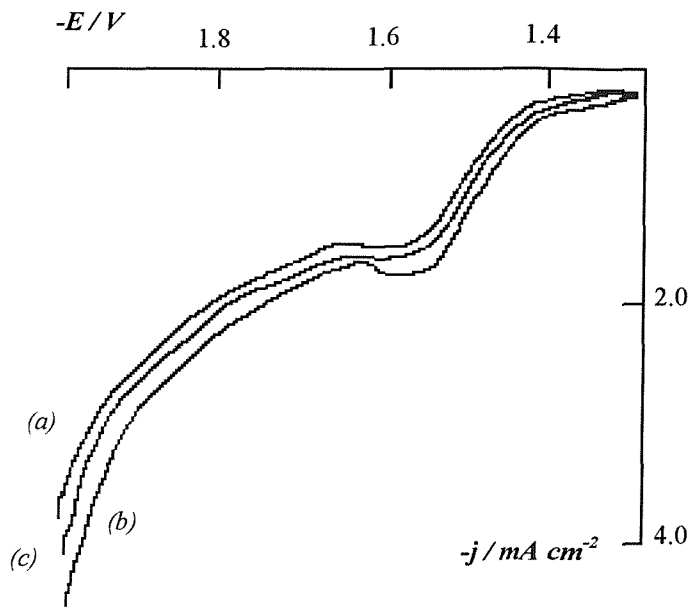

Figure 3.28 *- The back scans recorded after four continuous cycles from alkaline cyanide solutions containing: 0 g l^{-1} 2.5 g l^{-1}, 10 g l^{-1} of additive solution added to 1 litre of electrolyte*

3.4.2 SEM

Hull cell panels as well as silver coated brass strips have been plated from alkaline cyanide solutions which contained different concentrations of the organic additive (Copper Glo). The samples have been analyzed by the means of SEM; also, the EDS technique has been employed to detect their elemental composition.

Table 3.8 reports data collected from brass strip samples which were plated from solutions which contained various amounts of additive. All the samples studied showed no significant change in the ratio of metals with additive concentration.

Additive / g l^{-1}	*Cu / %*	*Zn / %*	*Sn / %*
1.25	51	10	39
5	52	8	40
10	52	8	40
20	52	9	39

***Table** 3.8 - The Cu - Zn - Sn ratio for alloys plated from solutions containing different amounts of additive.*

SEM performed on a sample which was plated from a solution containing 0 g additive solution to 1 litre of electrolyte showed a rough deposit with a structure composed of very small grains - figure 3.29.

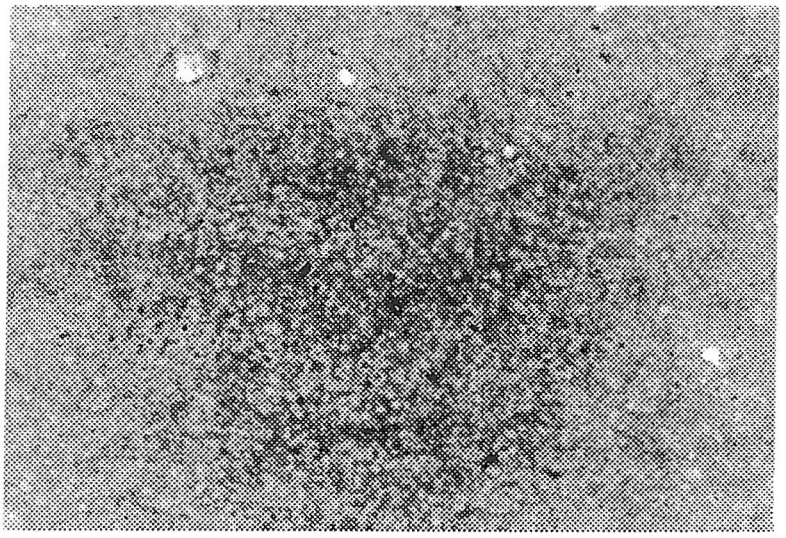

***Figure 3.29** - SEM of a brass strip sample plated from a solution containing 0 g additive solution to 1 litre of electrolyte. Deposition time = 120 s, j = 6 mA cm^{-2}*

scale : ⟷ 1μm

In contrast, when a brass strip sample was plated from a solution containing 10 g additive to 1 litre of electrolyte, a featureless, smooth deposit was observed by the SEM technique.- figure 3.30 -

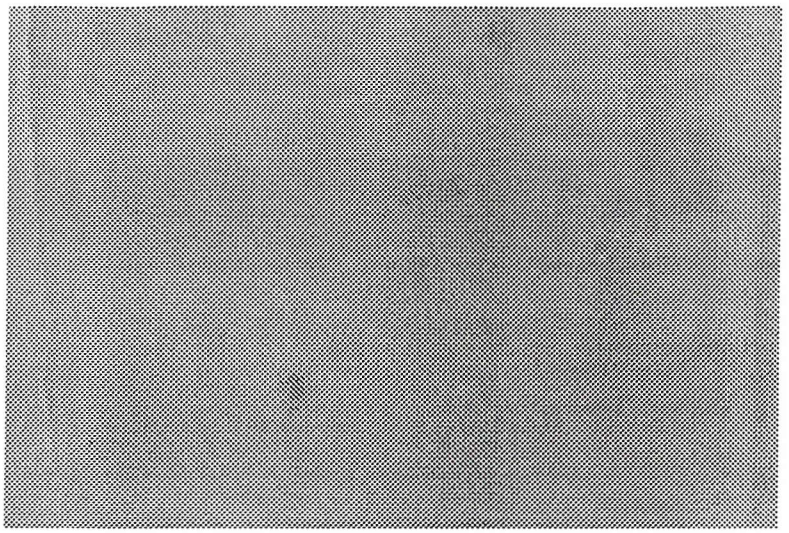

Figure 3.30 *- SEM from a brass strip sample plated from a solution containing 10 g additive solution to 1 litre of electrolyte. Deposition time = 120 s, j = 6 mA* cm^{-2}

scale: ⟷ 1 μm

3.4.3 Studies of the electroreduction of trimethylamine N - oxide and dimethyloctylamine N - oxide

It was of interest to examine whether amine oxides were electroactive in the plating medium or whether they lead to the transient H_2 evolution seen with Copper Glo. Data published in literature [45] shows that only cyclic amino oxides in their protonated form can undergo electroreduction. At pH > 9 the cyclic amino oxides become polarographically inactive. However, no data concerning the reduction of alkyl amino oxides in alkaline media has been published. Because the composition of the commercial plating additive, Copper Glo, was not known, two different amino oxides solutions have been examined.

These amino oxides were ***trimethylamine N-oxide (a)*** and ***dimethyloctylamine N-oxide (b)***

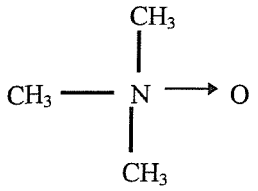

(a)

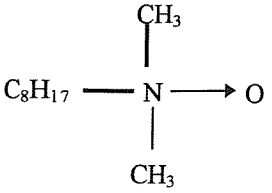

(b)

and they were employed in voltammetric experiments which were carried out at carbon or platinum microelectrodes.

- Linear sweep voltammetric experiments have been carried out from a solution which contained 10 mM ***trimethylamine N- oxide*** and 0.5 M Na_2SO_4, pH 12. These experiments have been performed at a Pt microelectrode. No reduction wave or other voltammetric feature was observed prior to hydrogen evolution at - 2250 mV vs. SCE.

- Similar results were recorded when it was attempted to reduce ***dimethyloctylamine N-oxide*** solutions at a carbon microelectrode.

- Figure 3.31 reports the forward scans recorded in two different alkaline cyanide solutions containing Cu(I), Sn(IV), Zn(II). The first one was the standard bath which did not contain any commercial additive. To this trimethylamine N-oxide (5g l^{-1}) was then added to form the second solution. Voltammetric experiments were performed with brass strip electrodes. None of the major features recorded in the presence of Copper Glo were observed with trimethylamine N-oxide. *E.g.* there is no reduction peak observed in the region of E = -1600 mV. Also no hydrogen was seen evolving in this potential region. This implies that the amino oxide functional group was necessary only to make the additive soluble.

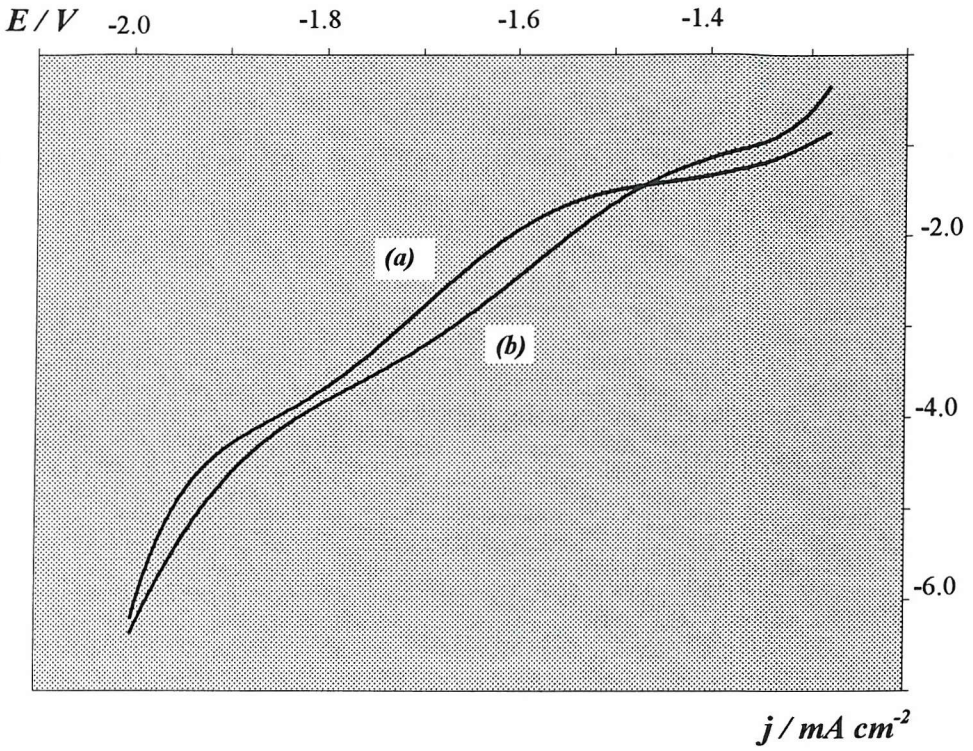

Figure 3.31 *- The forward scans recorded form the standard plating bath containing: 0 g l^{-1} of additive solution added to 1 litre of electrolyte (a), and 5 g l^{-1} trimethylamine N-oxide (b)*

3.4.4 Conclusion

- The voltammetry of the alkaline cyanide bath changes with the commercial additive. Small reduction currents are recorded from solutions low in additive. When the solution contains 2.5 g of additive solution to 1 litre of electrolyte or more, this reduction wave takes the shape of a sharp reduction peak.

- The reduction current recorded at E = -1600 mV increases with the concentration of additive in solution.

- The structure of the alloy changes with the additive concentration. An alloy with a rough structure is deposited from a solution containing low concentrations of additive. This structure becomes completely featureless when the additive concentration in solutions increases.

- The same alloy composition is found regardless of the additive concentration. The composition is within the following close limits:

Cu	51 - 52 %
Zn	8 - 10 %
Sn	39 - 40 %

- The amino oxides studied do not reduce at pH 12, nor do they influence the voltammetry in the same way as Copper Glo.

3.5 The effect of temperature on alloy deposition

The temperature of the bath is likely to have an important influence in the plating process. As stated in the Introduction, it quickens the surface diffusion of the adatoms which is expected to have an effect on the alloy structure and quality. Also, it increases the rate of all homogeneous chemical reactions as well as the exchange current density for the electron transfer reactions by the means of an Arhenius type equation. Lastly, the rate of diffusion increases with temperature.

Data published [20] reports that for other alkaline cyanide plating baths the temperature has to be controlled within strict limits. A low current efficiency is achieved when the electroplating bath is operated at room temperatures. On the other hand, high temperatures cause the decomposition of cyanide leading to an imbalance in the alloy metal ratio. Hence, the operating temperature must be a balance between a good current efficiency and a adequate quality and composition of the alloy coupled to bath stability.

Studies of the effect the temperature of the plating bath has on alloy deposition have been carried out in this section. Cyclic voltammetric and SEM techniques have been carried out on standard cyanide solutions operated at different temperatures

The solutions used in this section have been freshly prepared and had the following composition:

	$g\ l^{-1}$	mM
CuCN	9.1	102
$Zn(CN)_2$	5.4	46
$Na_2[Sn(OH)_6]$	5.7	24
Na_2CO_3	6.5	61
free NaOH	2.1	50
free NaCN	25	551
Copper Glo solution	5.0	

In these experiments, the solution temperature was strictly controlled at the chosen values by circulating water from a thermostat through a cell jacket. The electrodes employed were freshly cut silver coated brass strips.

3.5.1 Voltammtery

Voltammetric studies have been performed from solution which were thermostated at four different temperatures. In these experiments the potential have been scanned between: -1250 mV to -2000 mV vs. SCE at a scan rate of 20 mV s^{-1}. Figures 3.32 a, b, c show the potential - current response recorded from the standard plating bath solutions with temperatures of: 293 K, 313 K, and 343 K. When discussing these voltammograms the potential window could be divided into two separate regions. At potentials positive to -1750 mV, a few features are observed on the voltammograms. At 293 K, no current is visible on the voltammogram using the current sensitivity shown (figure 3.32 a). However, on a more sensitive scale, very small reduction waves are recorded at $E_{1/2}$ ~ - 1500 mV and $E_{1/2}$ ~ - 1700 mV. This currents could be associated with metal deposition, but their small magnitude explains why no alloy was observed on the electrode surface after a complete potential cycle. With a temperature of 313 K, two well defined reduction waves are observed. The first wave with a limiting current of 0.8 mA cm^{-2} was recorded at $E_{1/2}$ ~ - 1500 mV and it is followed by another with j_L = 0.6 mA cm^{-2} at $E_{1/2}$ ~ - 1700 mV. This rapid increase in the reduction current (Table 3.8) with increasing temperature could be attributed to an increase in the homogenous chemical reactions preceding the electron transfer.

Temperature / K	Current density at E = -1700 mV / mA cm^{-2}
293	0.8
313	1.2
333	5.2
343	9.5

Table 3.8 *showing the current density at E = -1700 mV recorded with different bath temperatures*

At the completion of the voltammogram, a thin layer of metal covered the electrode surface. At 333 K, a large increase in the reduction current is again recorded. This response has the shape of a peak and it has the value of 5.2 mA cm^{-2} (Figure 3.1 a). This particular curve was discussed largely in Section 3.1.

Figure 3.32 c shows the current - potential response obtained from the standard bath operated at 343 K. The reduction current recorded at $E_{1/2}$ = -1500 mV increases to 7 mA cm^{-2}. At E_P = -1700 mV a reduction peak of 2.5 mA cm^{-2} is also observed. Indeed, at this temperature the rate of homogenous chemical reaction is increased greatly. It should be stated also, that the rise in these reduction currents are also caused partially by the hydrogen evolution which was evolving in the potential region around -1.6 V when the bath was operated at 333 K and 343 K. With these temperatures, highly reflecting deposits were clearly visible after a single potential cycle.

A different behavior of these solutions is recorded at potentials between -1750 mV and -2000 mV. The current - potential response follows a different trend with temperature. At 293 K and 313 K the current corresponding to -2000 mV doubles its size compared to the one recorded at -1750 mV. In contrast, when the solution is operated at 343 K almost no increase is observed. In this potential range, the electrode reaction is mainly hydrogen evolution and the different responses may be due to the different H_2 evolution characteristics on the substrate and the electroplated alloy. It is clear from the discussion above that the temperature influences greatly the electrodeposition process. The comparison of the current density at -1700 mV with 6 mA cm^{-2} is a reasonable first estimate of the current efficiency to be expected in a commercial plating process. At low temperatures very small reduction currents are recorded and deposition takes place at a low rate and a low current efficiency is to be expected. In contrast, high temperatures lead to higher current densities as a result of an increase in the rate of the homogeneous chemical reactions preceding the electron transfer; thick alloy deposits are readily formed and a much better current efficiency will result.

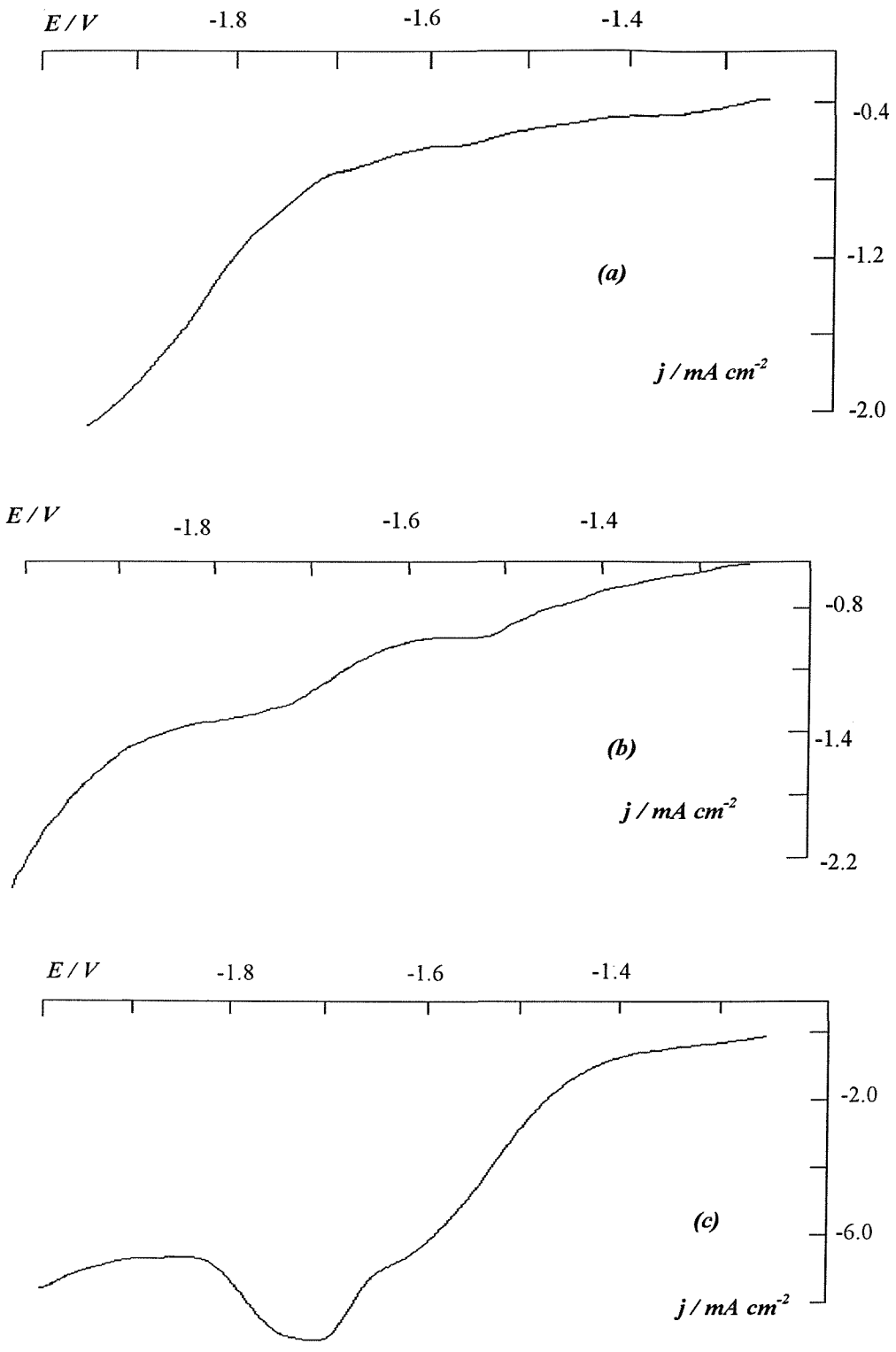

Figure 3.32 Cyclic voltammograms recorded at brass strip electrodes from a standard bath at different temperatures. (a): 293K, (b):313K ,(c): 343 K,

3.5.2 Chronopotentiometric experiments

A series of experiments were performed at fresh silver coated brass strip electrodes. In these experiments a current density of 6 mA cm^{-2} was applied for a period of 800 s. A uniform coat of alloy was deposited onto the electrode surface at all temperatures. Figure 3.33 shows the potential / time response recorded from a standard solution which was operated at 293 K, 313 K and 333 K. In all three experiments the potential falls rapidly to a value of about -1800 mV. This fall is caused by the charging of the double layer. At 293 K, this potential is maintained constant for a period of about 25 s before a very slow fall (of about 400 s) to a steady state value of $E_{S.S}$ = -2020 mV. It is believed that at -1800 mV the main electrode reaction is hydrogen evolution as probably, silver metal is a better catalyst for hydrogen evolution than the alloy itself.

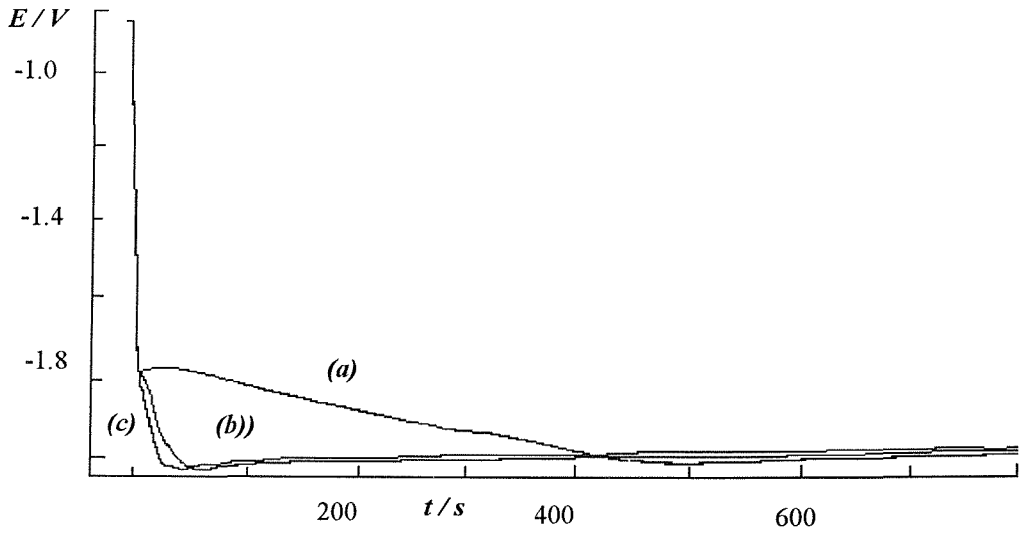

Figure 3.33 *Chronoamperometric experiments performed at brass electrodes with silver undercoat in a standard bath at different temperature. (a): 292 K, (b): 313 K , (c):333 K*

Certainly, a relatively high H_2 evolution current is observed at -1800 mV on the voltammogram at 293 K shown in figure 3.32 a. Then, this process is followed by slow alloy deposition. This long transition time explains the slowness of the deposition rate at room temperature. A reflective but very thin, deposit was obtained at this temperature after 800 s. With temperatures of 313 K and 333 K, these transition times decrease to less than 25 s and the alloy deposit is quickly formed on the electrode surface. It is clear therefore that the rate of deposition is very slow at 293 K but it increases rapidly with temperature.

3.5.3 SEM

Brass strips that had a silver undercoat were electrodeposited from a standard cyanide solution at four different temperatures: 292 K, 313 K, 333 K and 343 K. Reflective, uniform deposits were obtained in each experiment. However, at 293 K the deposit was thin as the EDS spectra showed a large silver peak along with the peaks for the three metals composing the alloy - figure 3.34.

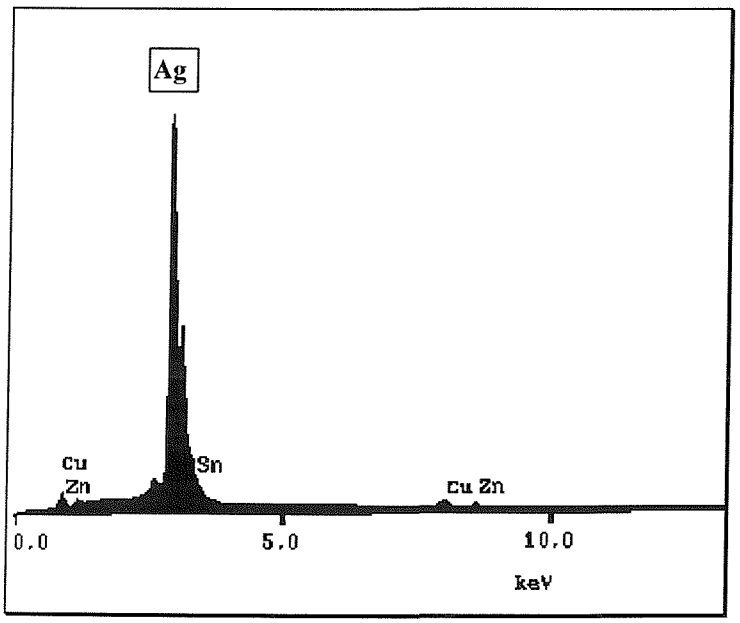

Figure 3.34 EDS of a brass sample with silver undercoat plated at 293 K

These samples were analyzed by the means of SEM and EDS techniques. All the micrographs taken from these samples showed featureless deposits. Also, the elemental composition shown in table 3.9 indicates a similar metal ratio regardless of the temperature of the bath.

Temp. / K	time / s	Cu / %	Zn / %	Sn / %
293	400	52	9	39
313	200	52	10	38
333	120	52	8	41
343	100	51	7	42

Table 3.9 *showing the alloy composition with bath temperature*

3.5.4 Conclusion

Studies carried out in this section show that :

- Reflective alloy deposits could be obtained at all temperatures studied, 293 K - 343 K.

- The composition of the alloy does not change with the temperature, the metal ratio falls within the range:

Cu	51 - 52 %
Zn	7 - 10 %
Sn	39 - 42 %

- The rate of alloy deposition is, however, a strong function of temperature. Thick deposits must be plated at elevated temperatures, if the process is to be completed within a reasonable period. At a constant current density of 6 mA cm^{-2} , the current efficiency is very poor at room temperature.

3.6 Studies of alkaline cyanide solutions containing one metal ion only

Data presented in previous sections showed the complexity of electrodeposition process of Cu - Zn - Sn alloy. It was shown that in order to obtain an alloy with a specific composition and appearance, the plating solution composition should be kept within tight limits and the whole process has to be strictly monitored. Any change in the bath parameters: e.g.: cyanide or hydroxide concentration, bath temperature, etc. would lead to an unsatisfactorily alloy with a completely different composition and / or appearance.

Also, studies reported in previous sections showed that an Cu - Zn - Sn alloy plated from baths in which the metal concentrations in solution was varied, not only had a different metal ratio, but often a different color. Moreover, voltammetric responses from such solutions were different. As a result, the need for a deeper knowledge of the electrochemical behavior of each metal ion in an alkaline cyanide solution emerged. For this, solutions which contained only Cu(I), Zn(II) or Sn(IV) were investigated by voltammetric techniques.

3.6.1 The reduction of Sn ion in an alkaline - cyanide bath

Studies of the Sn(IV) reduction were performed at brass strip electrodes in a solution with the following composition:

	$g\ l^{-1}$	mM
$Na_2[Sn(OH)_6]$	5.7	24
Na_2CO_3	6.5	61
free NaOH	2.1	50
free NaCN	25	551
Copper Glo solution	5.0	

The free cyanide / free hydroxide ratio has been kept at the same value as the solution on the plating line and the same additive addition had been made. Also, the bath have been operated at the same temperature as the plating line: 333 K.

3.6.1.1 Cyclic voltammetric experiments

Figure 3.35 shows a cyclic voltammogram recorded at a brass strip electrode from an electrolyte with the above composition. In this experiment, the potential was scanned between -1250 mV to -2000 mV vs. SCE at 20 mV s^{-1}.

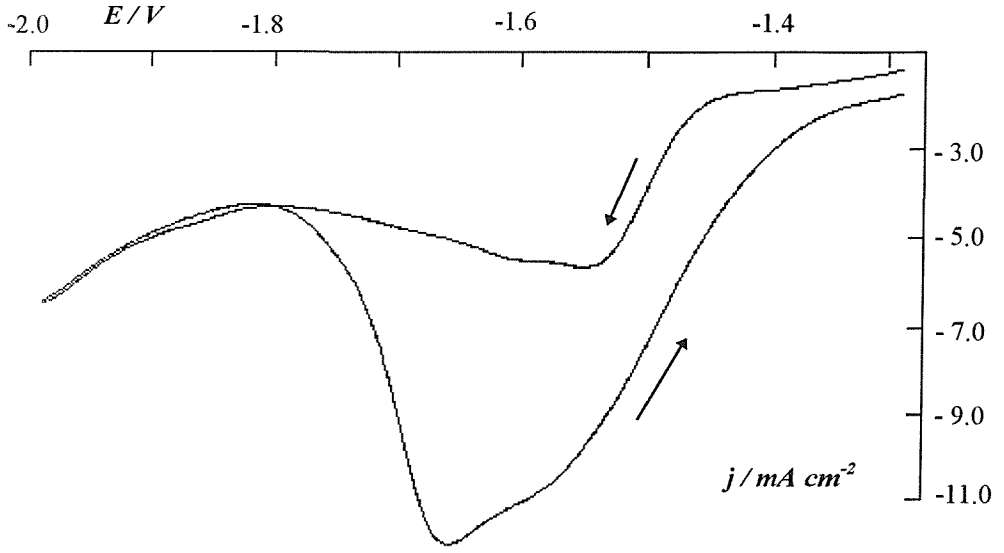

Figure 3.35 - Cyclic voltammogram recorded at a brass strip electrode from a solution containing Sn(IV), NaCN, NaOH, Na_2CO_3 and Copper Glo. Scan rate 20 mV s^{-1}

One main feature is observed on the forward scan consisting of a well defined but slightly peaked reduction wave of j_L = 5.5 mA cm^{-2} at $E_{1/2}$ = -1500 mV. This reduction wave is associated with tin deposition as a tin coat covered the electrode surface even when the

potential was scanned between -1250 mV to -1600 mV (see Table 3.10). Hydrogen was also seen evolving at a potential of around E = -1600 mV. This is not surprising since it is known that tin metal it is a good catalyst for hydrogen evolution. The back scan shows a large reduction peak of j_P = -11 mA cm^{-2} at E_P = -1650 mV during which vigorous hydrogen evolution was seen taking place. This could be the response at tin metal as a layer of metal was covering the electrode surface at the end of the forward scan. At the completion of this scan the deposit obtained had a milky, dull appearance.

Potential limits / mV	*deposit appearance*
-1250 : -2000	milky
-1250 : -1900	fairly milky
-1250 : -1800	reflecting, uniform
-1250 : -1700	reflecting, uniform
-1250 - -1600	reflecting but thin

Table 3.10 *- shows the deposit appearance when the potential have been cycled between different limits*

Table 3.10 shows data recorded during cyclic voltammetric experiments with different negative potential limits. A nice, shiny deposit was obtained only when the potential limit was restricted to -1800 mV. The milky deposit therefore results either from the rate of Sn deposition being too high to obtain a highly ordered deposit structure or from the influences of hydrogen evolution.

In the absence of the Copper Glo, a voltammogram between -1250 mV and -2000 mV showed no clear features, only a slow increasing current density (~ 7.0 mA cm^{-2} at a potential of -2000 mV) but the deposition of tin could be seen to occur. Indeed, the appearance was very similar to that in the presence of the additive.

3.6.1.2 Steady state experiments

In these experiments the electrode was plated with tin at a fixed potential for either 30 s or 120 s. During these experiments the steady state current density and also the deposit appearance was noted.

$E_{dep.}$ / V	i_L / mA cm^{-2}	*deposition time 120 s*	*deposition time 30 s*
-2.1	15.0	hazy	hazy
-2.0	6.7	hazy	hazy
-1.9	3.4	hazy	hazy
-1.8	2.3	hazy	shiny
-1.7	8	hazy	shiny
-1.6	8	little hazy	shiny
-1.5	5.3	shiny	shiny, but thin

Table 3.11 - Potential step experiments performed at different deposition times: 120 s or 30 s.

Table 3.11 shows the data collected from such studies. It can be seen that there is an agreement between data in this table and data presented in Table 3.10. When the electrodeposition is performed at negative potentials (e.g.: -2.0 V to -1.8 V) a milky, dull deposit is obtained regardless of the deposition time. With more positive potentials, the deposit is initially shiny and reflecting. However, even at this potential values, a milky deposit can be obtained if the deposition continues for longer periods of time so that a thick deposit is obtained.

3.6.1.3 Chronopotentiometric experiments

The chronopotentiometric response was recorded at several current densities. At a current density of 6 mA cm^{-2}, the potential rapidly relaxes to -2050 mV . The same potential - time response is recorded when higher current densities are applied. It was found that tin deposits

easily and rapidly at current densities higher than 2 mA cm^{-2}. At short times tin deposits are reflecting. In other conditions the deposits appear uniform but have a milky appearance.

3.6.1.4 Potential step experiments

In these experiments the nucleation and early growth of a tin layer was studied by the means of potential steps technique. Current / time transients have been recorded in a series of potential steps in which the potential was stepped from -1250 mV to values in the range -1320 mV to -1450 mV. Figure 3.36 shows that even if these potentials are well positive compared to the reduction wave on the cyclic voltammogram (figure 3.35), tin deposition occurs although at a low rate.

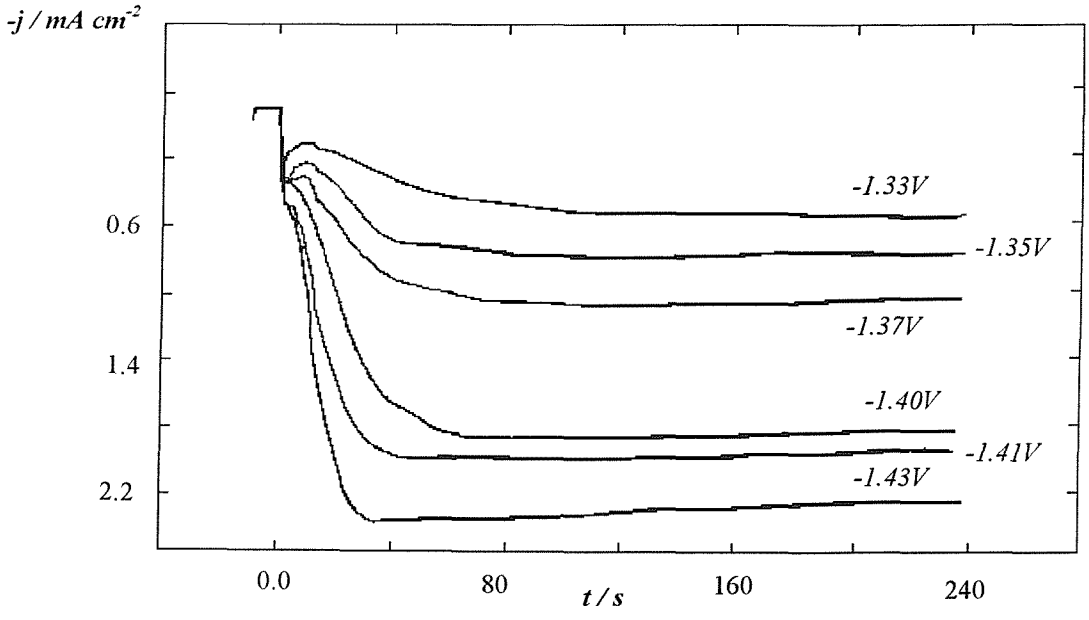

Figure 3.36 - I/t transients during a series of potential step experiments performed at a solution containing tin ions

At each potential there is an early fall in current followed by an increase in the cathodic current over a time scale of 30 - 50 s until a steady state is reached. The time scale for the rise in current is shortened as the potential is made more negative.

The transients recorded at low potential steps over a period of 40 s show a normal behavior for nucleation and growth of the deposit. The early part of the rising transient could be fitted to linear $I^{1/3}$ vs t plots as expected for continuous nucleation and three dimensional growth of centers under electron transfer control (figure 3.37).

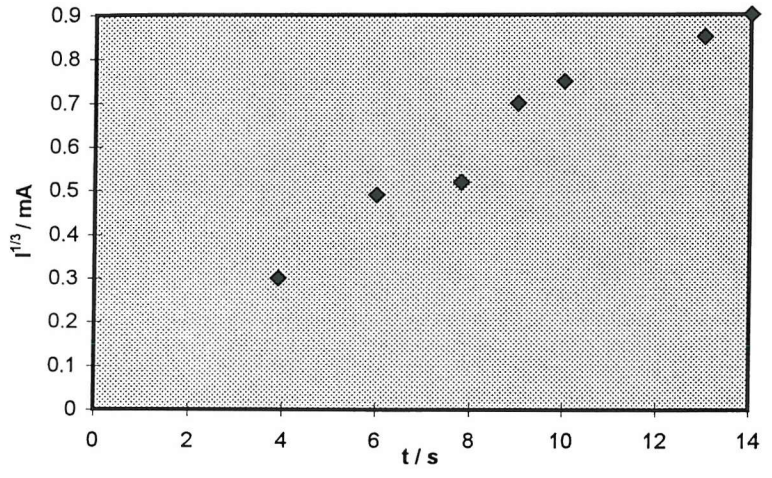

Figure3.37 $I^{1/3}$ / t *plots recorded at a potential step of -1400 mV*

3.6.2 Studies of solutions containing only Zn ions

Studies of the Zn(II) reduction have been carried out in a solution composed of:

	g l^{-1}	mM
$Zn(CN)_2$	5.4	46
Na_2CO_3	6.5	61
free NaOH	2.1	50
free NaCN	25	551
Copper Glo solution	5.0	

These experiments have been performed at brass strip electrodes of A = 1 cm^2 As on the plating line, the solution have been heated to 333 K.

3.6.2.1 Cyclic voltammetry

The cyclic voltammetry of the solution containing only Zn(II) generally gave rather featureless responses. On the forward scan, the current density increased smoothly and reached 15 mA cm^{-2} at - 1900 mV.

3.6.2.2 Deposition at constant potential

In these experiments, zinc metal has been deposited at different fixed potentials for various times until a layer of zinc was deposited onto the electrode surface.
Table 3.12 reports data collected during these studies. It could be seen that low current densities were observed at all potentials studied.

E_{DEP} / V	$j_{s.s}$ / mA cm^{-2}	deposition time / s	deposit appearance
-2.2	7	120	reflective
-2.1	4.3	300	reflective
-2.0	2	480	reflective
-1.9	1.6	540	reflective, thin
-1.8	3	600	reflective, thin

Table 3.12 *showing data recorded during a series of potential step experiments in a solution containing zinc ions*

A current density of 7 mA cm^{-2} was recorded at -2200 mV. At -2000 mV, the current density reached was only 2 mA cm^{-2}. Zinc is a poor H_2 evolution catalyst compared to Sn or Cu and this probably contributes to the lower current densities. Also, at -1800 mV the deposit obtained was very thin in spite of the long deposition time of 600 s.

3.6.2.3 Chronoamperometric experiments

Very unusual current - time transients have been recorded during these experiments (figure 3.38). At -1400 mV and -1500 mV the transients have the shape of symmetrical peaks, with charges far too large to be considered monolayers of material on the electrode surface. It could be possible that zinc deposition is later on inhibited by some other processes occurring at the electrode surface - e.g. additive adsorption. Also, small steady state currents were observed at the potentials studied (table 3.13)

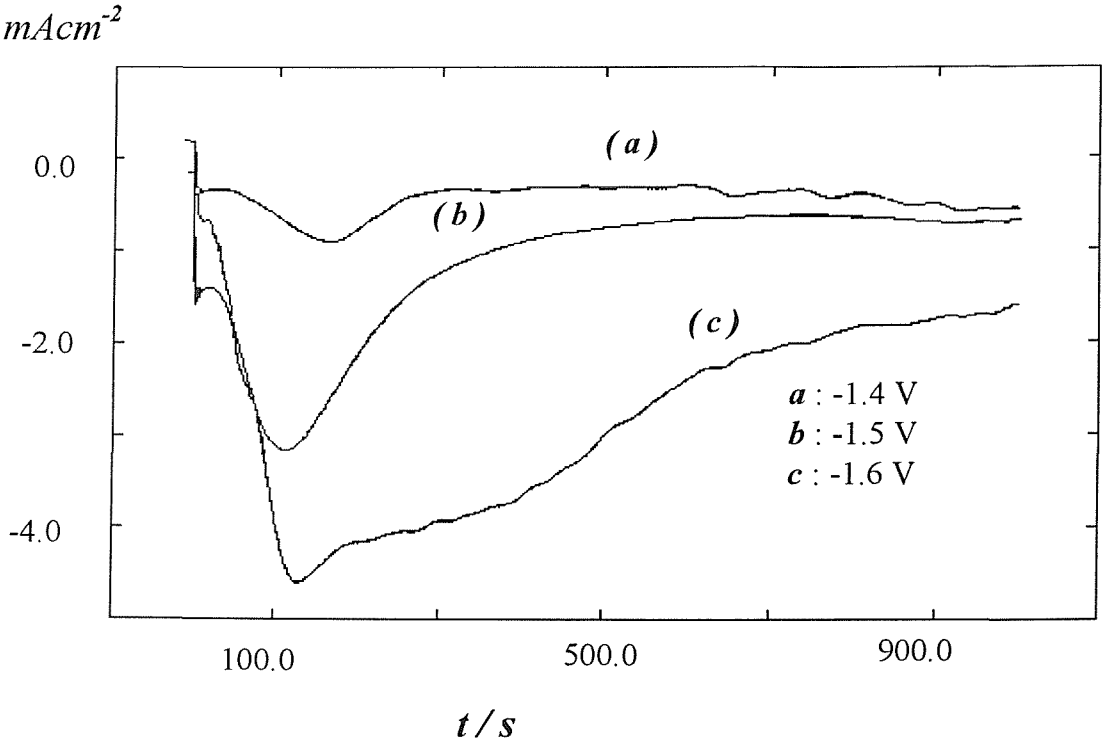

Figure 3.38 *I / t transients during potential step experiments performed at brass electrode from a solution containing Zn ions*

Transients recorded from solutions which did not contain Copper Glo did not show any of the peaks seen in figure 3.38 . The currents recorded from such solution were in the region of 0.4- 0.8 mA cm^{-2}

E_{dep} / V	$j_{s.s}$ / mA cm^{-2}	time / s	Appearance
-1.4	-0.5	1000 s	no deposit
-1.5	-0.7	1000 s	no deposit
-1.6	-2.0	1000 s	very thin deposit
-1.7		1000 s	thin deposit
-1.8		1000 s	reflective deposit

Table 3.13- *showing the steady state current in a series of potential step experiments performed in a solution containing zinc ions and additive*

3.6.2.4 Chronopotentiometry

When performed at fixed current, the deposition of zinc seems very slow to commence and it deposits at a slower rate than the other two metals. At a current density of 6 mA cm^{-2}, the steady state potential is reached after as long as 200 s..

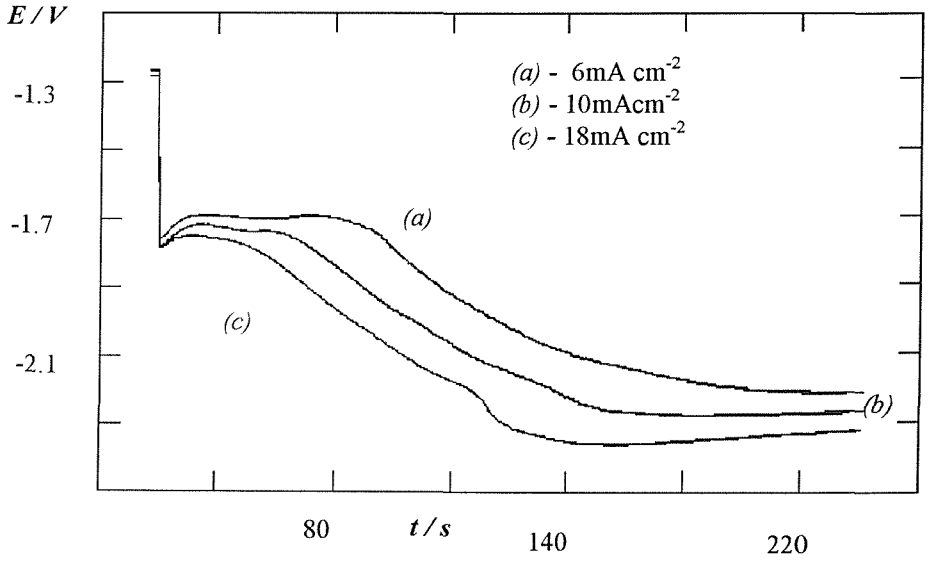

Figure 3.39 *- The change of potential in time for Zn electrodeposition at a fixed current density*

Despite the absence of current in the potential range around -1700 mV during voltammetry, the potential appears to remain in this potential range for over 50 s even at -18 mA cm^{-2}. The reasons for this behavior it is not clear.

3.6.3 Studies of solutions containing only Cu(I) ions

The electrochemistry of copper cyanide was monitored by the means of voltammetric experiments. The solution studied was composed of:

	$g\ l^{-1}$	mM
CuCN	9.1	102
Na_2CO_3	6.5	61
free NaOH	2.1	50
free NaCN	25	551
Copper Glo solution	5.0	

These experiments have been carried out at brass strip electrodes and the electrolyte has been thermostated at 333 K in a cell with a mantle.

3.6.3.1 Cyclic voltammetric experiments

Figure 3.40 shows a cyclic voltammogram recorded at a brass strip electrode. No clear features can be noted on this voltammogram. A sharp rise in the reduction current is recorded in the potential window studied. Also, hydrogen evolution started at -1700 mV and it become very vigorous towards the negative limit of -2000 mV.

The back scan does not show any oxidation peak and this shows the irreversibility if the process studied. After a complete scan a thin layer of copper metal was deposited onto the electrode surface. A large portion of the massive current density recorded at more negative potentials results from the hydrogen evolution.

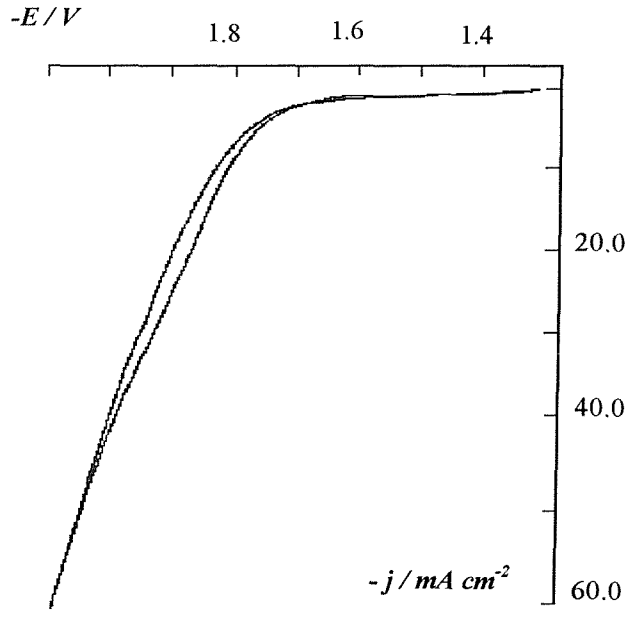

Figure 3.40- *cyclic voltammogram recorded at a brass electrode from a solution containing copper ion*

No copper was seen on the electrode surface when the potential was scanned between -1250 mV and -1900 mV or less. Same results were recorded when experiments were carried out from solutions without Copper Glo.

3.6.3.2 Steady state experiments

During these experiments a layer of copper metal was deposited onto the electrode surface at a fixed potential and then the potential was scanned back to -1250 mV. This scan was

found to have the same shape as the back scan on the cyclic voltammogram (figure 3.40). Very high current densities were recorded at all potentials studied. Also, the deposition time was increased as the deposition potential was made less negative. For instance, if at -2100 mV and -2000 mV only one minute was needed to deposit a nice deposit, at -1700 mV after seven minutes only a thin deposit was obtained (table 3.14).

E_{DEP} / V	$j_{S.S}$ / mA cm^{-2}	Deposition time / s	Deposit appearance
-2.2	75.5	60	uniform
-2.1	-	60	uniform
-2.0	41.3	60	uniform
-1.9	23	60	uniform
-1.8	6	360	uniform
-1.7	1.5	420	uniform but thin

Table 3.14 -showing data recorded from a set of potential step experiments at a solution containing copper ions and additive

3.6.3.3 Chronopotentiometric experiments

In this section the copper was deposited at fixed current densities for a period of 500 s and the potential / time response was monitored. Figure 3.41 shows that at 6 mA cm^{-2}, the steady state potential is reached only after a long period of time of about 300 s. It is possible that other electrode reactions than the nucleation and growth of copper occur in the first 300 s. This fact combined with the visible hydrogen evolution could explain why the copper deposits are so thin compared to expectations based on charge passed.

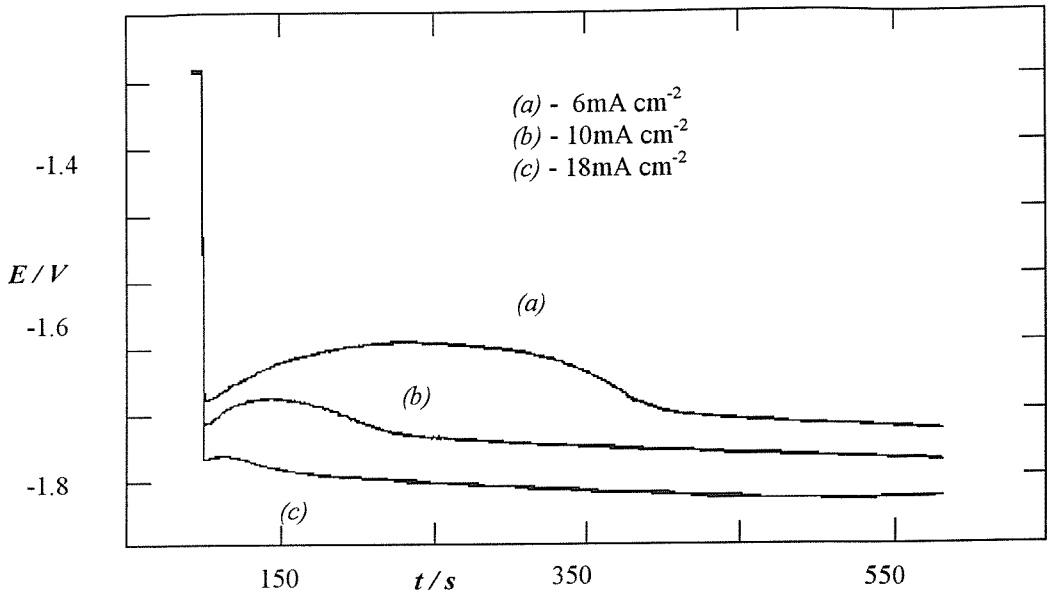

Figure 3.41 *- The change of potential in time for Cu electrodeposition at a fixed current density*

With higher current densities, copper deposits more rapidly and at a much lower steady state potential than required for Zn and Sn (table 3.15). Also, hydrogen evolution was becoming much vigorous with higher current densities.

current density / mA cm^{-2}	$E_{s.s}$ / V	time to observe deposit / s	H_2 evolution
6	-1.8	250	little
10	-1.85	100	vigorous
18	-1.9	45	very vigorous

Table 3.15*- Data showing the steady state potential with applied current density*

3.6.3.4 Potential step experiments

Over the potential range -1400 mV to -1600 mV, transients were featureless and very low currents were observed.

3.6.4 Conclusions

- It was shown that only the electrochemistry of tin is strongly influenced by the presence of the Copper Glo. The large reduction currents recorded from such solutions are associated with the hydrogen evolution which occurs in the wave region. No such major features are recorded in the absence of the additive or from solutions that contains zinc or copper ions only.

- Tin itself deposits easily even at potentials as low as -1500 mV. Milky, dull deposits are obtained at deposition times of 120s. However, these deposits can be reflecting and uniform if the plating time is shortened to 30 s.

- Copper and zinc deposit very slowly and at more negative potentials than the tin. For instance, at a deposition potential of -1800 mV, it takes 360 s for Cu and 600s respectively for Zn to plate a thin deposit.

- Sn has a critical role in allowing the deposition of the alloys.

3.7 The effect of metal concentration on the alloy deposition

A Cu - Zn - Sn cyanide bath can be used to electrodeposit alloys with a large range of compositions that satisfy different applications for metal coatings[18]. The different alloy compositions depend mainly on the metal ion concentration in solution as well as on other bath parameters - as studied in previous chapters.

The alloy studied in this project has several favorable properties. Firstly, unlike the other brasses it has a white, tarnish resistant color. Also, because of its non-magnetic properties as well as a good conductivity of radio frequency signals, it is suitable for electronic components. Lastly, its good mechanical properties such as its scratch-resistance and good abrasion-resistance make it employable for long periods of time before requiring replacement. Several papers in the literature[17-20] report that an alloy with 55-60 % copper, 10-20 % zinc and 20-30 % tin has such properties. However, the alloy studied in this project has a slightly different composition, which, as stated in Chapter I, is within the range: 47 - 51 % copper, 8 - 12 % zinc and 38 - 43 % tin. As a result of this discrepancy, a deeper investigation of the effect that changes in the metal ion concentrations have on the alloy composition, its appearance and electrochemistry was necessary.

The experiments carried out in this section were performed from solutions in which the concentration of one metal only was increased / decreased at the time. The concentration of the other two metals and of all other bath components were maintained constant. Voltammetric, SEM and EDS techniques were employed in such studies. The electrodes were made of brass or silver coated brass material. The experiments were performed at 333 K.

3.7.1 Cyclic voltammetry

3.7.1.1 Cyclic voltammetric studies on solutions containing high / low concentration of copper ions

The alkaline cyanide solutions employed in this section had concentrations of copper cyanide which were 0.5 and 1.5 the Cu(I) content of the standard bath.

	$g\ l^{-1}$	mM
CuCN	4.55 or 13.65	51 or 153
$Zn(CN)_2$	5.4	46
$Na_2[Sn(OH)_6]$	5.7	24
Na_2CO_3	6.5	61
free NaOH	2.1	50
free NaCN	25	551
Copper Glo solution	5.0	

Cyclic voltammograms have been performed at brass electrodes from the above solutions. The potential have been scanned between -1250 mV to -2000 mV vs SCE at a 20 mV s^{-1} scan rate. The potential - current response recorded from these two solutions is shown in Figures 3.42 a,b. When the plating bath is low in copper cyanide, two main reduction features are recorded on the forward scan. A well defined reduction wave of j_L = -4 mA cm^{-2} recorded at $E_{1/2}$ = -1450 mV, is followed by a second reduction peak of j_P = -2 mA cm^{-2} at E_P = -1650 mV. This wave is positive by -150 mV compared to the first reduction feature in the standard bath. Close to this peak, hydrogen evolution was seen evolving. During the back scan a large reduction peak of j_P = -8 mA cm^{-2} is recorded at E_P = -1580 mV. The large height of this peak results mainly from hydrogen evolution which was evolving vigorously in this region. Such peaks on the reverse scan again show the complexity of the deposition process in a solution low in copper cyanide. The deposit obtained after a complete potential

cycle had a yellow color; this shows that a completely different alloy is deposited from such solutions. Voltammograms recorded after a few complete scans showed a much larger reduction peak of about -14 mA cm^{-2}. This could be explained by the different response given by the yellow alloy compared to the brass electrode.

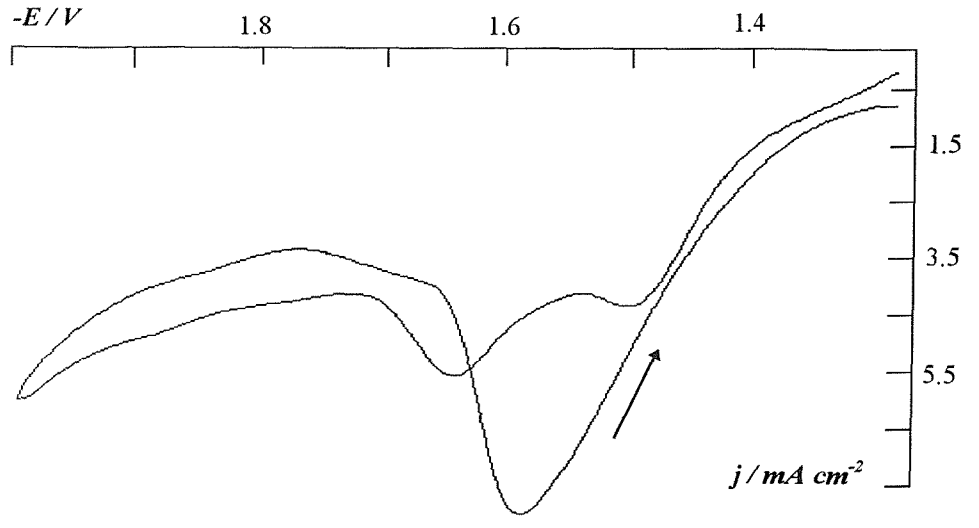

Figure 3.42 a *- Cyclic voltammogram recorded from solutions low in copper ions. Working electrode: brass strip, Reference electrode: SCE, scan rate: 20 mV* s^{-1}*. T = 333 K*

A totally different response is recorded from a plating solution high in copper cyanide (figure 3.42 b). A well defined reduction wave of j_L = -3 mA cm^{-2} is obtained at $E_{1/2}$ = -1600 mV. The back scan shows a drawn out reduction wave which resembles the back scan recorded from a standard plating solution. The current is always lower than for the solution with 4.55 g l^{-1} CuCN and this also suggests that not all the current observed on voltammograms is for metal deposition. During the potential cycle, no hydrogen was seen evolving. With this solution, the brass electrode was covered completely with a film of white alloy.

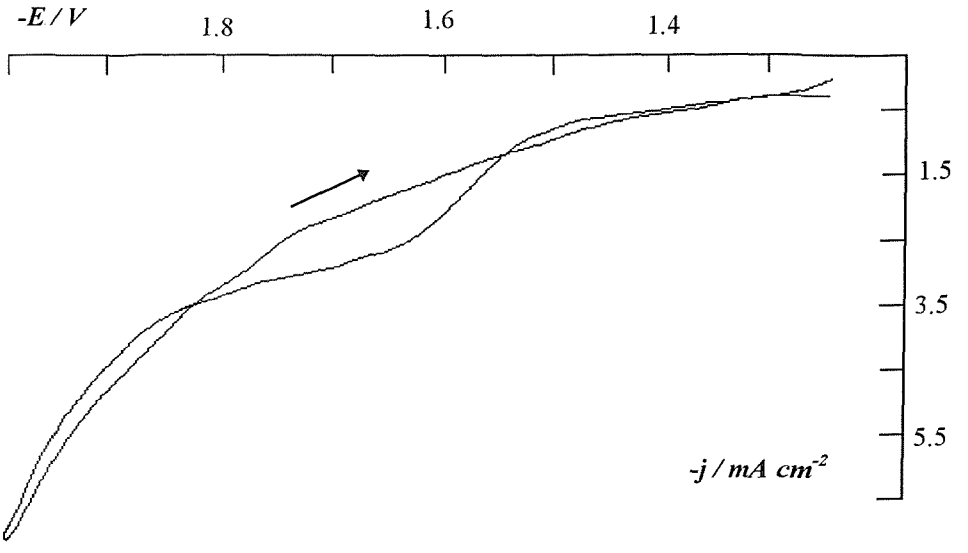

Figure 3.42 b *- Cyclic voltammogram recorded from a solution high in copper ions. Working electrode: brass strip, Reference electrode: SCE, scan rate: 20 mV s^{-1}. T = 333 K*

The electrochemistry changes with the copper cyanide concentration. This can be seen both from the voltammetry and the appearance of the deposit.

3.7.1.2 Cyclic voltammetric studies on solutions containing high / low concentration of tin ions

Cyclic voltammetric studies have been performed on cyanide solutions which contained 0.5 and 1.5 concentration of sodium stannate in the standard solution. These solutions had one of the following concentrations:

	g l^{-1}	mM
CuCN	9.1	102
$Zn(CN)_2$	5.4	46
$Na_2[Sn(OH)_6]$	2.85 or 8.4	14 or 42
Na_2CO_3	6.5	61
free NaOH	2.1	50
free NaCN	25	551
Copper Glo solution	5.0	

The cyclic voltammetric studies have been carried out at fresh brass electrodes at 333 K. The potential has been scanned between the same limits: -1250 mV and -2000 mV vs. SCE at a scan rate of 20 mV s^{-1}. Figures 3.43 a,b, show the current potential response recorded from such solutions. It could be seen that both figures have a common feature consisting of a reduction wave / peak at $E_{1/2}$ = -1600 mV.

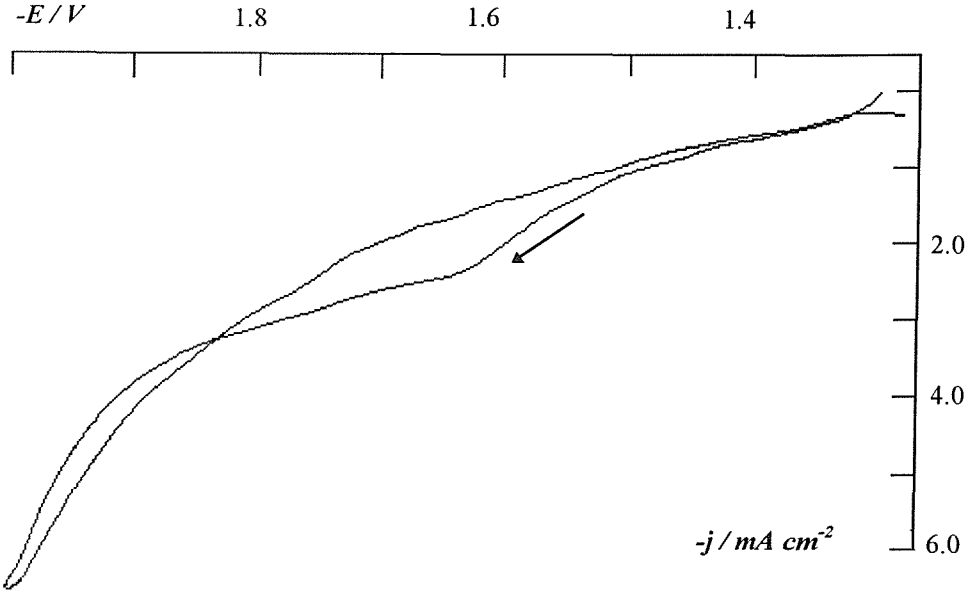

Figure 3.43 a *- Cyclic voltammogram recorded at brass strip electrodes from solutions containing low tin ions. Working electrode: brass strip, reference electrode: SCE, scan rate: 20 mV s^{-1}. T: 333 K*

When the plating bath is low in sodium stannate, a drawn out reduction wave of j_L = -2.5 mA cm^{-2} is recorded at $E_{1/2}$ = -1600 mV. No hydrogen evolution was observed evolving until towards the negative limit.

A much higher reduction current is recorded from a solution high in Sn(II) - figure3.43b. This current takes has the shape of a reduction peak of j_L = - 5.5 mA cm^{-2} and could be partially attributed to hydrogen evolution which was evolving in this region.

The back scan of both solutions resembles the back scan of a standard plating solution. With both solutions, after a complete cycle the surface of the electrode was covered with a complete film of reflective and uniform alloy.

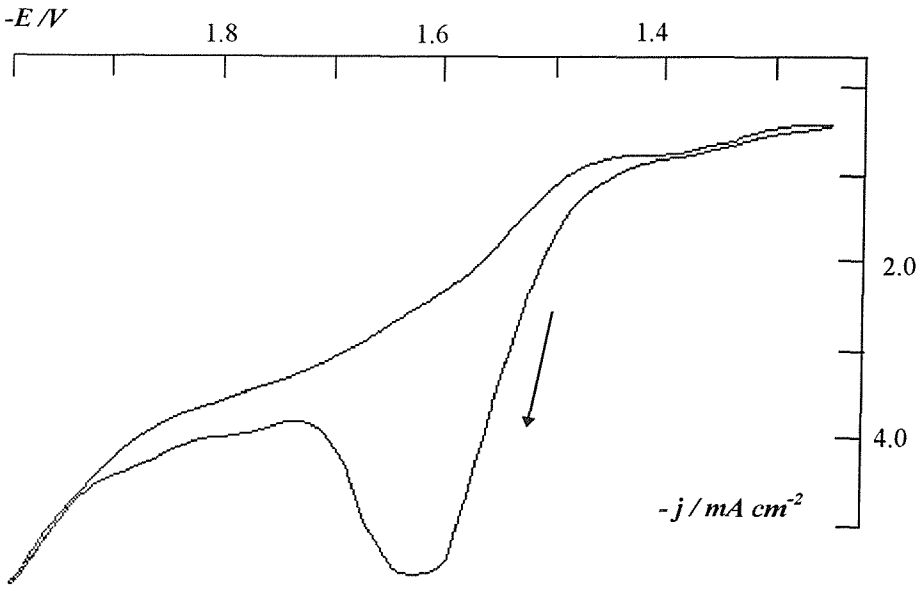

Figure 3.43 b - Cyclic voltammograms recorded at brass strip electrodes from solutions containing high tin ions. Working electrode: brass strip, reference electrode: SCE, scan rate: 20 mV s^{-1}. T: 333 K

3.7.1.3 Cyclic voltammetric studies from solutions containing high / low concentration of zinc ions

In this section, the experiments have been carried out from cyanide solutions which contained 0.5 and 1.5 the concentration of zinc cyanide that in the standard bath. These solutions had one of the following concentrations:

	$g\ l^{-1}$		mM	
CuCN	9.1		102	
$Zn(CN)_2$	2.7	7.7	23	69
$Na_2[Sn(OH)_6]$	5.6		28	
Na_2CO_3	6.5		61	
free NaOH	2.1		50	
free NaCN	25		551	
Copper Glo solution	5.0			

This studies have been performed at brass electrodes by scanning the potential between -1250 mV to - 2000 mV vs. SCE at a scan rate of 20 mV s^{-1}. Figures 3.44 a, b show the response obtained from the above two solutions.

When the plating was performed in a solution low in zinc cyanide, a small reduction peak of j_L = -2.7 mA cm^{-2} was recorded at E_P = -1500 mV. This peak could be attributed equally to metal deposition as well as to hydrogen evolution which was evolving at the electrode surface. Then, a second reduction wave with a well defined plateau of 1 mA cm^{-2} occurs at $E_{1/2}$ = -1600 mV.

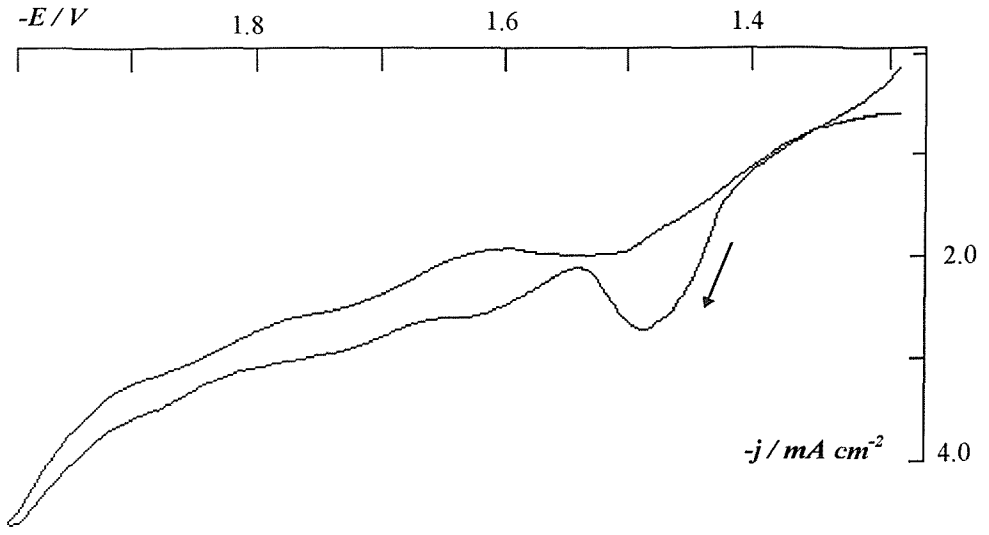

Figure 3.44 a *- Cyclic voltammogram recorded at brass electrodes from solutions low in zinc ions. Working electrode: brass strip, Reference electrode: SCE, scan rate: 20 mV* s^{-1}

More drawn out reduction waves were recorded from solutions high in zinc ion -figure 3.44b. There is a first wave of 2.5 mA cm^{-2} which occurs at $E_{1/2}$ = -1550 mV followed by another one of the same value at $E_{1/2}$ = -1800 mV.

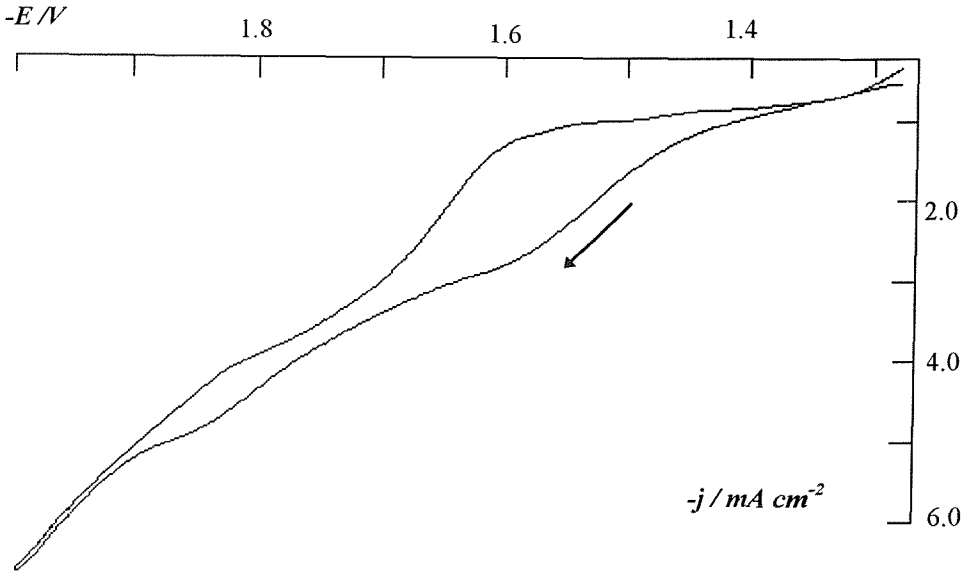

Figure 3.44 b *- Cyclic voltammogram recorded at brass electrodes from solutions high in zinc ions. Working electrode: brass strip, Reference electrode: SCE, scan rate: 20 mV* s^{-1}

A complete layer of alloy covered the electrode surface after the completion of a full potential scan. It was noted also, that the amount of hydrogen evolving in these experiments was far less that in the standard bath.

3.7.2 SEM

Hull cell panels as well as silver coated brass strips have been plated from solutions in which the metal concentration have been increased / decreased one at the time. These samples have been analyzed visually as well by the means of the scanning microscopy. Also, the composition of each alloy was estimated with the aid of the EDS technique.

The Hull cell panels plated from alkaline-cyanide solutions low in copper cyanide had a hazy deposit in the region of the plate corresponding to j = 6 mA cm^{-2}. Also, the micrograph showed a rough deposit composed of globular grains of about 0.25 μm diameter - figure 3.45. Such deposits were found to have a high tin content with the composition Cu - Zn - Sn of 30 - 7 - 63.

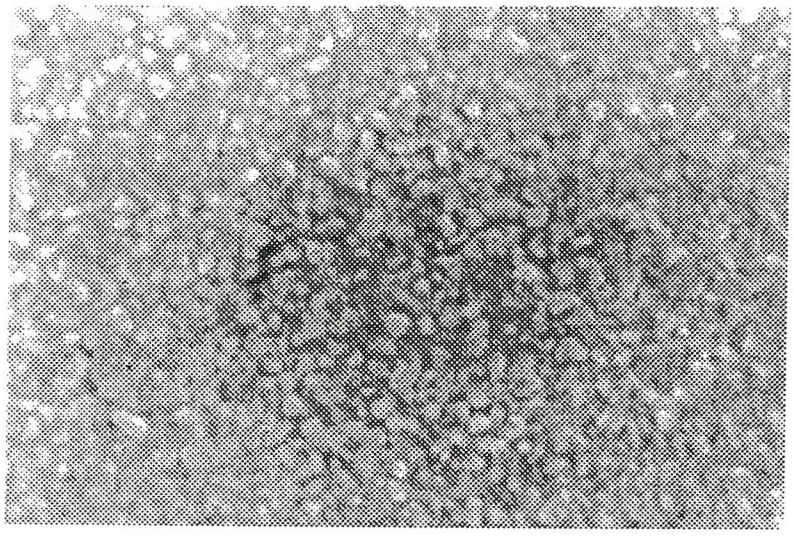

Scale : ⟷ 1 μm

Figure 3.45 *- SEM of a Hull Cell sample at the position of 6 mA cm^{-2} plated from a solution low in copper cyanide*

When the plating bath was high in copper cyanide the whole area of the Hull cell panel was covered with a yellow deposit. This deposit was becoming reddish towards the side corresponding to a high current density. When the region of the plate corresponding to j = 6 mA cm^{-2} was analyzed, the alloy was found to have a high copper content and low tin

content with the composition: Cu - Zn - Sn of 63 - 6 - 31. The micrograph - figure 3.46 - showed a poor deposit composed of scattered clusters of grains of about 0.5 μm diameter.

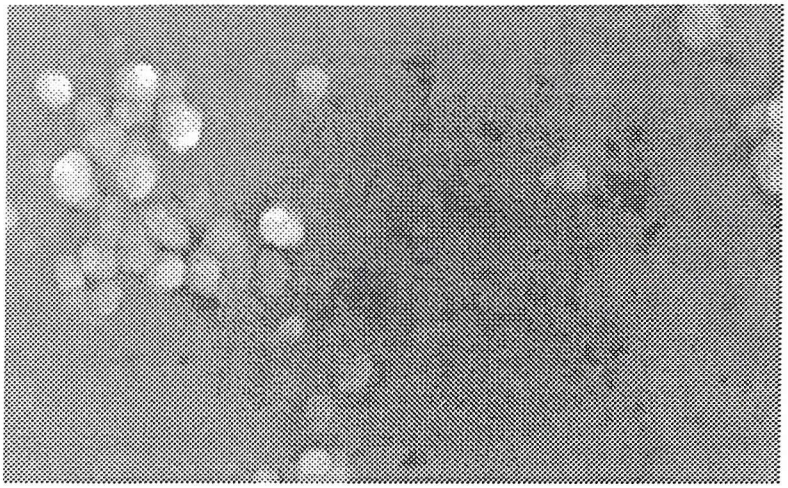

Figure 3.46 *- SEM of a Hull Cell sample at the position of 6 mA* cm^{-2} *plated from a solution high in copper cyanide*

Scale: ⟷ 1 μm

When the plating was carried out from an alkaline-cyanide bath high in sodium stannate, the Hull cell test led to a hazy deposit covering the center of the panel. The deposit corresponding to j = 6 mA cm^{-2} - figure 3.47 - was found to be granulated and formed of angular spherulites with the composition Cu - Zn - Sn of 43 - 7 - 50.

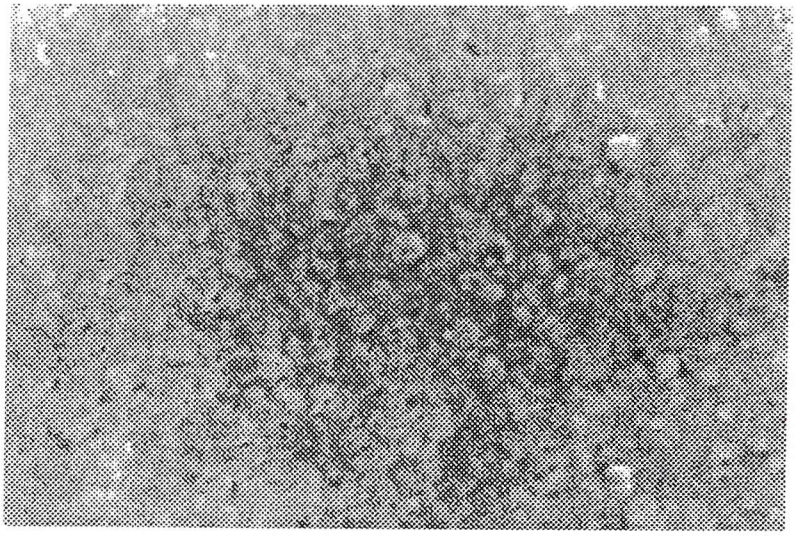

Figure 3.47 *- SEM of a Hull Cell sample at the position of 6 mA* cm^{-2} *plated from a solution high in sodium stannate*

Scale: ⟷ 1 μm

An alloy plated from a solution low in tin had the same appearance as the one obtained from a solution high in copper. The Hull cell test showed the same reddish deposit on the side corresponding to a high current density. The composition of the deposit corresponding to 6 mA cm^{-2} was found: Cu - Zn - Sn of 65 - 8 - 27.

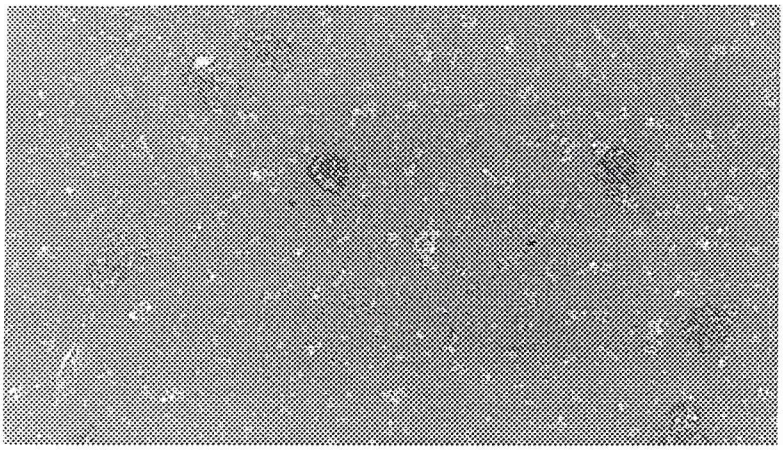

Figure 3.48 *- SEM on a less sensitive scale of a Hull Cell sample at the position of 6 mA* cm^{-2} *plated from a solution low in sodium stannate*

Scale: ⟷ 10 μm

Also, this deposit was formed of the same scattered clusters of grains - figure 3.48.

The best deposit was obtained from solutions high in zinc cyanide, which was very highly reflecting. The composition found in such alloys was found to be close that from the standard bath. However, the micrograph - figure 3.49 - did not show a featureless deposit, as expected, but one scattered with small grains of 0.1 μm diameter.

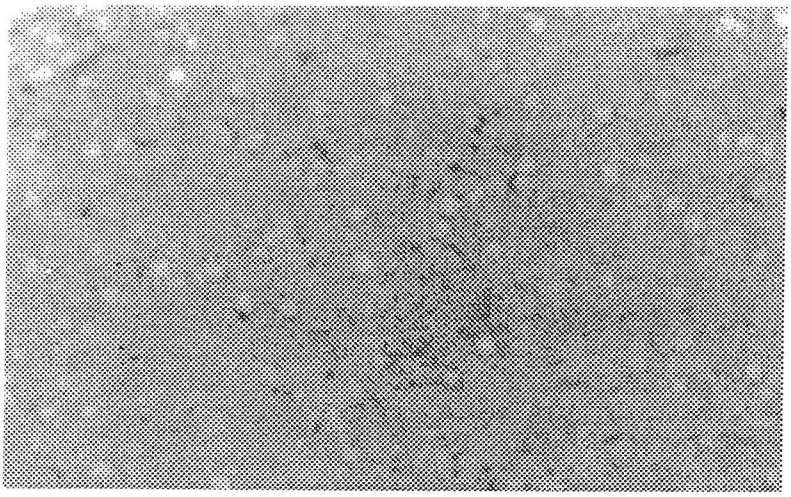

Figure 3.49 *- SEM of a Hull Cell sample at the position of 6 mA* cm^{-2} *plated from a solution high in zinc cyanide*

Scale: ⟷ 1 μm

An alloy plated from a solution low in zinc cyanide showed a high tin content and a rough grainy deposit - figure 3.50.

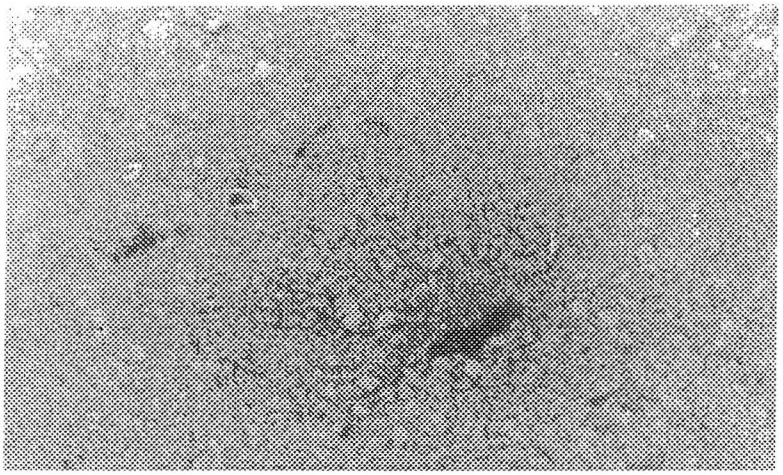

Figure 3.50 *- SEM of a Hull Cell sample at the position of 6 mA* cm^{-2} *plated from a solution low in zinc cyanide*

Scale: ⟷ 1 μm

It could be concluded therefore that the plating bath is much more tolerant to changes in zinc but less to the other two metal ions. When the bath has an increased amount of zinc cyanide, an alloy similar to the one studied in this project is obtained. Otherwise, alloys with completely different compositions and appearance are obtained.

Table 3.16 shows data collected from such experiments. It can be seen that there is a good agreement Hull cell experiments and experiments carried out at brass strip electrodes.

	STRIP			Hull Cell		
	Cu	**Zn**	**Sn**	**Cu**	**Zn**	**Sn**
1.5 Cu	62	7	31	63	6	31
0.5 Cu	32	10	58	30	7	63
1.5 Sn	45	8	47	43	7	50
0.5 Sn	62	9	29	65	8	27
1.5 Zn	53	15	32	52	12	36
0.5 Zn	52	4	44	50	2	47

Table 3.16*-data collected from Hull cell samples and brass strip samples with silver undercoat. The current density: 6 mA* cm^{-2}.

3.7.3 Conclusions

- The voltammetry of the plating bath changes with the metal concentration. Large reduction peaks are recorded when the solution is low in copper or high in tin. In the other situations, the peaks take the form of nice reduction waves with well defined plateau. The results are consistent with the voltammetry being determined mainly by the Cu(I)/Sn(IV) ratio.

- The peak close to -1600 mV previously associated with hydrogen evolution, is only observed when deposits have a high tin content and the additive is present.

- Deposits with different compositions were plated from these solutions. As a rule, an increase/ decrease in the plating bath metal concentration leads to an increase / decrease of the metal. However, an increase in zinc concentration does not seem to produce dramatically large changes in the metal ratio.

	Cu %	*Zn %*	*Sn %*
0.5 Cu	30-32	7-10	58-63
1.5 Cu	62-63	6-7	31
0.5 Zn	50-52	2-4	44-47
1.5 Zn	52-53	12-15	32-36
0.5 Sn	62-65	8-9	27-29
1.5 Sn	43-45	7-8	47-50

Table 3.17 - the change in alloy composition with metal concentration

- The structure of the alloy changes with the metal ratio(table 3.17). A deposit that is high in copper and low in tin is composed of clusters of spherulites which are scattered over a featureless layer of alloy. This leads to a deposit with dark appearance. On the contrary, a

deposit which is low in copper and high in tin is very rough and is composed of compacted circular grains of about 0.25 μm diameter. This is the "milky" deposit seen on the plating line in some conditions.

3.8 The effect of carbonate concentration on alloy composition

The role of the carbonates in the plating bath is to provide buffering in the solution layer close to the cathode and to contribute to conductivity [44]. During its life time the plating bath becomes more concentrated in carbonate as a result of reaction between the CO_2 from the atmosphere and hydroxide. Studies carried out in this section aim to identify how a change in the carbonate concentration would affect the plating process.

3.8.1 Cyclic voltammetry

Cyclic voltammetric experiments have been carried on solutions with the standard bath composition and also solutions where the concentration of sodium carbonate have been varied to: 3.25 g l^{-1}, and 26 g l^{-1}. The same potential current response was recorded with all these solutions. The voltammetry had identical characteristics to that for a standard solution and it was reported in section 3.1 (figure 3.1A). Reflective, uniform alloys were plated from all solutions during a single potential cycle..

3.8.2 EDS

The composition of alloys plated from standard solutions with 6.5 gl^{-1}, and 20 gl^{-1} sodium carbonate have been analyzed with the aid of EDS technique. The alloys have been plated on brass strip electrodes with a silver undercoat at E = -2050 mV for 120 s. Some of the samples were also cut out from Hull Cell panels plated at I = 2 A for120 sec.

The table 3.18 shows the composition of such samples.

Na_2CO_3 / g l^{-1}	Conditions	Cu / %	Zn / %	Sn / %
6.5	Ag undercoat brass strip. E = -2050 mV for 120 s	51	8	41
6.5	Hull Cell deposition j = 6 mA cm^{-2} for 120 s	51	7	42
20.0	Ag undercoat brass strip. E = -2050 mV for 120 s	51	8	41
20.0	Hull Cell deposition j = 6 mA cm^{-2} for 120 s	50	7	43

Table 3.18 *- studies of the variation of alloy composition with carbonate concentration*

Data in table 3.18 shows that there is no change in the alloy composition with the increase in carbonate. This was the case with both electrode strips and Hull Cell panels.

3.8.3 Conclusion

- No change in voltammetry was found in plating baths with different carbonate concentrations.

- An increase in the carbonate does not affect the alloy metal ratio.

3.9 Studies of the aging of the electroplating bath

The effect of the bath age on the plating process was studied by the means of cyclic voltammetry and EDS analysis. Fresh standard solution was prepared and cyclic voltammograms were run with a fresh solution, after the solution was 1 day old and then two weeks old. The free cyanide - hydroxide ratio have been adjusted prior to each experiment.

3.9.1 Cyclic voltammetry

The same cyclic voltammetric response was recorded from all three solutions. The same reduction peak was recorded at E_P = -1700 mV (figure 3.1A). This shows that no changes in metal speciation or homogenous decomposition of additive occurs during two weeks.

3.9.2 EDS

Brass strip electrodes which had a silver undercoat were plated at E = -2050 mV for 120 s from these solutions. Reflective, uniform deposits were obtained in all three experiments. The EDS showed that the metal ratio of these deposits is similar, see table 3.19.

Age of solution	*Cu / %*	*Zn / %*	*Sn / %*
fresh	49	9.0	42.0
1 day old	50	7.5	41.5
14 days old	50	8.0	42.0

***Table 3.19** - the Cu-Zn-Sn alloy composition with different age of the bath.*

Studies Performed on Parts from the Plating Line and on Commercial Solutions

Previous chapters showed that an alloy with a desired quality and composition can be obtained only in strictly controlled conditions. For instance, changes in the composition of the plating bath: e.g. free CN/OH ratio, ion metal concentration, temperature, can lead to a deposit which cannot meet the specification for which it has been designed. All these experiments were carried out with freshly prepared solutions. Although these preparations use most of the chemicals and procedures as employed in the plating shop in Bicester, the solutions were not aged. Nor were the solutions compositions subjected to uncertainties resulting from factors such as drag out, anode chemistry, atmospheric CO_2.

It is also known that during its lifetime, many changes occur in the plating bath. There are daily consumption of chemicals through the: (i) plating process itself, (ii) drag out while transferring the parts from one tank to another, (iii) changes in the bath as a result of factors such as hydrolysis, anodic oxidation, CO_2 absorbtion, (iv) various additions of chemicals and additive. For instance, a loss in the free hydroxide occurs as a result of its reaction with CO_2 from the atmosphere, hydrolysis of some species such as CN^-, etc. This could lead to a build up in some of the chemicals which already exist in the bath: e.g. sodium carbonate. Also, the organic additive, may undergo decomposition reactions and, in time, the products could poison the bath itself. It should be stressed that during its lifetime, there are daily additions of additive based on the Hull Cell test only and not on a specific analytical method. No spectroscopic or chromatographic method for the additive is presently available.

4.1 Samples meeting specification

During the duration of the project, a number of connectors deemed to be of satisfactory quality have been examined by SEM and EDS. In general, no information is available about the history of the bath used. SEM are shown for typical components, labeled samples A-G.

Sample H is the SEM of a feature found within the coating of a component which passed quality control and, certainly, no consequences of the feature could be seen by eye.

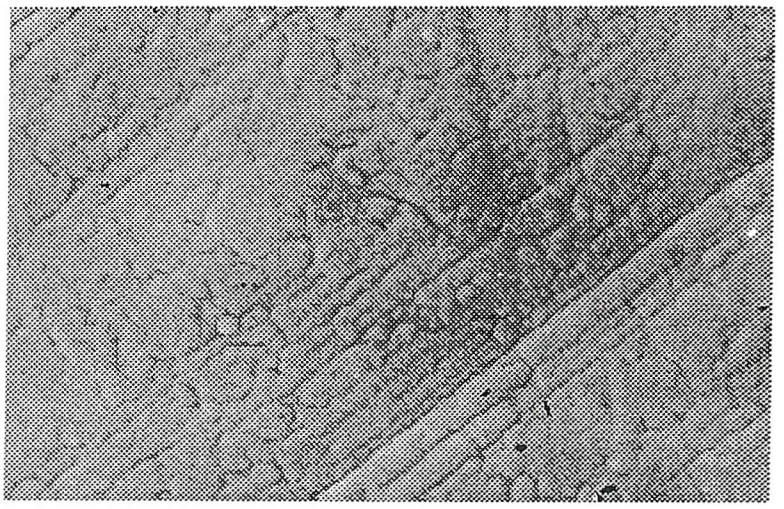

Sample A *-supplied on 20/2/1998*
SEM on a less sensitive scale

scale ⟷ 10 μm

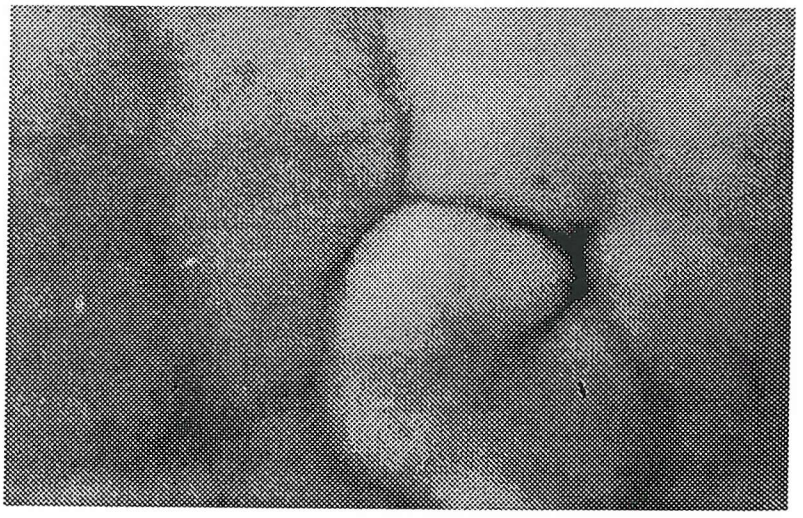

Sample B *-supplied on 18/2/98*

scale ⟷ 1 μm

Sample C *-supplied on 2/2/1998*

scale ⟷ 1 μm

Sample D *-supplied on 18/2/1998*
SEM on a less sensitive scale

scale ⟷ 10 μm

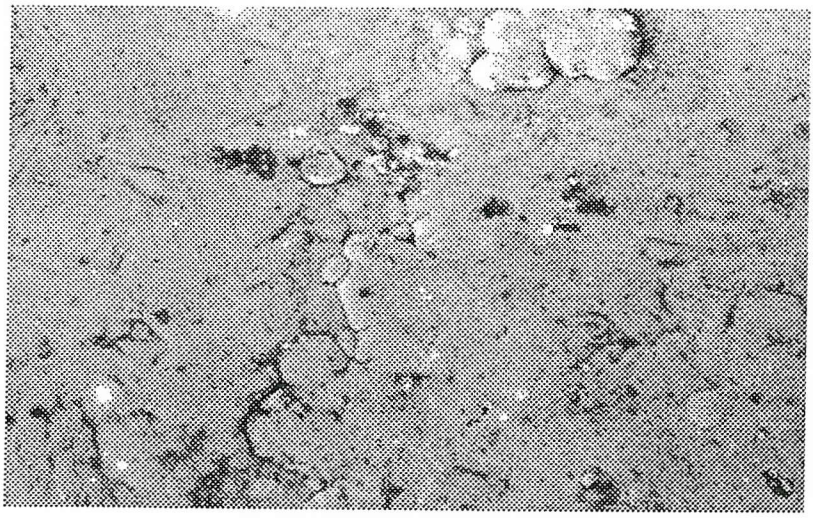

Sample E*-supplied on 2/9/1998*
SEM on a less sensitive scale

scale ⟷ 10 μm

Sample F *-supplied on*
12/8/1998
SEM on a less sensitive scale

scale ⟷ 10 μm

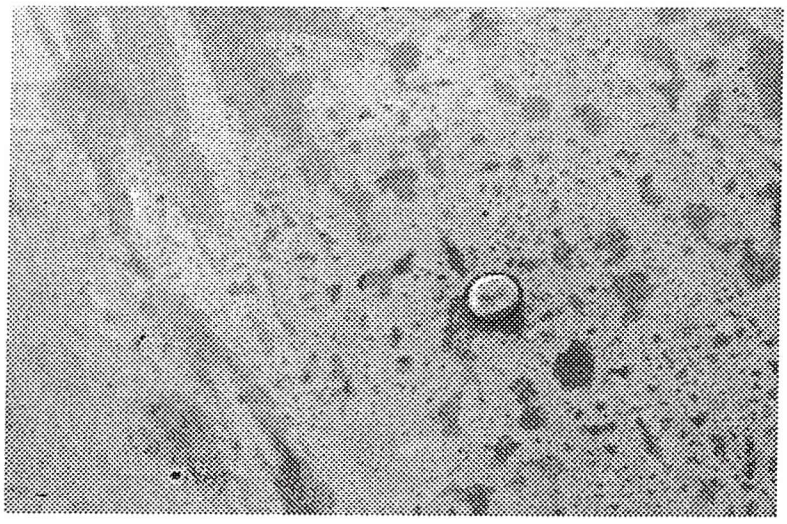

Sample G *-supplied on*
19/8/1998
SEM on a less sensitive scale

scale ⟷ 10 μm

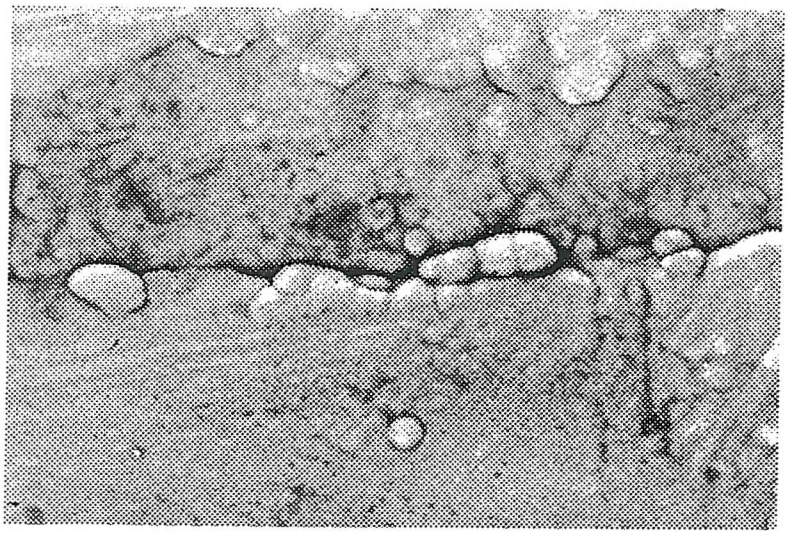

Sample H *-supplied on*
12/8/1998

scale ⟷ 10 μm

In can be seen that the morphologies are not identical. In general, however, each surface seems to be uniform in appearance and to be made up from overlapping rounded but rather flat features. Certainly, there is an absence of well defined hemispherical or angular crystallites found in other situations.

All these samples have been analysed by EDS and the following compositions were found:

Sample No.	Cu / %	Zn / %	Sn %
A	50	14	36
B	47	11	41
C	48	9	42
D	49	11	40
E	48	12	40
F	48	11	41
G	49	12	39
H	50	13	37

***Table 4.1** - the alloy composition of connectors plated at Huber & Suhner at Bicester*

It can be seen the all the alloy compositions fall within a narrow range :

- Cu: 48-52%
- Zn: 9-14%
- Sn: 36-42%

4.2 Studies of the bath aging

A number of connectors have been analyzed by the means of SEM and EDS techniques. These samples were collected from the North and South plating lines at Huber and Suhner - Bicester, and were obtained as a function of bath operating time during 1998. All the plates appeared of acceptable quality and were reflecting and free of visible defects. While the plating lines were subject to the routine, daily quality control and additions, it was not recorded how the samples relate to the additions etc. nor the position of the connector on the jig.

Table 4.2 reports the elemental analysis from all these samples:

	Bath Operating life / Ah	**Elemental Compositions / %**		
		Cu	**Zn**	**Sn**
North	~0	48.2 ± 0.7	8.7 ± 0.4	43.1 ± 0.5
	1563	46.9 ± 0.5	9.9 ± 0.4	43.2 ± 0.2
	2646	52.9 ± 0.7	15.1 ±0.5	32.0 ±0.4
	3697	48.2 ± 1.4	12.4 ± 0.5	39.4 ± 1.3
	6109	47.5 ± 1.0	13.9 ± 0.2	38.6 ± 1.0
South	~0	49.3 ± 0.5	9.8 ± 0.2	40.9 ± 0.6
	1756	44.2 ± 0.2	11.1 ± 0.5	44.7 ± 0.5
	2466	48.4 ± 0.2	11.3 ± 0.2	40.2 ± 0.3
	3829	49.3 ± 0.4	12.7 ± 0.4	37.9 ± 0.6
	4650	47.9 ± 0.4	11.9 ± 0.4	40.2 ± 0.7

Table 4.2 - elemental composition of alloy deposits detected by EDS analysis as a function of bath operating time. $i \approx 6$ mA cm^{-2}

Data in table above are the average and standard deviation of 4 - 10 measurements on the same sample. It could be seen from the standard deviations that although the variation is larger than would be expected for a limited area of one sample. There are some clear conclusions:

- the alloy composition is usually in the range:

  Cu 47-50 %, Sn 38-43 % and Zn 9-13 %

  and this is similar to the data reported for Southampton solutions in the last chapter. A few samples show more significant variations and it was suspected that the bath had not been recently adjusted before the component was plated.

- with bath operating time the Cu shows no trend but the Sn decreases and the Zn increases.

Figure 4.1, 4.2, 4.3 show SEM performed on connectors which were plated from the North line. Figure 4.1 shows a connector plated from a ≈ 0 Ah bath. This is a relatively thick deposit compared with these in chapter 3. It also shows a more structured surface not dissimilar to those reported earlier for satisfactory components.

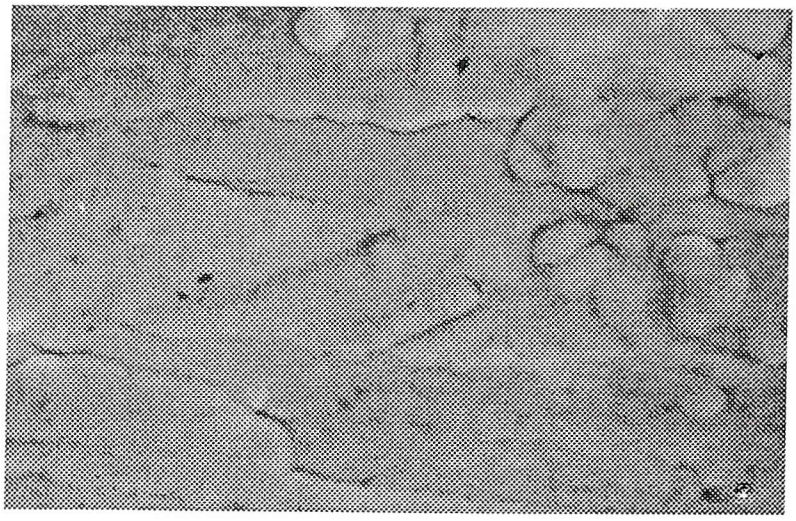

scale ⟷ 10 μm

Figure 4.1 *- SEM on a less sensitive scale of a connector plated from a 0 Ah bath*

Figure 4.2 shows an expanded view of some of the features. It is clear that the surface is made up of overlapping hemispheres and other rounded features and the grain boundaries are readily visible. This is a significantly different surface from these produced by plating onto strips of Hull cell plates under normally the same conditions, see chapter 3. The latter appear featureless at the same magnification.

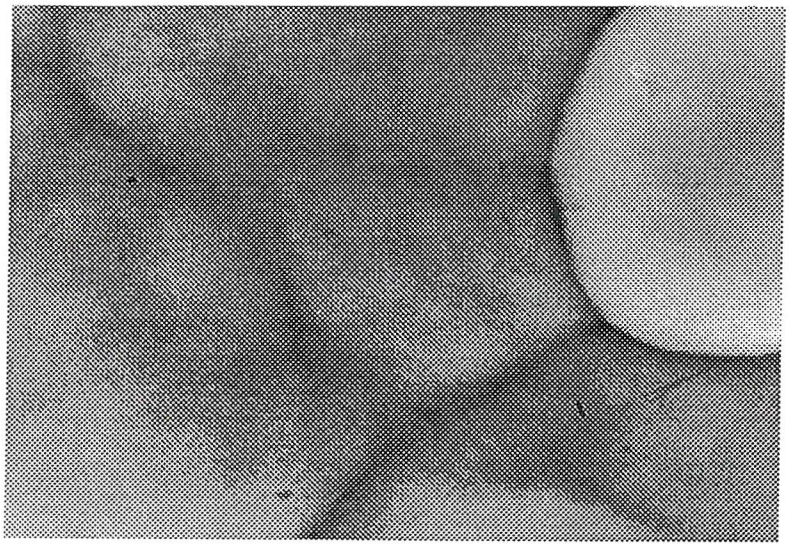

scale ⟷ 1 μm

Figure 4.2 *- SEM of a connector plated from a 0 Ah bath*

After the bath had been operated for 3697 Ah, the deposit starts losing this structure (figure 4.2). Lines, perhaps resulting from polishing, are visible along with a few hemispherical growths. Overall, the surface is much rougher than those described in chapter 3. The components, however, do have a uniform coating which is pleasing to the eye.

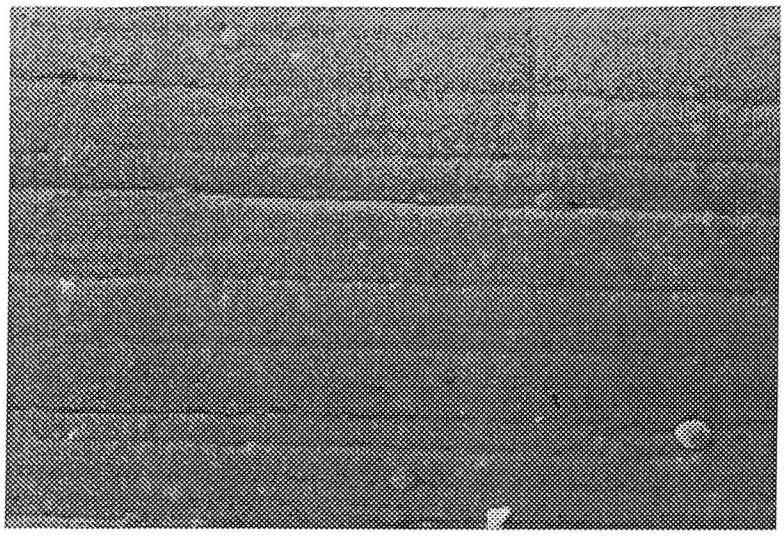

Figure 4.2 *- SEM on a less sensitive scale plated from a bath operated for 3697 Ah*

scale ⟷ 10 μm

At 6109, when the bath is normally replaced, the alloy structure has become very fine, and it follows many parallel lines although a number of circular pits can be observed: figure 4.3.

Figure 4.3 *- SEM on a less sensitive scale of a connector plated from a 6109 Ah bath*

scale ⟷ 10 μm

The SEM from the South line showed a similar trend.

4.3 Hull cell test plates

A Hull cell deposition is used as the routine method to monitor the state-of-health of the commercial plating line solutions. The state-of-health is, however, assessed from the overall appearance of the coated plate. Most of the plate should be covered by a uniform, reflective coating without any misty white areas but at the higher current density side, there should be tiger stripes. Indeed, the quality control requires an assessment of the area covered by the tiger stripes and the method is based on experience. A bath coming towards the end of the useful bath life, the tiger stripe darkens and extends towards the center of the plate but at the position equivalent to 6 mA cm^{-2}, the deposit remains uniform and reflective. The experience in Bicester, however, does not extend to any knowledge of the deposit structure in the area of the plate corresponding to the commercial current density (~ 6mA cm^{-2}).
Also, the charge passed during the 120s plating time used in the standard test is not enough to deposit an alloy thick enough at the position equivalent to 6 mA cm^{-2} that could be analyzed by the means of EDS. As a result, EDS data obtained from Hull cell samples supplied by Huber and Suhner was not reliable. For example, for a plate without Ag undercoat, a typical Cu-Zn-Sn analysis is: 61-25-14. When Ag coated under the same conditions lead to a Cu-Zn-Sn ratio of 50-10-40. The small content of tin found at the position of plating current density (ie. 10 - 20 % Sn) results from the electron beam passing through the electroplate into the base plate (which is composed of copper and zinc only).

However, these samples could be studied by SEM. Variation in the alloy morphology at different current density positions could be identified. Samples supplied by Huber & Suhner were studied in terms of "good deposit" and "tiger striped" deposit.
At the position of 6 mA cm^{-2}, a smooth, highly reflective deposit is obtained. The SEM is shown in figure 4.4 and some lines and uncovered area are apparent. This is not surprising for a very thin deposit. The lines probably reflect polishing scratches on the base plate.

Figure 4.4 *- SEM of a Hull Cell sample plated from a standard solution at the position of 6 mA cm^{-2}*

scale ⟷ 1 μm

This deposit becomes rougher at positions on the plate corresponding to higher current density. Figure 4.5 reports the SEM at 27 mA cm^{-2} and many lines are observed along with small hemispherical grains which are scattered over the whole area.

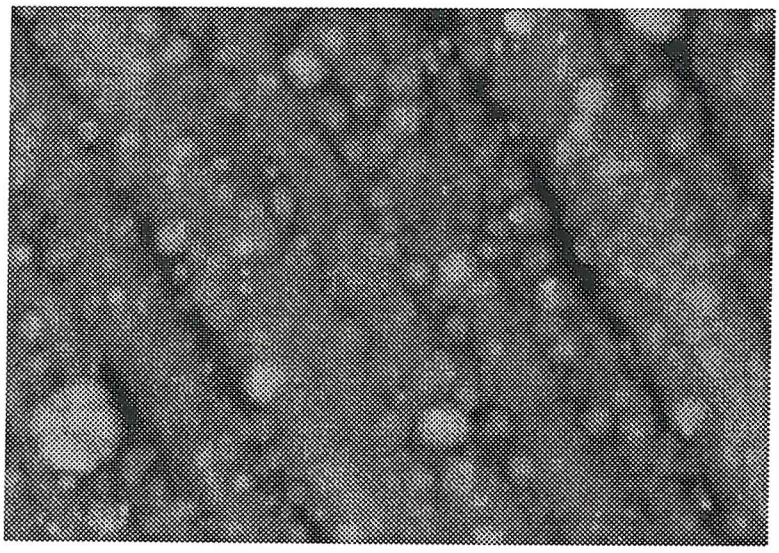

Figure 4.5- *SEM of a Hull Cell sample plated from a standard solution at the position of 27 mA cm^{-2}*

scale ⟷ 1 μm

At a current density of 45 mA cm^{-2}, in the region of the tiger stripes, the deposit becomes made of overlapping hemispherical or angular centers. Qualitatively, the EDS confirms that this structure corresponds to a deposit high in copper (giving the darker appearance by eye).

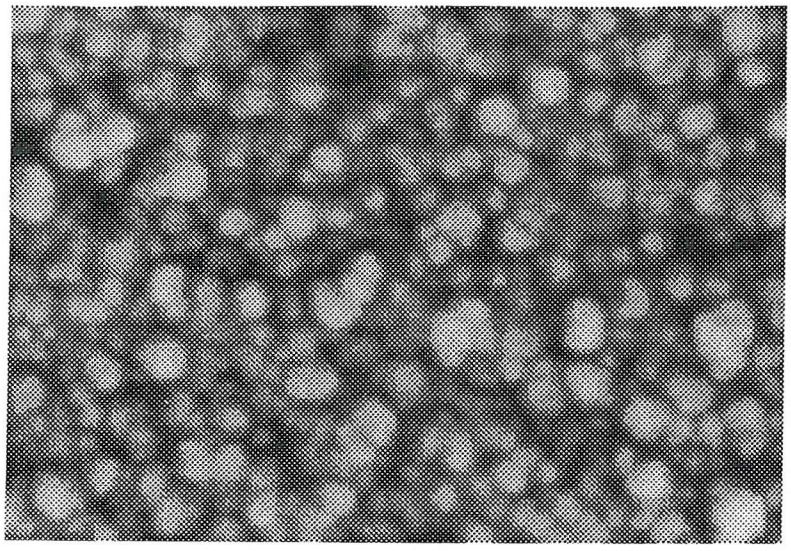

Figure 4.6- *SEM of a Hull Cell sample plated from a standard solution at the position of 45 mA cm^{-2} - tiger stripe*

scale ⟷ 1 μm

4.4 Jig cell

In addition to the Hull cell test, another test procedure based on a "Jig Cell" has been used by Huber & Suhner. In this cell a shaped brass workpiece, see figure 4.7, is moved up and down opposite a flat counter electrode. This arrangement again gives a distribution of current densities over the workpiece. The samples were plated at a current density of ~ 6 mA cm^{-2} for 5 min or 20 min from standard solutions at the Huber & Suhner laboratory. All the samples provided had three distinct areas: highly quality deposit, areas with a tarnished and poorly reflective finish and areas with a "lined appearance"- figure 4.7. It is thought that this "lined" defects were caused by the hydrogen which was trapped in the bent section at the lower end of the panel.

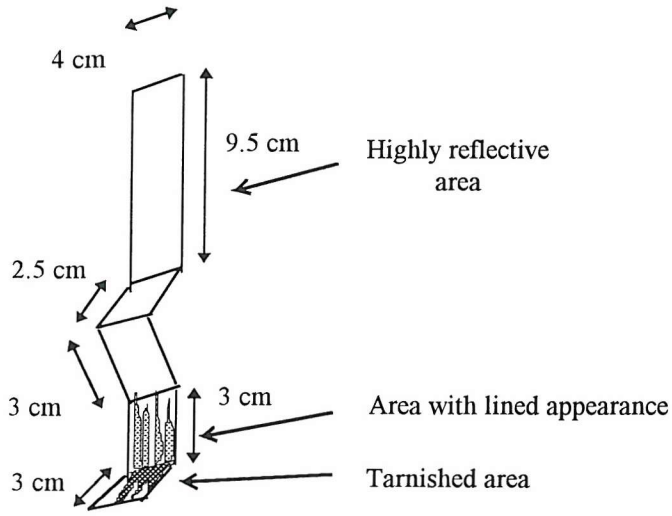

Figure 4.7 *- a diagram of a Jig Cell panel*

In this study, SEM and EDS data were collected from three different regions of the panels: the uniform highly reflecting deposit, the area with sharp linear imperfections and the area with a hazy, tarnished appearance. It was found that the defective areas were made up of large crystallites. For instance, the tarnished area is formed of overlapping, large crystallites of up to 1μm diameter (figure 4.8).

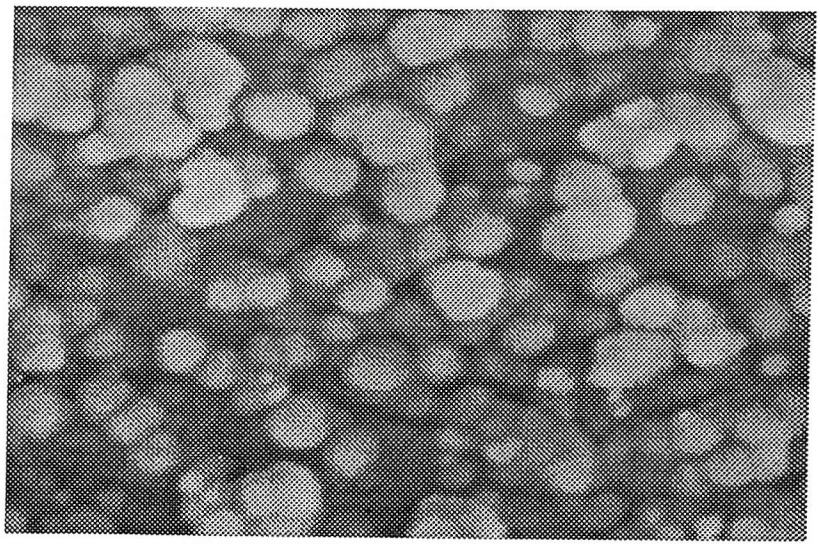

Figure 4.8 *- SEM of a jig sample plated from a standard solution for 5 min at the position of tarnished deposit*

This grains become of a more angular and irregular shape at the position of lined defects (figure 4.9).

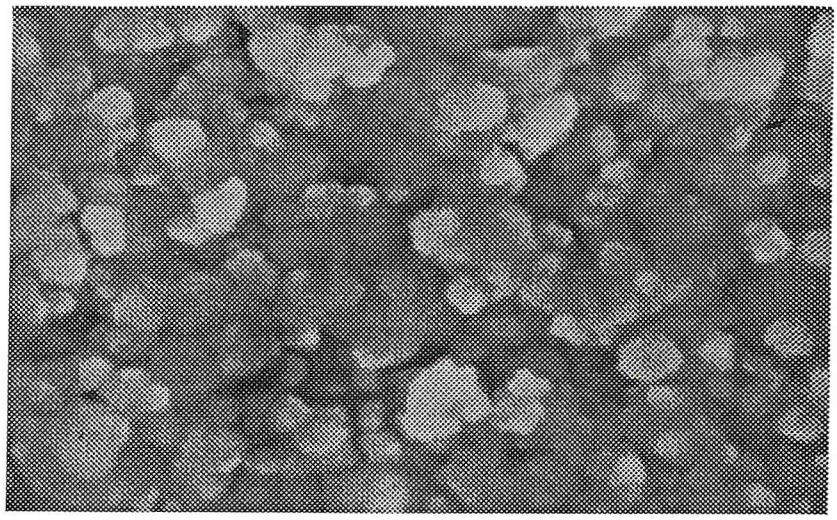

Figure 4.9 *- SEM of Jig Cell sample plated from a standard solution for 5 min at the position of lined defects*

scale ⟷ 1 μm

The SEM of the high quality deposits(both 5 and 20 minute deposits) show a very smooth and featureless deposit(figure 4.10). However, some cracks are seen which may indicate stress in the alloy (perhaps during cooling).

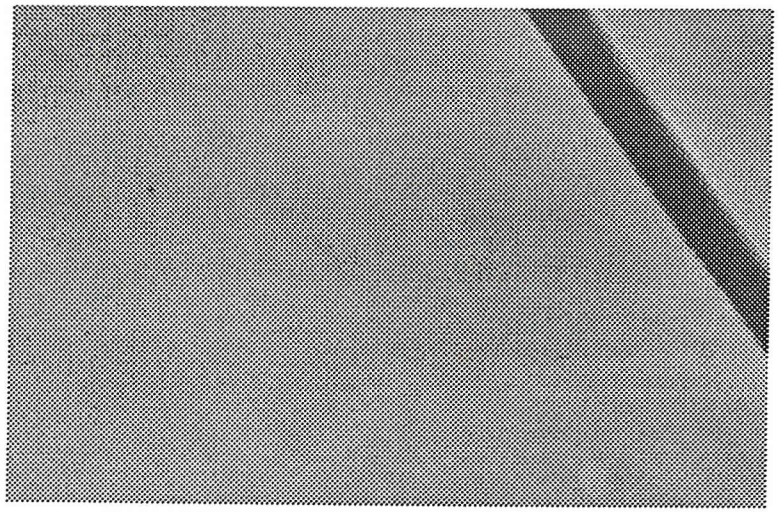

Figure 4.10 *- SEM of a Jig Cell sample plated from a standard solution for 5 min at the position of a reflective area*

scale ⟷ 1 μm

Table 4.3 reports EDS analysis of Jig Cell samples which were plated at 1 A for 5 min or 20 min. It can be seen that there is no significant difference between the two thickness of deposit and the defective area corresponds to high zinc and low in tin. All are high in copper.

	Cu	Sn	Zn
Highly reflective deposit			
5 minute	55	35	10
20 minute	56	36	8
Area with striped defects			
5 minute	58	32	11
20 minute	56	35	9
Tarnished area			
5 minute	58	26	16
20 minute	60	25	15

***Table 4.3** - EDS data from Jig Cell deposits*

The metal contents at all positions are significantly different from these found from Hull cell, strip plating or component plating. It is therefore difficult to interpret the data. There is the suspicion that the beam is going through the alloy deposit during the EDS analysis.

4.5 Cyclic voltammetry at a solution from the plating line

Several samples of solution from the commercial plating line supplied by Huber & Suhner at Bicester have been examined by cyclic voltammetry. This experiments were carried out a fresh brass electrode of 1 cm^2. The potential was cycled between -1250 mV to -2000 mV. In

all cases it was thought that the solutions were in good condition although the lifetime of the baths are not known.

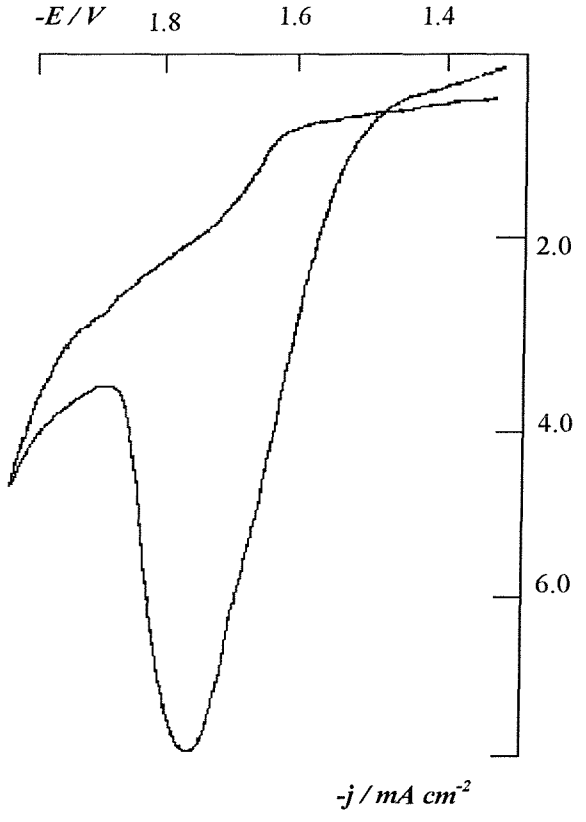

Figure 4.11 *- Cyclic voltammogram recorded at a brass strip electrode from a plating bath supplied by Huber & Suhner at Bicester. Scan rate: 20 mV s^{-1}, Temperature: 333 K*

Figure 4.11 reports the current-potential response recorded with one solution. A large reduction peak of j_P = 8 mA cm^{-2} is recorded at E_P = -1700 mV vs. SCE. This peak is caused by the hydrogen which started evolving at around -1500 mV. Also, in the steady state (the back scan), a reduction wave of about 2 mA cm^{-2} is recorded. This response is consistent with the response obtained from a standard solution high in additive (10 g additive solution to 1 l electrolyte) which was prepared in Southampton.

Cyclic voltammograms recorded on Huber & Suhner solutions on several occasions had a similar form of curve but the peak height varies as would be expected for variable additive concentration

4.6 Rejected connectors with defects

In these experiments SEM and EDS has been used to identify the alloy morphology and the local alloy composition respectively on reject connectors with tiger stripes or tarnished deposits. These samples were supplied by Huber & Suhner Bicester .

A tarnished connector, figure 4.12, was found to have a deposit which was scattered with hemispherical grains of up to 0.5 μm diameter. This alloy was found to be slightly low in copper and slightly high in tin with a composition Cu-Zn-Sn of 42-11-47.
In the laboratory, such deposits may be produced by using either a low hydroxide or copper ion concentration, or a high tin or cyanide concentration.

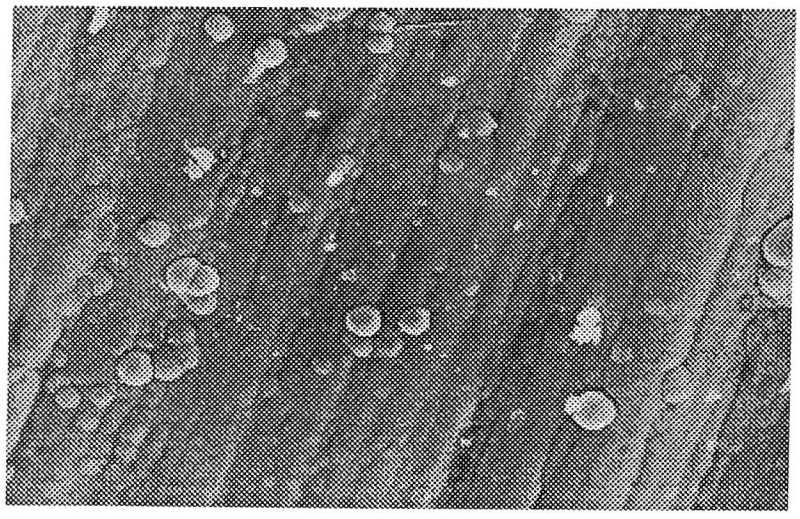

Figure 4.12 *- SEM of a tarnished connector*

Figure 4.13 shows an SEM of a tiger stripe type defect which is composed of a rough deposit with many overlapping centers.. This deposit was found to be high in copper and low in tin with an

alloy composition of Cu-Zn-Sn: 64-10-26. An alloy with this ratio could be plated in the laboratory from solutions that were high in copper hydroxide or low in tin or cyanide.

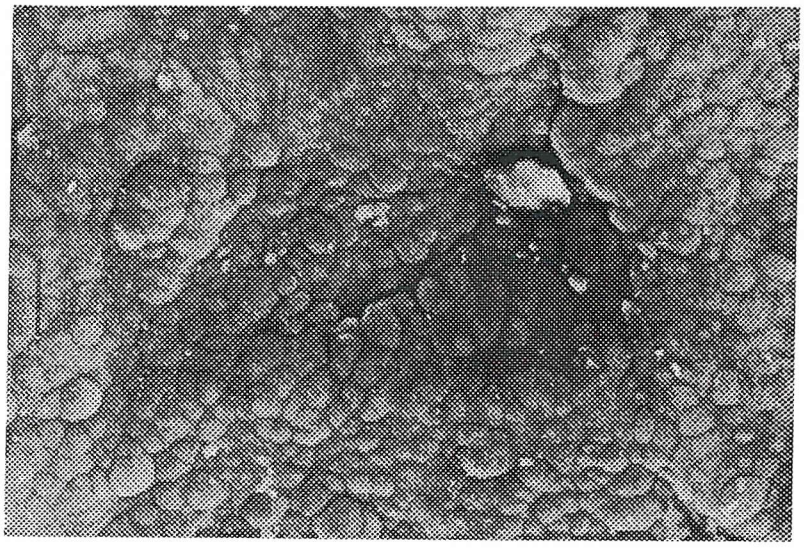

scale ⟷ 1 μm

Figure 4.13 *- SEM of a connector with tiger stripes*

4.7 Connectors from different plating lines

The composition and morphology of connectors which have been plated at Huber & Suhner plating lines in the USA and Switzerland have been examined. Although these connectors were classified as "good" plates, the US sample had a dull and poorly reflective appearance.

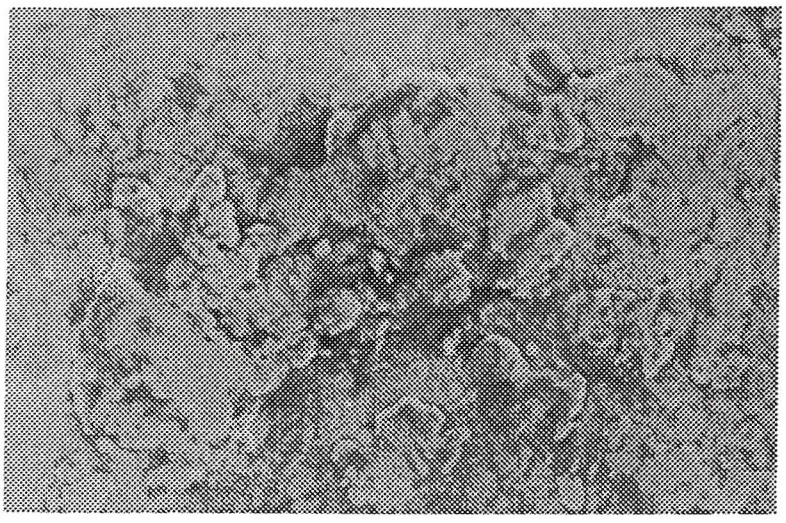

Figure 4.14 *SEM on a less sensitive scale of a connector plated on the USA line*

scale ⟷ 10 μm

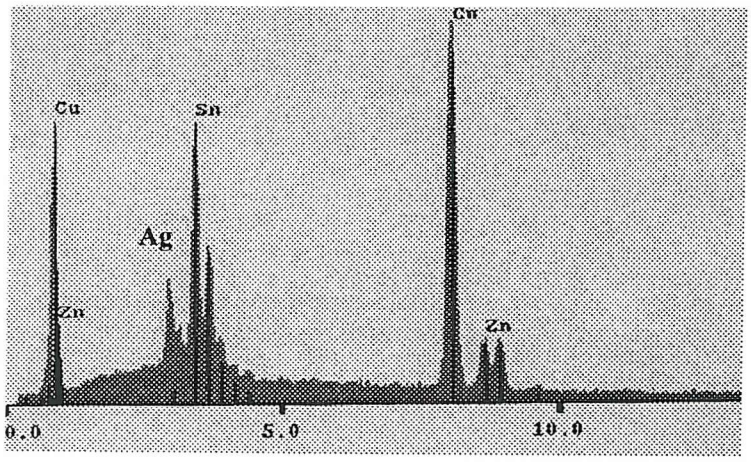

Figure 4.15 *- EDS spectra of a sample plated at Huber & Suhner USA line*

The SEM of this connector, figure 4.14, showed a faulty deposit with a rough, non-uniform structure. Its composition was found to be high in copper and low in tin, with a ratio Cu-Zn-Sn of 60-10-30. Also, the large silver peak on the EDS spectra (figure 4.15) shows that this deposit was very thin. An alloy with a similar metal content was produced in the laboratory from solutions high in copper or hydroxide or low in cyanide or tin.

A much more uniform deposit was observed on a connector plated a Switzerland: (figure 4.16). This sample, was classified as "good" and it had a reflective, uniform deposit. It is not as featureless as some deposits examined during the project.

Figure 4.16 *SEM on a less sensitive scale of a connector plated on the Switzerland line*

scale ⟷ 10 μm

The EDS showed an alloy with the ratio, Cu-Zn-Sn of 58-9-33. However, this deposit was thick, as the EDS spectra did not show any silver peaks (figure 4.17) These two connectors have an alloy composition different from a typical alloy plated at Huber & Suhner Bicester. They are high in copper and low in tin.

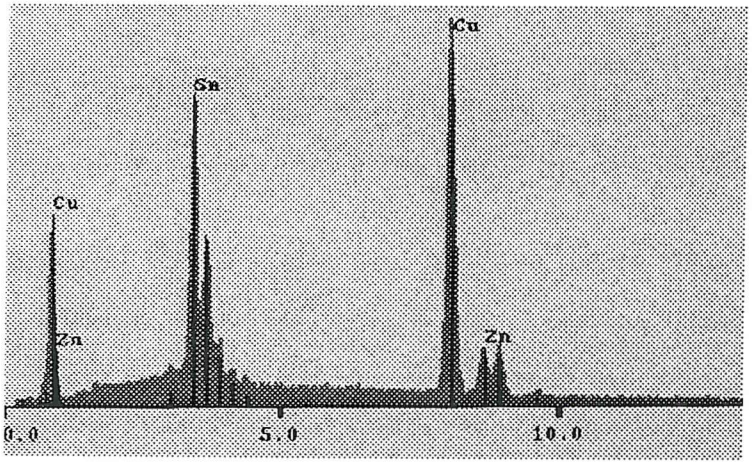

Figure 4.17*- EDS spectra of a sample plated at Huber & Suhner Switzerland*

Figure 4.18 shows the structure of a connector plated at Bicester. The composition of such deposit was:

Cu 48 %, Sn 42 % and Zn 10 %.

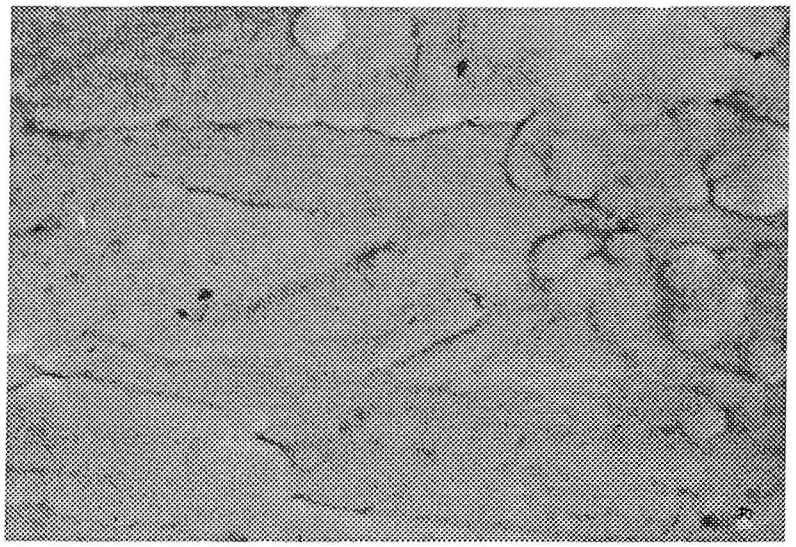

scale ⟷ 10 μm

Figure 4.18 *SEM on a less sensitive scale of a connector plated on the Bicester line on a freshly made bath*

4.8 Conclusions

- Hull Cell test with a brass panel shows the change in structure of the deposit with the current density. At low current densities(6 - 10 mA cm^{-2}) the deposit is featureless and it follows the polishing lines of the substrate. As the current density increases, the structure roughens, with angular or circular grains.

- There is a clear evidence that change in deposit morphology occurs with the aging of the bath. The uniform deposit with a clear structure observed at early bath age become featureless as the bath reaches the end of its useful life.

- This change is observed from the trend in metal ratio during the bath lifetime: copper tends to stay constant, there is an increase in zinc and a decrease in tin

- Different deposit composition are achieved from the three different plating lines. The US plating line gives thin deposits which are high in copper and low in tin. These deposits are

poorly reflective. Samples from the Switzerland have a good appearance; however, the same trend is obtained from the Switzerland plating lines: high copper and low tin.
the alloy composition from Huber & Suhner at Bicester always in the range:

Cu 47-50 %, Sn 38-43 % and Zn 9-13 %

- Cyclic voltammetry of the plating solution provided by Huber & Suhner at Bicester shows the same response as the one performed in laboratory on a fresh bath with 10 g additive to 1 litre of electrolyte. The same reduction peak of i= 8 mA cm^{-2} is recorded at E_P = -1700 mV. Other commercial solutions show similar voltammetry although the peak current density is variable which may reflect different additive concentrations.

The Effect of the Anode on Plating Process

The deposition of the alloy at the cathode involves the 1 e reduction of Cu(I) and the 2 e^- reduction of Sn(IV) and Zn(II) and the deposition of the alloy is accompanied by significant H_2 evolution. The deposition of 1 Kg of alloy requires the passage of >25.2 F (or > 672 Ah of charge. The same charge must pass at the anode and possible reactions include:

$4\ OH^- - 4e^- \rightarrow O_2 + 2H_2O$

$2\ CN^- - 2e^- \rightarrow (CN)_2$

$CN- + 2OH- -2e \rightarrow CNO- + H_2O$

$CN^- + 2OH^- -10e^- \rightarrow CO_2 + NO_3^- + 5H_2O$

$CuCN + CN^- -1e^- \rightarrow Cu(CN)2$

additive $-ne^- \rightarrow$?

Without precise knowledge of the anode chemistry, the mass balance in the bath cannot be predicted. Certainly, if CN^- in not oxidized or undergoes a $10e^-$ oxidation, cyanide will build up in solution. If the additive undergoes oxidation, unknown species will be formed. In the commercial plating bath, carbon anode are used.

Voltammetric experiments were therefore carried out a C anode in order to give a preliminary view as the anode chemistry in the bath. The electrode used cut form a carbon anode from the plating line at Bicester had an area of 0.5 cm^2.

Four solutions were studied:

- 1 M NaOH
- 1 M NaOH + 0.1 M NaCN
- 1 M NaOH + 0.1 M NaCN + 5 g l copper Glo
- standard plating bath

and the voltammograms are reported in figure 5.1. The response for 1M NaOH shows relatively low currents although there is a small oxidation wave around +500 mV and further oxidation positive to + 600 mV. The second solution shows a well defined oxidation wave $E_{1/2}$ = + 300 mV and limiting current density of 10 mA cm^{-2}. Clearly, cyanide is oxidizing and the limiting current density suggests a multielectron oxidation of the cyanide. On addition of the Copper Glo, however, there is no substantial change in the response indicating that the additive is probably not oxidized.

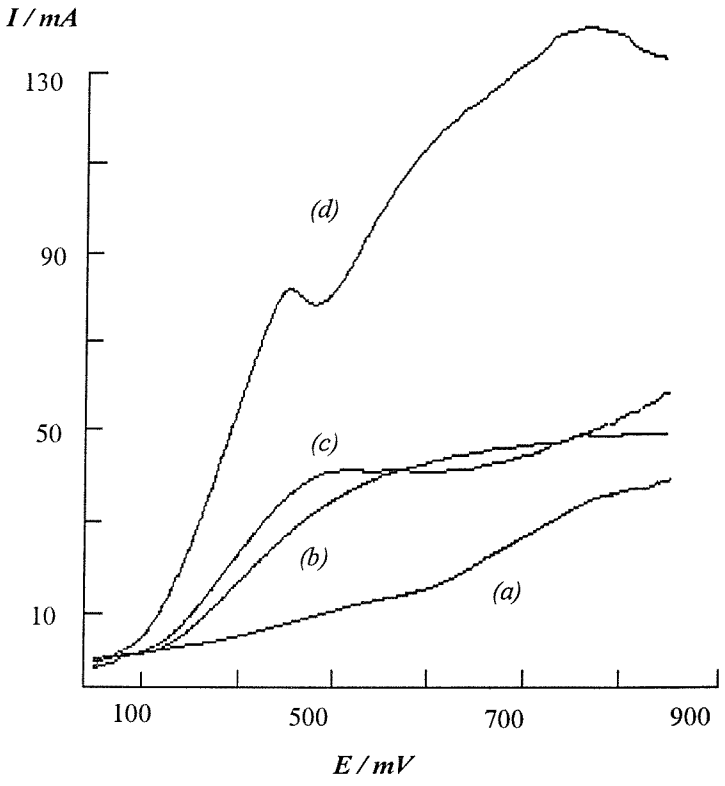

Figure 5.1 *- The potential current data recorded at a carbon electrode with different solution. (a) : 1 M NaOH, (b): 1 M NaOH + 0.1 M NaCN, (c): 1M NaOH + 0.1 M NaCN + 5g Copper Glo solution / 1 litre electrolyte, (d): standard plating bath. Working electrode: carbon, Temperature 333 K*

The voltammogram for the standard plating bath solution again shows an oxidation wave at $E_{1/2}$ = + 300 mV and it is larger. This is not surprising since the free CN^- concentration is 551 mM. The voltammograms shows a second oxidation wave at more positive potential but this is unlikely to be involved in the commercial bath (because of the high current density for the first oxidation wave) and may be due to the oxidation of Cu(I) or Sn(IV).

Clearly, the main oxidation process in the commercial electroplating bath is the oxidation of cyanide. The products of this reduction has not been defined but they could influence plating performance as they built up during the bath lifetime.

Overall Conclusions and Discussion

The commercial electroplating bath, tradename SUCOPLATE, with the composition

	$g\ l^{-1}$	mM
CuCN	9.1	102
$Zn(CN)_2$	5.4	46
$Na_2[Sn(OH)_6]$	5.7	24
Na_2CO_3	6.5	61
free NaCN	25	551
free NaOH	2.1	50
Copper Glo solution	5.0	

has been investigated. It is normally operated at 333 K with a current density of 6 mA cm^{-2}.

Using freshly prepared solutions, it has been confirmed that the bath gives adherent and highly reflecting electroplates on either brass or silver coated brass electrodes. The composition of such deposits were found to be:

Cu	47 - 50%
Zn	9 - 13%
Sn	38 - 43%

Indeed, Cu-Zn-Sn alloys with this composition can be plated under a range of controlled current or controlled potential conditions. When the deposition of the alloy is carried out at a current density of 6 mA cm^{-2} for 120 s, the potential of the substrate quickly reaches a steady state value of -2050 mV vs SCE and some hydrogen evolution accompanies alloy deposition. An alloy with the same composition is obtained when the deposition is carried out at -2050 mV vs SCE for 120 s. When deposition is carried out for much longer periods

either with a constant current or constant potential, the deposit becomes less reflecting and SEM shows that it becomes rougher.

It should be stressed that the composition of the alloy deposited, Cu/Zn/Sn ≈ 48/10/42 is quite different from the ratios of the molar concentrations of the metal in solution, ie. 60/28/12. This difference indicates that the deposition of the alloy cannot be mass transfer controlled and that the rate of deposition of the three metals is determined by kinetic factors. This is consistent with calculations which show that the mass transport limited current would be much higher than 6 mA cm^{-2} (and some of the applied current produces hydrogen and not alloy deposit). Moreover, the same conclusion is evident from all voltammetric experiments. Cyclic voltammograms are always complex. Steady state voltammetry at freshly plated alloy electrodes at 333 K does lead to a single reduction wave at -1650 mV vs SCE and a limiting current of ~ 2 mA cm^{-2}; this wave is not observed for solutions containing only one of the metal ions and is extremely small at room temperature. Overall, it would appear that the rate of deposition of the metals is determined by chemical reactions, probably associated with changes in metal ion speciation, which precede the electron transfer step. A number of experiments confirmed the key role for Sn(IV) in catalyzing alloy deposition.

Cyclic voltammograms on the standard electrolyte showed a large reduction peak in the region of E_P = -1700 mV. This peak can be seen to be associated with hydrogen evolution evolving vigorously during this part of the experiment. Hydrogen evolution was also seen in deposition and other experiments but only as a transient phenomenon and in the steady state it generally decreased to a much slower rate. Studies performed on other solutions showed that the peak was only observed when deposits have a high content in tin and the additive, Copper Glo was also present in the solution. The role of tin is not surprising since it is known that tin is a good catalyst for hydrogen evolution. The height of this peak was found to vary with the additive concentration in the bath. When no additive was present in the bath, only a reduction wave was recorded, and the alloy was found to have a rough structure, formed of small, round features. As the additive concentration increases, the

reduction wave takes the form of an increasing peak and the structure of the alloy becomes completely featureless (in the laboratory plating of strips). However, the change in the additive concentration did not produce any change in the alloy composition. This may indicate that one role for the additive is to cause hydrogen evolution at an early stage and that this leads to changes in the current distribution for metal deposition during the early stages of alloy layer formation, eg. leading to a different pattern of nucleation.

A large number of experiments have been carried out where the concentration of each of the bath components is varied systematically.

It was found that the free cyanide and free hydroxide concentrations have a substantial influence on the Cu/Sn ratio. The Cu/Sn increases in the bath in either low in cyanide or high in hydroxide and decreases when the solution is high in cyanide or low in hydroxide. The zinc content is less sensitive to the CN^-/OH^- ratio although it is high in the concentrated hydroxide solution. All the deposits are strongly adherent and uniform but the appearance and morphology of these deposits appear to be totally determined by the alloy composition.

Changes in the concentrations of the metal ions lead to alloys with a Cu or Sn contents > 60 % with consequent changes in the appearance of the deposits and morphologies on a 1 μm scale when examined by SEM. When the Cu(I) and Sn(IV) concentrations are varied, the trend in the metal content of the alloy is entirely predictable; an increase in relative amount of one ion leads to an increase in that metal in the alloy. It is, however, mainly the Cu and Sn contents which vary and the zinc content of the alloy is quite constant. When the Zn(II) concentration is varied, it is the amount of Zn and Sn which change. These trends are surprising since Cu(I) and Zn(II) are complexed by cyanide and Sn(IV) by hydroxide. But, again, it must be concluded that the relative rates of reduction of the three metal ions are determined by kinetic factors and little by thermodinamics. The quality of deposits is generally good; uniform and adherent deposits are obtained over a surprisingly wide range of conditions in this alkaline cyanide bath.

The above results can be understood through the role of the ligands in the system; cyanide complex the Cu(I) and Zn(II) while Sn(IV) is complexed by the hydroxide ion:

- high copper contents result from the solution being high in Cu(I), low in Sn(IV), low in cyanide or high in hydroxide. Conversely, low copper contents result from solutions low in Cu(I), high in Sn(IV). high in cyanide or low in hydroxide. High copper contents are also the norm at high current densities.
- high tin contents result from solutions being high in Sn(IV), low in Cu(I), high in cyanide or low in hydroxide. Low tin result from solutions low in Sn(IV), high in Cu(I), low in cyanide or high in hydroxide.
- high and low zinc contents result for variation of the Zn(II) concentrations but the zinc content is less sensitive to the cyanide and hydroxide concentrations.

A high copper content gives rise to a deposit which is poorly reflecting, darker and even brown to the eye. By SEM they usually can be seen to be made up of overlapping hemispherical centres. High tin content leads to plates with a tarnished white appearance and SEM shows them to consist of small angular crystallites. Such features can be seen on defective components from the plating line.

Studies were carried out at solutions containing only one of the metal ions, Sn(IV), Cu(I) or Zn(II). It was found that tin deposits easily at very low negative potentials. Milky deposits were obtained at deposition times of 120s. At shorter deposition times, 30s, however, the tin deposits were reflective and uniform. Copper and zinc deposits were obtained at a very slow rate and at much more negative potentials. For example, it takes 600 s for Zn and 360 s respectively for Cu to deposit at a deposition potential of -1800 mV. Also, no reduction peak could be seen on the voltammograms. Indeed, the cyclic voltammetric experiments carried out in such solutions showed different behaviour from the alloy plating bath. A large reduction wave accompanied by hydrogen evolution was recorded from solutions containing Sn ions only and additive. Copper ions did not show any reduction waves. However, it is thought that as the copper ion reduces at more negative potentials, this wave is masked by

the hydrogen evolution which occurs at such potential values. The cyclic voltammetry of the solution containing only Zn(II) generally gave rather featureless responses. On the forward scan, the current density increased smoothly and reached 15 mA cm^{-2} at - 1900 mV.

Studies carried out at different temperatures, 293 K - 343 K, showed no change in the composition of the alloy but the rate of alloy deposition is a strong function of temperature. Thick deposits must be plated at elevated temperatures, if the process is to be completed within a reasonable period. At a constant current density of 6 mA cm^{-2}, the current efficiency is very poor at room temperature; almost all the current is consumed in hydrogen evolution.

A change in the carbonate concentration do no seem to influence nor the alloy composition neither its morphology and appearance.

The organic additive concentration does not produce any change in the alloy composition but it has a very strong effect on the appearance on deposit. The best reflecting deposits were plated from a bath containing twice the amount of copper Glo in the commercial bath. (10 g l^{-1}). The mechanism of operation of the additive has not been defined. Crucially, the structure of Copper Glo is not fully known. Copper Glo leads to hydrogen evolution as a transitory event and this is clearly seen, for example, during cyclic voltammetry (both as current and visibly as bubbles) from solutions high in tin content. The hydrogen evolution is observed only over a narrow potential range and stops after a short period of alloy deposition if the potential is held in this potential region. Almost certainly, this behavior is associated with the adsorption of an organic molecule(s) over this potential range and it could be that this adsorption is more favorable on a tin containing surface since the additive only leads to characteristic behavior for such surfaces. During many experiments, eg. constant current or constant potential, this H_2 evolution occurs only for a short period during the early stages of deposition. This suggests that the additive acts by influencing the early stages of metal deposition, perhaps through the rate of formation of nuclei of the alloy phase. H_2 evolution is occurring, it will influence the current distribution over the surface of

the substrate and make it more uniform. In addition, certainly during constant current plating, the rate of reduction of the metal ions will be reduced by the occurrence of the H_2 evolution. Thus a possible mode of action for the additive is to slow down the nucleation and early growth of the alloy phase (and the H_2 evolution will contribute to the current) and hence to create a basis for further growth of a deposit smooth on a sub-micron scale. On the other hand, none of the effects of the additive could be reproduced with simple amine oxides and such amine oxides were not reduced cathodically in the bath solutions. It must be concluded that the N-oxide group is not the active functional group in the additive molecule. Its role is probably only to enhance the solubility of the additive in aqueous solutions.

A preliminary study of the anode chemistry in the plating bath was undertaken with a sample of anode carbon from the plating line. The main process is the oxidation of cyanide. The products of this process has not been defined but they could influence plating performance as they built up during the bath lifetime.

Huber and Suhner have developed a reliable Hull cell test for the state of health of the plating line solution. It is, however, based on the appearance of the whole test panel and is a qualitative test which uses the experience of the operator; good quality deposits are observed over much of the plate even when the bath needs to be replaced. It cannot, however, be assumed that the alloy deposited at the position equivalent to a current density of 6 mA cm^2 will be identical to those produced in strip plates or commercial components under the same conditions. Moreover, the alloy morphology at different current density positions were readily identified. At the position of 6 mA cm^{-2} a highly reflective deposit was obtained and the SEM were essentially featureless. The deposits becomes rougher with increasing current density. At 45 mA cm^{-2}, in the region of tiger stripes, the deposit becomes made of overlapping hemispherical or angular centers. Also, EDS analysis performed on Hull cell samples showed that at high current densities there is an increase in the copper content at the expense of tin.

The same alloy composition was found for the plated panels and strips in Southampton and panels as well as satisfactory components from the Bicester lines. In addition the voltammetry of solutions supplied from the Bicester line were consistent with data from fresh solutions prepared in Southampton. On the other hand, there were significant differences in alloy composition and morphology of components supplied from other Huber & Suhner facilities in Switzerland and USA. There was some evidence that the alloy composition changed with the operating life of the bath; the copper was found to remain constant there was an increase in zinc and decrease in tin with operating time. This trend in composition seemed to result from change in the bath due to anode chemistry since the same variations were not reproduced from solutions simply left to stand for the same period.

When rejected components were examined by SEM and EDS, the faulty regions showed the expected effects. The metal ratios were outside the acceptable range and the morphology reflected the alloy composition. This is, however, clearly not the whole story since the rejected components only had defects in particular areas. Hence, the defects do not arise only from the bath composition going out of specification. There must also be mass transport or current distribution effects which combine with a bath composition slightly out of specification to produce defects in particular areas on the components and/or positions on the jig.

References

1. Raub C.J ,- *Comprehensive Treatise of electrochemistry* Vol 2, eds. O'M Bockris J., Conway B. E., Yeager E., White R.E., (1981), Plenum Press, New York, pp.381-397
2. Kuhn A.T.,(ed.), *Industrial Electroplating Process* (1971) Elsevier, London
3. Brenner A., *Electrodeposition of Alloys - Principles and Practice,* Vol. 1 and 2, New York, Academic Press, (1963)
4. Pletcher D., Walsh F.C., *Industrial Electrochemistry.* 2nd edition (1990), Chapman and Hall, London
5. Southampton Electrochemistry Group, *Instrumental Methods in Electrochemistry,* 1st edition (1985), Ellis Horwood Ltd., Chichester
6. Pletcher D. - *A First Course in Electrode Process,* 1st edition (1991), The Electrochemical Consultancy, Romsey
7. Brett C., Brett O. - *Electrochemistry Principles, Methods and Applications* (1993), Oxford University Press , Oxford
8. Lowenheim F.A. - *Modern Electroplating,* 3rd edition (1974), Wiley Interscinece, New York
9. Gileadi E., Kirowa-Einser E., Penciner, *Interfacial Electrochemistry. An Experimental Approach,* (1975), Addison-Wesley Reading, Mass.
10. *Canning Handbook of Electroplating,* 21st edition (1970), W. Canning & Co. Ltd., Birmingam
11. Ivascanu S.,Gutt G., Gutt S., Gramaticu M., Apostolescu M. - *Revista de chimie,* (1983), Vol. 34, pp. 500
12. Sanicky M. - *Plating and Surface finishing,* (1986), Aug., pp.10
13. Sanicky M. - *Plating and Surface finishing,* (1985), Oct., pp. 20
14. Silaimani S. M., Thangavelu P.R., John S. - *Bulletin of Electrochem.,* (1998), Vol 14, pp. 157
15. Hull R.O., - *Am. Electroplating Soc.,* (1939), Vol.27, pp. 52

16.Pinner. R. - *Copper and Copper Alloy Plating,* 2 nd. Edition, (1964), Copper Development Association, London

17.Diggin M.B, Jernsted G.W - *Proc. Amer. Electoplating* Soc. (1944), Vol 32, pp. 247

18.Mohler.J.B - *Metal Finishing,* Oct. (1955), Vol 53, pp.47

19.Jacky G. F. - *Plating,* Sept., (1971), pp. 883

20.Jordan M. - *The Electrodeposition of Tin and its Alloys,* (1995), Eugen Leuze Publishers, Germany,

21.*Encyclopedia of Elchem. of the Elements,* Vol 2, Ed. Bard J. A., Marcel Dekker, (1978), Inc. New York, pp. 438

22.Sinitski R.E, Srinivasan V., Haynes R - *J. Electrochem. Science and Technology,* Jan. (1980), Vol 127, No.1, pp. 47

23.Abbott D.- *Inorganic Chemistry,* (1965), Mills & Boon Ltd.

24.Katagiri A., Inoue H., Ogure N., *J. Applied Electrochem.,* (1997), Vol.27, pp.529

25.Deryn Chu, Fedkiw P., *J. Electroanal. Chem.,* (1993), Vol. 345, pp. 107

26.Hartherley P.G., Carpenter P.J.,- *Trans. Inst. Metal. Finishing,* (1995), Vol. 73, pp. 85

27.Thompson M. R. - *Trans. Electrochem.,* (1941), Vol. 79, pp. 433

28.Glasstone S. - *J. Chem. Soc.,* (1929), pp. 702

29.Otero T.F. - *Personal Communications*

30.Penneman R. A., Jones L. H.- *J. Chem. Physics,* Febr., (1956), Vol. 24, pp. 293

31.*Comprehensive Coordination chem.,* Vol. 6, (1987), Perganon Press, Oxford, pp.4

32.Hedges E.S. - *Tin and its Alloys,* (1960), London, Edward Arnold

33.Jongkind J. C., Cargo F.B., *Plating,* Sept., (1970), pp. 901

34.Hull R. O., Wernlund C. J. - *Trans. Electrochem. Soc.,* (1941), Vol. 48, pp. 407

35.Bockris J. O'M., Nagy Z., Damjanovic A. - *J. Electrochem. Soc.,* (1972), Vol. 119, pp 290

36.Gerischer H.- *Anal. Chem.,* Jan., (1959), Vol. 31, pp. 33

37.Sharpe A.G. - *The Chemistry of Cyano Complexes of Transition Metals,* (1976), Academic Press, London

38.Jongkind J.C. - *Plating,* (1968), pp.722

39.Fulton J., Swinehart D. F.- *This Journal*, (1954), Vol 76, pp. 864

40.Hajdu J., Zehnder J. A.- *Plating*, (1971), pp. 458

41.Sillen L. G. - *Stability Constants Metal-Ion Complexes*, (1964), The Chemical Society, London

42.Smith R, Martell A. - *Critical Stability Constants* Vol 4, (1976), Plenum Press, New York

43.Kragten J. - *Atlas of Metal-Ligant Equilibria in Aqueous Solutions* , Ellis Howard Ltd., Chichester

44.Mandich N. V.- *Trans. Inst. Metal. Finishing*, (1991), Vol 40, pp. 24

45.*Encyclopedia of Elchem. of the Elements*, Ed. Bard J. A., Marcel Dekker, Inc. New York, (1978), Vol 13, pp.310